



# THESE

*Présentée à*

**L'École Nationale d'Ingénieurs de Sfax**

*En vue de l'obtention du*

**DOCTORAT**

Dans la discipline  
*Ingénierie des Systèmes Informatiques*

*Par*

**Nouha Baccour Sellami**

---

**Link Quality Estimation in Wireless Sensor Networks:  
Analysis, Design, and Experimentation**

---

*Soutenu le 7 Mai 2012, devant le jury composé de :*

M.	Mohamed Jmaiel (Professeur)	Président
M.	Rafik Braham (Professeur)	Rapporteur
M.	Abdelfettah Belghith (Professeur)	Rapporteur
M.	Maher Ben Jemaa (Maître de conférences)	Examineur
M.	Habib Youssef (Professeur)	Directeur de Thèse
M.	Anis Koubâa (Maître de conférences)	Co-encadreur de Thèse

*To my parents and my two brothers  
To my husband and my daughter  
To my mother in law and my grand mother*



# *Acknowledgments*

First, I would like to express a deep gratitude to my thesis supervisor Prof. Habib Youssef for his guidance and support throughout my thesis. I am so grateful to have had the opportunity to work with an outstanding professor and a superb person like him. I really enjoyed all the work meetings that we had together. At each meeting, I learned something new in networking in general and also get very interesting suggestions and critics for my research work.

Second, I would like to thank my thesis co-supervisor Dr. Anis Koubâa for his outstanding supervision leading towards this thesis. Particularly, I am so thankful for the so many things I learned from him. Among other things, he taught me how to write high quality papers and also professional e-mails. I would also thank him for the several hours he has dedicated to my research work and for the uncountable meetings and interactions that we had together discussing in depth my work progress.

Next, I would like to thank Prof. Mário Alves for being following the development of this thesis and providing insightful comments and guidance. I would like to thank him for seeing the usefulness of my work and for his considerable efforts to make my work more visible to the research community.

I also owe special thanks to all ReDCAD research unit members, especially Emna, Fatma, Kaouthar, Afef, Amina, Imene, Riadh, Slim, Ismail, Soumaya, Emna, Lamya, and Afef for the great environment inside our lab. Moreover, I would like to express a deep gratitude to Prof. Mohamed Jmaiel, the head of ReDCAD, for his exceptional support and encouragement. He has always made me feel like I am one of his own students and does not hesitate to provide help and advices. I am really indebted to him.

Many thanks goes to my friends Boudour, Manel, and Olfa for their support and encouragement during the difficult moments of this thesis.

I would like to express my appreciation to Maissa Ben Jamâa, Denis do Rosário, and Wala Meftah for their implementation efforts that contributed significantly to the results presented in thesis. Their efforts were made in the context of their Masters. I must confess that I was lucky to work with brilliant students like them. Special thanks goes to Maissa Ben Jamâa not only for her valuable contribution, but also for her exceptional human quality.

Finally, I would like to convey my sincere and deep gratitude to my parents Mohamed and Fatma, my two brothers Rami and Hamdi, my husband Riadh, and my mother in law Nabiha. Without their patience, encouragement, and support, I could not have finished this thesis.

This thesis was performed within ReDCAD research unit at ENIS (Ecole Nationale d'Ingénieurs de Sfax, University of Sfax), in collaboration with (1) CISTER Research Unit at ISEP/IPP (Instituto Superior de Engenharia do Porto/ Instituto Politécnico do Porto), (2) COINS Research Unit at CCIS/IMAMU (College of Computer and Information Sciences / Al-Imam Mohamed bin Saud University), and (3) Prince Research Unit at the University of Sousse; and it was partially funded by the Portuguese Science Foundation under the CISTER Research Unit (FCT UI 608), by the CONET European Network of Excellence, and by the EMMON European project.

# *Abstract*

Stringent cost and energy constraints in large-scale wireless sensor networks (WSNs) impose the use of low-cost radio transceivers that transmit low-power signals. This fact makes radiated signals very prone to noise, interference, and multi-path distortion. Consequently, radio links in WSNs are extremely unreliable, which affects the network performance. This raised the need for link quality estimation as a fundamental building block for network protocols and mechanisms (e.g., medium-access control (MAC), routing, mobility management, and topology control), in order to mitigate link unreliability.

Link quality estimation in WSNs is a challenging problem due to the lossy and dynamic behavior of the links. This dissertation addresses the design, evaluation and experimentation of new methodologies for more reliable link quality estimation in WSNs. We first present a comprehensive overview of fundamental concepts related to link quality estimation. For instance, we analyse the empirical characterization of low-power links. We also identify the main requirements and building blocs for link quality estimation and give a taxonomy and classification of existing link quality estimators (LQEs) in WSNs. In doing so, we realize that none of existing LQEs has been thoroughly evaluated. Hence, we conduct an extensive comparative performance study of most well-known LQEs. The evaluation methodology consists in analyzing their statistical properties independently of any external factor, such as collisions and routing. Our study is carried out using TOSSIM 2 simulation as well as real experimentation with RadiaLE, a testbed we designed and implemented to automate the experimental evaluation of LQEs. Both experimental and simulation results demonstrate that existing LQEs are not sufficiently reliable. This is due to the fact that they only assess a single link aspect (e.g. reception ratio, packet retransmissions count) thus providing a partial link characterization. We then propose F-LQE (Fuzzy Link Quality Estimator), a new estimator that overcomes the limitations of existing LQEs by considering important link properties that impact link quality, namely delivery, asymmetry, stability, and channel quality. We resort to fuzzy logic to express and combine these link properties. A thorough performance analysis, based on both simulation and real measurements, shows that F-LQE is more reliable and stable than existing estimators. To demonstrate the applicability and usefulness of F-LQE, we assess its impact on the performance of collection tree routing — specifically the CTP (Collection Tree Protocol). We first design FLQE-RM, a routing metric based on F-LQE. Then, we compare its impact on the performance of CTP with that of representative routing metrics. Experimental results show that FLQE-RM outperforms these routing metrics: It improves the end-to-end-delivery, reduces the number of packet retransmissions, reduces the hop count, and improves the topology stability.



---

## Contents

---

<b>Introduction</b>	<b>1</b>
<b>1 Link Quality Estimation in Wireless Sensor Networks</b>	<b>7</b>
1.1 Introduction	7
1.2 Radio communication hardware	7
1.3 Overview of low-power links	9
1.3.1 Spatial characteristics	10
1.3.2 Temporal characteristics	13
1.3.3 Link asymmetry	16
1.3.4 Interference	17
1.3.4.1 External interference	18
1.3.4.2 Internal interference	19
1.3.5 Implication on communication protocols	20
1.4 Fundamentals of link quality estimation	20
1.4.1 Steps for link quality estimation	21
1.4.1.1 Link monitoring	21
1.4.1.2 Link measurements	22
1.4.1.3 Metric evaluation	23
1.4.2 Requirements for link quality estimation	23
1.5 A Survey on link quality estimators	24
1.5.1 Hardware-based LQEs	25
1.5.2 Software-based LQEs	28
1.5.2.1 PRR-based	28
1.5.2.2 RNP-based	29
1.5.2.3 Score-based	31
1.6 Conclusion	33
<b>2 Performance Evaluation of Link Quality Estimators</b>	<b>35</b>
2.1 Introduction	35
2.2 Related work	36
2.3 LQEs under evaluation	37
2.4 Evaluation methodology	38



2.4.1	Links establishment . . . . .	39
2.4.2	Link measurements collection . . . . .	40
2.4.3	Data analysis . . . . .	41
2.5	Evaluation platforms . . . . .	41
2.5.1	TOSSIM 2 simulator . . . . .	41
2.5.1.1	Overview of TOSSIM 2 channel model . . . . .	42
2.5.1.2	Advantages and shortcomings of TOSSIM 2 channel model . . . . .	43
2.5.2	RadiaLE experimental testbed . . . . .	44
2.5.2.1	Existing experimental testbeds . . . . .	44
2.5.2.2	Overview of RadiaLE . . . . .	46
2.5.2.2.1	Hardware components . . . . .	47
2.5.2.2.2	Software components . . . . .	47
2.5.2.2.3	Traffic patterns . . . . .	50
2.6	Performance analysis . . . . .	50
2.6.1	Experimental study . . . . .	50
2.6.1.1	Experiments description . . . . .	50
2.6.1.2	Experimental results . . . . .	52
2.6.1.2.1	Reliability . . . . .	54
2.6.1.2.2	Stability . . . . .	55
2.6.2	Simulation study . . . . .	56
2.6.2.1	Simulations description . . . . .	56
2.6.2.2	Simulation results . . . . .	56
2.6.2.2.1	Reliability . . . . .	57
2.6.2.2.2	Stability . . . . .	58
2.6.2.3	TOSSIM 2 realism . . . . .	58
2.7	Summary of the results . . . . .	58
2.8	Conclusion . . . . .	59
<b>3</b>	<b>F-LQE: A Fuzzy Link Quality Estimator for Wireless Sensor Networks</b>	<b>61</b>
3.1	Introduction . . . . .	61
3.2	Related work . . . . .	61
3.3	Fuzzy logic for link quality estimation . . . . .	63
3.4	Overview of F-LQE . . . . .	64
3.4.1	Link quality metrics . . . . .	64
3.4.1.1	Packet delivery . . . . .	65
3.4.1.2	Stability . . . . .	65
3.4.1.3	Asymmetry . . . . .	66
3.4.1.4	Channel quality . . . . .	68
3.4.2	Combination of link quality metrics . . . . .	68
3.4.2.1	Fuzzy rule . . . . .	68
3.4.2.2	Membership functions . . . . .	68
3.4.2.3	F-LQE expression . . . . .	71
3.5	Performance analysis . . . . .	72
3.5.1	Methodology . . . . .	72
3.5.2	Experimental results . . . . .	72
3.5.2.1	Reliability . . . . .	72
3.5.2.1.1	Temporal behavior . . . . .	72
3.5.2.1.2	Link quality estimates distribution . . . . .	74

3.5.2.2	Stability . . . . .	76
3.5.3	Simulation results . . . . .	76
3.5.3.1	Reliability . . . . .	76
3.5.3.1.1	Temporal behavior . . . . .	77
3.5.3.1.2	Link quality estimates distribution . . . . .	78
3.5.3.2	Stability . . . . .	79
3.6	Conclusion . . . . .	79
<b>4</b>	<b>Boosting Collection Tree Routing Protocols Through Fuzzy Link Quality Estimation</b>	<b>81</b>
4.1	Introduction . . . . .	81
4.2	Related work . . . . .	82
4.2.1	Collection tree routing protocols . . . . .	82
4.2.2	Link quality based routing metrics . . . . .	82
4.3	Overview of CTP (Collection Tree Protocol) . . . . .	83
4.3.1	Link estimator . . . . .	84
4.3.2	Routing engine . . . . .	85
4.3.3	Forwarding engine . . . . .	85
4.4	Towards an efficient F-LQE based Routing Metric (FLQE-RM) for tree routing . . . . .	85
4.4.1	Design requirements . . . . .	86
4.4.2	Potential solutions . . . . .	86
4.4.3	Integration of potential solutions in CTP . . . . .	87
4.4.3.1	Beacon-driven link quality estimation . . . . .	88
4.4.3.2	LQI for channel quality assessment . . . . .	88
4.4.3.3	Link direction . . . . .	88
4.4.3.4	Parent update . . . . .	89
4.4.3.5	Routing engine . . . . .	89
4.4.4	Simulation study of the potential solutions . . . . .	89
4.4.4.1	Evaluation methodology . . . . .	89
4.4.4.2	Simulation description . . . . .	91
4.4.4.3	Simulation results . . . . .	91
4.5	Experimental performance evaluation of FLQE-RM . . . . .	93
4.5.1	Evaluation methodology . . . . .	93
4.5.2	Experiments description . . . . .	94
4.5.3	Experimental results . . . . .	94
4.5.3.1	Performance for different testbeds . . . . .	94
4.5.3.2	Performance as a function of the traffic load . . . . .	96
4.5.3.3	Performance as a function of the number of source nodes . . . . .	98
4.5.3.4	Performance as a function of the topology . . . . .	99
4.5.3.5	Results review . . . . .	99
4.5.3.6	Memory footprint and computation complexity . . . . .	101
4.5.3.7	Discussion . . . . .	101
4.6	Conclusion . . . . .	102
	<b>Conclusion</b>	<b>103</b>



---

## List of Figures

---

1.1	TMote antenna details . . . . .	9
1.2	Spatial characteristics: PRR as a function of distance between receiver node and sender node. . . . .	10
1.3	Radio irregularity and interference range [1]. Node B cannot communicate with node C as it is out of its communication range. However, B prevents C to communicate with A due to the interference between the signal sent by B and that sent by A. . . . .	12
1.4	Contour of PRR from a central node: anisotropy of link quality [2].	12
1.5	Links with very low or very high average PRRs are more stable than links with moderate average PRRs. Outdoor environment, using TelosB sensor motes and -25 dBm as output power (using RadiaLE testbed [3]). . . . .	14
1.6	The PRR/SNR curve. For <i>SNR</i> greater than 8 dBm, the <i>PRR</i> is equal to 100%, and for <i>SNR</i> less than 1 dBm, the <i>PRR</i> is less than 25%. In between, a small variation in the <i>SNR</i> can cause a big difference in the <i>PRR</i> ; links are typically in the transitional region. Outdoor environment, using TelosB sensor motes and -25 dBm as output power (using the RadiaLE testbed [3]). . . . .	15
1.7	IEEE 802.15.1 (Bluetooth), IEEE 802.11b, and IEEE 802.15.4 spectrum usage [4]. . . . .	17
1.8	Steps for Link Quality Estimation. . . . .	21
1.9	Taxonomy of LQEs. . . . .	25
1.10	PRR vs RSSI curve. . . . .	25
2.1	Nodes distribution forming a radial topology . . . . .	40
2.2	Illustration of TOSSIM 2 channel model reliability: the three reception regions . . . . .	43
2.3	Testbed Hardware and Software architectures . . . . .	46
2.4	ExpCtrApp Java application main functionalities . . . . .	48
2.5	DataAnlApp Matlab application main functionalities . . . . .	49

2.6	Interaction between mote $N_1$ , mote $N_i$ and the PC, allowing for a Bursty or Synchronized traffic exchange between the two Motes. When $N_1$ and $N_i$ finish their transmission, the PC triggers a new Bursty or Synchronized traffic exchange between $N_1$ and $N_{i+1}$ .	51
2.7	Depolyment of the Radial topology at an outdoor environment	52
2.8	Empirical CDFs of LQEs, based on all the links in the network (Default Setting).	52
2.9	Scatter plot of each LQE according to distance in meters (Default Setting). Note we subtract 1 from ETX, to account only for the retransmitted packets.	53
2.10	Temporal behaviour of LQEs when faced with links with different qualities (Default Setting)	54
2.11	Stability of LQEs, for different network settings.	54
2.12	Empirical CDFs of LQEs, based on all the links in the simulated network, and observed by Tossim 2 simulation.	57
2.13	Temporal behaviour of LQEs when faced with links with different qualities, observed by Tossim 2 simulation	57
2.14	Stability of LQEs, observed by Tossim 2 simulation.	58
3.1	Algorithm of SF computation. $P$ is the number of computed <i>PRRs</i> , initially $P = 0$ and <i>PRR_vect</i> is an array that contains a set of measured <i>PRRs</i> .	66
3.2	Hardware-based metrics as a function of PRR. These curves are obtained from experimentation with RadiaLE (refer to (refer to Table 2.2 — Default Setting)).	67
3.3	Definition of membership functions	69
3.4	SF threshold determination based on curves obtained from real experimentation with RadiaLE (refer to Table 2.2 — Default Setting)).	69
3.5	PRR/SNR curve obtained from real experimentation with RadiaLE (refer to Table 2.2 — Default Setting)). For ASNR greater than 8dBm, the PRR is equal to 100%, and for ASNR less than 1 dBm, the PRR is less than 25%. In between, a small variation in the ASNR can cause a big difference in the PRR; links are typically in the transitional region.	70
3.6	PRR/SNR curve obtained from simulation with TOSSIM 2 (indoor environment[5]). For ASNR greater than 9dBm, the PRR is equal to 100%, and for ASNR less than 5 dBm, the PRR is less than 25%. In between, a small variation in the ASNR can cause a big difference in the PRR; links are typically in the transitional region.	70
3.7	Temporal behaviour of LQEs when faced with links with different qualities (Default Setting)	73
3.8	Scatter plot of each LQE according to distance (Default Setting).	74
3.9	Empirical CDFs of LQEs (Default Setting).	75
3.10	Sensitivity to transient fluctuation in link quality, for different network settings.	75
3.11	Temporal behaviour of link quality estimators when faced to links with different qualities, observed by Tossim 2 simulation.	76

3.12	Scatter plot of each link quality estimator according to distance, observed by Tossim 2 simulation. . . . .	77
3.13	Empirical CDFs of link quality estimators, observed by Tossim 2 simulation. . . . .	78
3.14	Sensitivity to transient fluctuation in link quality, observed by Tossim 2 simulation. . . . .	79
4.1	Distribution pattern of 80 sensor nodes and a single sink node, in a non-uniform grid topology. . . . .	90
4.2	Impact of routing metrics on CTP performance (Tossim 2 simulation results) . . . . .	92
4.3	Impact of FLQE-RM, four-bit, and ETX on CTP performance, using Indriya testbed (refer to Table 4.2 — Set 1). . . . .	95
4.4	Impact of FLQE-RM, four-bit and ETX, on CTP performance, using MoteLab testbed (refer to Table 4.2 — Set 1). . . . .	96
4.5	Performance as a function of the traffic load (refer to Table 4.2 — Set 2). . . . .	97
4.6	Performance as a function of the number of source nodes (refer to Table 4.2 — Set 3). . . . .	98
4.7	Performance as a function of the topology (refer to Table 4.2 — Set 4). . . . .	99



---

## List of Tables

---

1.1	Characteristics of typical WSN radios. . . . .	8
1.2	Comparison and classification of LQEs. . . . .	26
2.1	Characteristics of link quality estimators under evaluation . . . .	39
2.2	Experiment scenarios. Burst(N, IPI, P) and Synch(W, IPI); N: Number of packets per burst, IPI: inter-packets interval, P: number of bursts, W: total number of packets. . . . .	53
2.3	Comparison of considered LQEs . . . . .	59
4.1	Characteristics of F-LQE based routing metrics . . . . .	88
4.2	Experiment sets. . . . .	94
4.3	Overall results for Indriya experiments, where 121 nodes are data sources and the node with ID equal to 1 is selected as root, aver- aged over all considered traffic loads. . . . .	100
4.4	Overall results for Indriya experiments, where the traffic load is fixed to 0.125 pkt/s and the node with ID equal to 1 is selected as root, averaged over all considered number of source nodes. . .	100
4.5	Overall results for Indriya experiments, where 121 nodes are data sources and the traffic load is fixed to 0.125 pkt/s, averaged over all considered Root ID assignments. . . . .	100
4.6	Memory footprint of four-bit, ETX, and FLQE-RM. . . . .	101



### Research context and motivations

A Wireless Sensor Network (WSN) is a set of sensor devices, each equipped with a low-power processing unit, a wireless communication interface, one or more sensors to measure properties of the environment and eventually an actuator to act on the network. When deployed in large quantities in a sensor field, sensor devices can automatically organize themselves to form a multi-hop Ad Hoc network to communicate with each other and with one or more sink nodes.

The design and deployment of sensor devices into a network imposes new resource constraints in comparison with traditional wireless networks. These constraints take various forms such as energy, size, CPU and memory. Indeed, sensor nodes are intended to be deployed in large scale in a monitored environment. The large-scale factor commonly found in WSN applications imposes the need for low-cost and reduced size sensor nodes. Further, sensor nodes are likely to be battery powered, and it is often difficult to change or recharge batteries for these nodes. Hence, energy requirements impose low communication rates and ranges and low duty cycles. These limitations in energy, size and cost lead to reduced CPU and memory resources.

Stringent cost and energy constraints in large-scale WSNs impose the use of low-cost radio transceivers that transmit low-power signals (typically, 0 dBm as maximum power). This fact makes radiated signals very prone to noise, interference, and multi-path distortion. Furthermore, these radio transceivers rely on antennas with non-ideal radiation patterns, which leads to anisotropic connectivity. Consequently, radio links in WSNs are extremely unreliable and often unpredictable. They experience quality fluctuation over time [6, 4] and space [7, 8], and their connectivity is typically asymmetric [7, 9]. The unreliability of WSN links greatly affects the network performance. This raised the need for link quality estimation as a fundamental building block for the design of network protocols and mechanisms, including medium-access control (MAC), routing, mobility management, and topology control.

Link quality estimation enables network protocols to mitigate and to overcome link unreliability. For instance, link quality estimation is instrumental

for routing protocols to maintain correct network operation [10, 11, 12, 13, 14, 15, 16, 17]. Delivering data over high quality links (i.) improves the network delivery by limiting packet loss and (ii.) maximizes its lifetime by minimizing the number of retransmissions, and avoiding route reselection triggered by link failures. Link quality estimation also plays a crucial role for topology-control mechanisms to maintain the stability of the topology [8, 18, 9]. High quality links are long-lived, therefore, efficient topology control mechanisms rely on the selection of high quality links in order to maintain robust network connectivity for long periods, thus avoiding unwanted transient topology breakdowns.

In this context, this thesis addresses the design, evaluation and experimentation of new methodologies for more reliable link quality estimation in WSNs.

## Problem statement

### Problem 1

Basically, link quality estimation consists in evaluating a metric — a mathematical expression, within an estimation window  $w$  (e.g., at each  $w$  seconds, or based on  $w$  received/sent packets). We refer to this metric as Link Quality Estimator (LQE). The accuracy of LQEs greatly impacts the efficiency of network protocols. For instance, many routing protocols, rely on link quality estimation to select high quality routes for communication. The more accurate the LQE is, the more correct the decision made by routing protocols in selecting such routes. This is just one example on how important it is to assess the performance of the LQE before integrating it into a particular network protocol.

Unfortunately, existing LQEs have not been properly evaluated. One of the reasons is the impossibility, or at least the difficulty, to provide a quantitative evaluation of the accuracy of LQEs. In fact, in link quality estimation there is lack of a real metric of reference based on which the accuracy of the estimators can be assessed. In classical estimation theory an estimated process is typically compared to a real known process using a certain statistical tool (e.g. least mean square error or regression analysis). However, such comparison is not possible in link quality estimation, since: (i.) there is no metric that is considered as the “real” one to represent link quality; and (ii.) link quality is represented by quantities with different natures, since some estimators are based on the computation of the packet reception ratio (PRR), some others are based on packet retransmission count (i.e. RNP) and some others are hybrid and more complex. Hence, the first question addressed in this thesis is the following:

*Is it possible to design a benchmark for a thorough performance evaluation of LQEs?*

This question raises two main challenges: The first challenge is to define the performance criteria for the assessment of LQEs. Particularly, giving that the accuracy of LQEs cannot be assessed quantitatively due to the lack of an objective metric, we aim at introducing a solution for a qualitative assessment of the accuracy. The second challenge is to design benchmark scenarios allowing for the computation of LQEs regardless their nature (e.g., sender-side vs receiver-side, hardware-based vs software-based, simple vs composite, etc.).

These scenarios define (i.) how to establish a rich set of links exhibiting different qualities and (ii.) what are the convenient traffic patterns to be exchanged over these links enabling LQEs computation through packet-statistics collection.

## Problem 2

Existing LQEs can be classified as either hardware-based or software-based. Hardware-based LQEs such as the Received Signal Strength Indicator (RSSI), are directly read from the radio transceiver, i.e., they do not require any additional computation. Most software-based LQEs enable to either count or approximate the packet reception ratio or the average number of packet transmissions/ retransmissions.

Existing LQEs, hardware or software based, do not seem to be accurate because they can only assess a particular link property and thus provide a partial characterization of the link. For example, the Packet Reception Ratio (PRR) can only capture link delivery property. It ignores other important properties that impact the link quality, such as asymmetry or stability. A link may have a good PRR and thus appears as a “good quality link”, whereas the link involves several MAC retransmissions due to its high asymmetry (some acknowledgements are not delivered). Hence, the link state provided by PRR, i.e., “good quality link”, is not correct. The link has a good delivery but it has also high asymmetry, so that overall, it is not a good quality link. This is just a simple example to illustrate that accurate link quality estimation requires the combination of several and appropriate link metrics rather than considering a single link metric. Hence, the second question addressed in this thesis is the following:

*Is it possible to design a LQE that provides a holistic characterization of low-power links while taking into account different aspects/properties that impact their quality e.g., asymmetry, stability, channel quality?*

We believe that such holistic link quality estimation can be achieved through a composite LQE that combines several link metrics. Each metric captures a particular link property. However, two main challenges should be addressed: The first challenge is how to identify link properties and derive appropriate metrics for their assessment. A vast array of research works tackled the empirical characterization of low-power links through real-world measurements with different platforms, under varying experimental conditions, assumptions, and scenarios (e.g., [6, 4, 8, 2, 1, 19, 20, 21]). These works presented radically different (and sometimes contradicting) results. Therefore, there is the need to deeply analyze their outcomes, and identify the most relevant key observations. Such observations would be helpful to determine the most important properties that impact the quality of low-power links. The second challenge is how to combine selected metrics, given that they have not necessarily the same nature. This challenge should be carefully addressed as a LQE can involve appropriate link metrics but the resulting link quality estimate is not sound due to the inadequacy of the combination technique. For example, Rondinone et al. [22] suggest combining PRR and RSSI metrics through the multiplication of PRR by the normalized average RSSI. Another alternative would be the combination through a weighted sum.

## Research contributions and Structure

The main research contributions of this thesis are as follow:

**A survey of link quality estimation in low-power WSNs** (supported by [23] and reflected in Chapter 1). This research work summarizes relevant lessons learned throughout a several year experience on link quality estimation in WSNs. It represents the first attempt to analyze and understand the fundamental concepts related to link quality estimation. In the first part, we start with an overview of the most common WSN radio technology. Basically, we show that sensor nodes typically employ inexpensive low-power radio transceivers. This fact, together with the harsh characteristics of the physical environment turn the underlying links unpredictable and experience spatiotemporal variations and asymmetry. Then, we synthesize the vast array of empirical studies on low-power links into a set of high-level observations. Such observations are useful for the design of efficient LQEs as well as other mechanisms at higher-layers (e.g., node deployment, routing, mobility management), as they heavily depend on the underlying radio links. In the second part, we address the statistical estimation of low-power links, which is the fundamental part of this research work. In this part, we first identify the main requirements and the building blocks in link quality estimation. Then, we present a taxonomy and classification of existing LQEs. This part shows that research on link quality estimation is challenging and several issues are still unexplored. Especially, although several link quality estimators are available in the literature, none of them has been thoroughly evaluated.

**The design and implementation of RadiaLE: a framework that automates the experimental evaluation, design and optimization of LQEs** (supported by [3] and reflected in Chapter 2 — Section 2.5.2.2). RadiaLE is available as open-source at [24]. It comprises the hardware components of the WSN testbed and a software tool for setting-up and controlling the experiments. RadiaLE is more than an experimental testbed. It stands for a methodology that allows (i) to properly set different types of links and different types of traffic, (ii) to collect rich link measurements, and (iii) to validate LQEs using a holistic and unified approach. RadiaLE presents several advantages compared to existing testbeds such as providing abstractions to the implementation details and the flexibility and completeness of the collected database.

**A comparative performance study of most well-known LQEs, using both simulation and experimentation** (supported by [25] and [3], and reflected in Chapter 2). Simulations were carried out using TOSSIM 2 simulator, while real experiments were conducted using our testbed RadiaLE. We are the first to produce such comparative study. We start by discussing related work and describing LQEs under evaluation. Then, we present our methodology for the performance evaluation of LQEs. Shortly, our methodology consists in analyzing the statistical properties of LQEs, independently of any external factor, such as collisions (each node transmits its data in an exclusive time slot) and routing (a single-hop network). These statistical properties impact the performance of LQEs, in terms of reliability and stability. Then, we present an overview of the considered evaluation platforms, namely TOSSIM 2 for simulations and RadiaLE for real experimentation. Both experimental and simulation results demonstrate that none of the existing LQEs is sufficiently reliable as they

either overestimate or underestimate link quality. This is due to the fact that each LQE is only able to assess a single link aspect (e.g. reception ratio, packet retransmissions count) thus providing a partial link characterization. In our study, we also examined the accuracy of the wireless channel model in TOSSIM 2 by comparing simulation results with experimental results. We showed that TOSSIM 2 channel model seems to be efficient and reliable as it provides a reasonable tradeoff between accuracy and simplicity.

**The design and evaluation of F-LQE, a new LQE based on Fuzzy Logic that overcomes the limitations of existing LQEs** (supported by [26] and reflected in Chapter 3). In contrast to existing LQEs, which only assess one single link property thus providing a partial view on the link, F-LQE considers four link properties (packet delivery, asymmetry level, stability, and channel quality). Link properties are usually imprecisely measured and Fuzzy logic provides a convenient language to express, model, and combine such imprecise knowledge. Thus, F-LQE combines link properties, expressed in linguistic terms (e.g., “good packet delivery”, “low asymmetry”), in a fuzzy rule. The evaluation of the fuzzy rule returns the degree of membership of the link in the fuzzy subset of good quality links, i.e., the goodness level of the link, which is a score between 0 and 1. An extensive performance analysis based on both simulation and real experimentation shows that F-LQE outperforms existing estimators, in terms of reliability and stability.

**Impact of F-LQE on the performance of collection tree routing** (supported by [27] and reflected in Chapter 3). Link quality estimation in WSNs has a fundamental impact on the network performance. In this research work, we demonstrate the applicability and usefulness of F-LQE by assessing its impact on the performance of collection tree routing, — specifically the CTP (Collection Tree Protocol) [12]. The first part of this research work is dedicated for related work and an overview of CTP. In the second part, we design a routing metric based on F-LQE. We first describe design requirements. Then, we propose four potential solutions. Each solution evaluates the path cost based on link F-LQE estimates but using a different expression. Based on extensive simulations, we evaluate the performance of potential solutions by analyzing their impact on the performance of CTP tree routing. Our simulation study allowed us to select the most efficient solution among proposed F-LQE based routing metrics. We call this solution FLQE-RM. Simulation results also show that FLQE-RM establishes and maintain the routing tree better than four-bit, the default routing metric of CTP. In order to validate FLQE-RM metric, we extended the simulation study to a large scale experimental study, using real WSN platforms. In this experimental study, we compare the impact of FLQE-RM on CTP performance with that of four-bit and ETX, which are two representative routing metrics in WSN community. Experimental results show that our routing metric outperforms four-bit and ETX: It improves the end-to-end-delivery, reduces the number of packet retransmissions, reduces the hop count, and improves the topology stability.

## Main publications supporting this thesis

[M1] Nouha Baccour, Anis Koubâa, Luca Mottola, Marco Zuniga, Habib Youssef, Carlo Boano, and Mário Alves, “Radio Link Quality Estimation in Wireless

Sensor Networks: a Survey”, ACM Transactions on Sensor Networks, volume 8, issue 4, November 2012.

[M2] Nouha Baccour, Anis Koubâa, Maissa Ben Jamâa, Denis do Rosário, Habib Youssef, Mário Alves and Leandro Becker, “RadiaLE: a Framework for Designing and Assessing Link Quality Estimators in Wireless Sensor Networks”, Ad Hoc Networks journal (Elsevier), Volume 9, Issue 7, September 2011.

[M3] Nouha Baccour, Anis Koubâa, Habib Youssef, Maissa Ben Jamâa, Denis do Rosário, Mário Alves and Leandro Becker, “F-LQE: A Fuzzy Link Quality Estimator for Wireless Sensor Networks”, In Proc. of the 7th European Conf. on Wireless Sensor Networks (EWSN 2010). Springer, 240–255.

[M4] Nouha Baccour, Anis Koubâa, Maissa Ben Jamâa, Habib Youssef, Marco Zuniga, and Mário Alves, “A Comparative Simulation Study of Link Quality Estimators in Wireless Sensor Networks”, In Proc. of the 17th IEEE/ACM Int. Symposium on Modelling, Analysis and Simulation of Computer and Telecommunication Systems (MASCOTS '09). IEEE, 301–310.

## Other publications supporting this thesis

[O1] Nouha Baccour, Maissa Ben Jamâa, Denis do Rosário, Anis Koubâa, Habib Youssef, Mário Alves and Leandro B. Becker, “A TestBed for the Evaluation of Link Quality Estimators in Wireless Sensor Networks”, In Proc. of the 8th ACS/IEEE International Conference on Computer Systems and Applications (AICCSA 2010). IEEE, 1-8.

[O2] Nouha Baccour, Maissa Ben Jamâa, Denis do Rosário, Anis Koubâa, Mário Alves, Leandro B. Becker, Habib Youssef, and Hossein Fotouhi. “Demo abstract: RadiaLE: a framework for benchmarking link quality estimators”, The 7th European Conference on Wireless Sensor Networks (EWSN 2010), Springer.

[O3] Maissa Ben Jamâa, Nouha Baccour, Anis Koubâa, Denis do Rosário, Mário Alves, Leandro Becker, Habib Youssef, and Mohamed Jmaiel, “Demo abstract: A TestBed for the evaluation of Link Quality Estimators in WSNs”, The First International School on Cyber-Physical and Sensor Networks (SensorNets 2009). (Best Demo Award)

[O4] Nouha Baccour, Anis Koubâa, Habib Youssef, and Mário Alves. “Poster abstract: Simulation analysis and validation of a Fuzzy Link Quality Estimator”, The First International School on Cyber-Physical and Sensor Networks (SensorNets 2009).

[O5] Nouha Baccour, Anis Koubâa, Wala Mefteh, Maissa Ben Jamâa, Habib Youssef, and Mário Alves, “Boosting Collection-Tree Routing Protocols Through Enhanced Link Quality Estimation”, Technical Report (available at request)

[O6] Nouha Baccour et al., “Radio Link Quality Estimation in WSNs and Co-operating Objects”, Springer Booklet, estimated publication date: late 2012.

# CHAPTER 1

---

## Link Quality Estimation in Wireless Sensor Networks

---

### 1.1 Introduction

Link quality estimation has been attracting a lot of attention in the WSN community as it emerges as a fundamental building block for several protocols and mechanisms such as MAC, routing, mobility management and localization. The design of effective link quality estimation mechanisms requires a deep and clear understanding of link characteristics in order to identify the aspects that reflect its quality.

Empirical studies have shown that WSN links — also referred to low-power links, are extremely unreliable: link quality fluctuations over time [6, 4] as well as space [7, 8, 28, 18], the prevalence of intermediate-quality links [29] and the asymmetric connectivity [7, 9]. This unreliability is mainly due to the low-cost and low-power radio transceivers typically employed in WSNs. These radio transceivers transmit low-power signals, which makes radiated signals more prone to noise, interference and multi-path distortion. Furthermore, these transceivers rely on antennas with non-ideal radiation patterns, which leads to anisotropic behaviour.

This chapter provides a thorough overview of low-power links starting from their empirical characterization, arriving to their statistical estimation. An overview of the most common WSN radio transceivers is also presented as they represent a major cause of low-power links unreliability. Further, this chapter provides a global taxonomy and classification of the existing Link Quality Estimators (LQEs).

### 1.2 Radio communication hardware

As link quality strongly depends on the radio hardware platform, it is important to survey the characteristics of radios typically employed in WSN nodes. These characteristics are summarized in Table 1.1. To tackle the energy issue, early

hardware platforms such as ChipCon CC1000 and RFM TR1000, leveraged radio chips operating in sub-GHz frequencies. These transceivers offer low power consumption in both transmission and receive modes. On the other hand, the low data rate prevented using these devices in scenarios different from low-rate data collection.

Model	Frequency	Max Data Rate	Modulation	TX Current	RX Current	TX Power
CC1000	3000-1000 Mhz	76.8 kbps	2-FSK	18.5 mA	9.6 mA	10 dBm
nRF903	433 or 915 Mhz	76.8 kbps	GFSK	19.5 mA	22.5 mA	10 dBm
TR1000	916 Mhz	115.1 kbps	OOK/ASK	12 mA	3.8 mA	0 dBm
CC2420	2.4 Ghz	250 kbps	DSSS/O-QPSK	17.4 mA	19.7 mA	0 dBm
CC2500	2.4 Ghz	512 kbps	2-FSK	12.8 mA	21.6 mA	1 dBm
PH2401	2.4 Ghz	1 mbps	GFSK	< 20 mA	< 20 mA	2 dBm

Table 1.1: Characteristics of typical WSN radios.

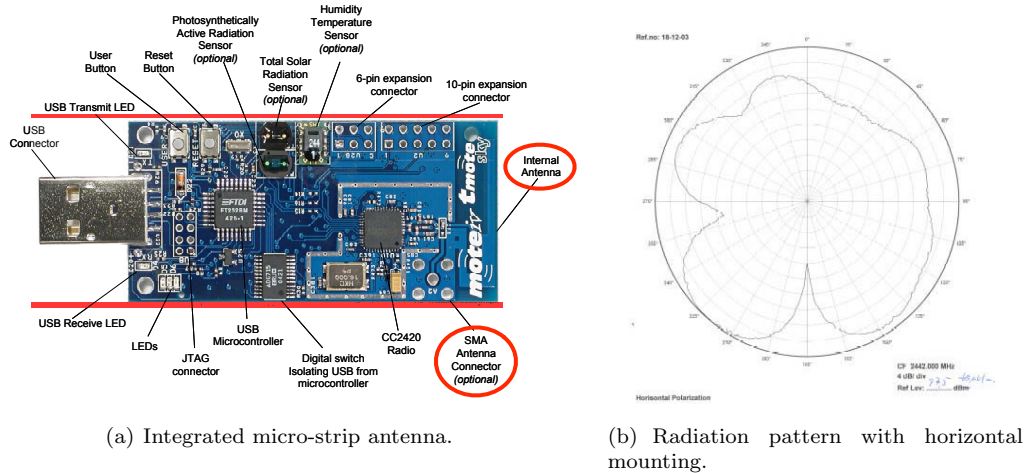
The need for higher data rate motivated the design of radios working in the 2.4 GHz ISM band, such as the well-known ChipCon's CC2400 and CC2500 families. Compliance to IEEE 802.15.4 also fostered a wider adoption of these radio chips, which are commonly found in several current WSN platforms. The tendency for high data rate is brought to an extreme when Bluetooth or WiFi chips are used. These are often found in hybrid configurations where a high-data rate radio is coupled to a low-power one. For instance, the BTnode [30] platform uses a Bluetooth-compliant device next to a CC1000 chip. Such design allows greater flexibility and alternative uses of the WSN devices, e.g., as passive sniffers of ongoing traffic for debugging purposes [31].

The radio hardware platform used often represents one of the main causes of low-power links unreliability. First, sensor devices are often shipped with low-gain antennas integrated in the board. For instance, in the widespread TMote/TelosB devices (Figure 1.1(a)) [32], the antenna is integrated in the PCB (Printed Circuit Board), and the actual radiation pattern is irregular (Figure 1.1(b)), although designed to be omni-directional. Such irregularity stems from several factors, e.g., the presence of the node circuitry. These aspects complicate the operation of MAC and routing protocols, which are traditionally based on the assumption of uniform communication ranges and symmetric links. A common design choice in real-world deployments is the replacement of the standard antenna [33], as it brings increased communication range and higher reliability without incurring extra energy costs. For instance, antennas of up to 8.5 dBi were used in harsh environments by exploiting the on-board SMA connectors [34]. Directional antennas, which are able to direct the transmission power in given directions, were also proposed. However, they lack flexibility in freely reconfiguring the network topology and node locations [35].

Second, real-world deployments showed how the performance of popular radio transceivers have a strong dependency on environmental factors such as temperature [36, 37], as well as how higher transmission frequencies tend to be more susceptible to humidity [38]. These factors drastically impact the quality of WSN links, particularly the ones deployed outdoors.

Third, radio hardware inaccuracy creates asymmetry in link connectivity, i.e., the quality of the link in one direction is different from that in the other direction. In fact, nodes neither have the same effective transmission power





(a) Integrated micro-strip antenna.

(b) Radiation pattern with horizontal mounting.

Figure 1.1: TMote antenna details

nor the same noise floor or receiver sensitivity. This discrepancy in terms of hardware calibration leads to link asymmetry [8, 18, 39, 40].

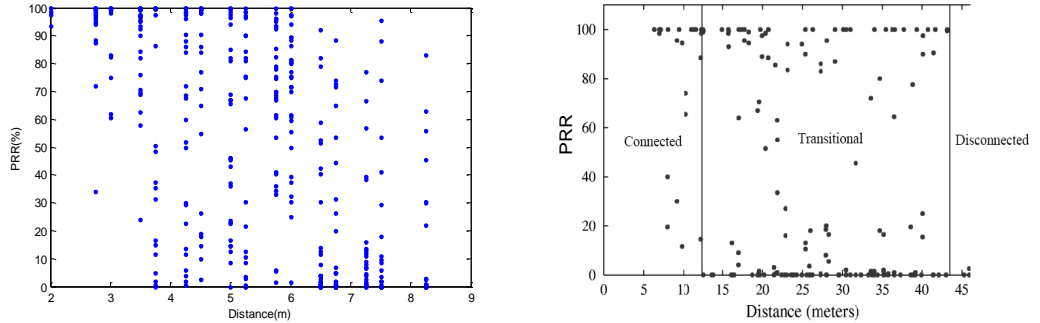
### 1.3 Overview of low-power links

The propagation of radio signals is affected by several factors that contribute to link quality degradation. Three factors include (i.) the multi-path propagation effect, which depends on the environment, (ii.) the interference, which results from concurrent transmissions within the current wireless network or between cohabiting wireless networks and other electromagnetic sources; and (iii.) hardware transceivers, which may distort sent and received signals due to their internal noise. In WSNs, these radio transceivers transmit low-power signals, which makes radiated signals more prone to noise, interference and multi-path distortion.

Several research efforts have been devoted to an empirical characterization of low-power links. These studies have been carried out using (i.) different WSN platforms having different radio chips (TR1000, CC1000, CC2420, etc), (ii.) different operational environments (indoor, outdoor) and (iii.) different experimental settings (e.g., traffic load, channel). Therefore, they presented radically different (and sometimes contradicting) results. Nonetheless, these studies commonly argued that low-power links experience complex and dynamic behavior.

Although several low-power link characteristics are shared with those of traditional wireless networks, such as Ad Hoc, mesh, and cellular networks, the extent of these characteristics is more significant with low-power links (e.g. a large transitional region or extremely dynamic links) and makes them even more unreliable. This might be an artifact of the communication hardware used in WSNs [4, 20].

In this section, we synthesize the vast array of empirical studies on low-power links into a set of *high-level observations*. We classify these observations into



(a) The transitional region, for an outdoor environment, using TelosB sensor motes and -25 dBm as output power (using the RadiaLE testbed [3]).

(b) The three reception regions, for an outdoor Habitat environment, using Mica 2 sensor motes and -10 dBm as output power [18].

Figure 1.2: Spatial characteristics: PRR as a function of distance between receiver node and sender node.

spatial and temporal characteristics, link asymmetry, and interference. Such observations are helpful not only to design efficient Link Quality Estimators (LQEs) that take into account the most important aspects that affect link quality, but also to design efficient network protocols that deal with links unreliability. Beforehand, we briefly present a set of basic metrics that were examined by previous empirical studies to capture low-power link characteristics:

- **PRR** (Packet Reception Ratio)—sometimes referred to as PSR (Packet Success Ratio). It is computed as the ratio of the number of successfully received packets to the number of transmitted packets. A similar metric to the PRR is the PER (Packet Error Ratio), which is  $1 - PRR$ .
- **RSSI** (Received Signal Strength Indicator). Most radio transceivers (e.g., the CC2420) provide a *RSSI register*. This register provides the signal strength of the received packet. When there are no transmissions, the register gives the noise floor.
- **SNR** (Signal to Noise Ratio). It is typically given by the difference in decibel between the pure (i.e., without noise) received signal strength and the noise floor.
- **LQI** (Link Quality Indicator). It is proposed in the IEEE 802.15 standard [41], but its evaluation is vendor-specific. For the CC2420 [42], which is the most widespread radio, LQI is measured based on the first eight symbols of the received packet as a score ranging from 50 to 110 (higher values are better).

### 1.3.1 Spatial characteristics

It was demonstrated in several work that the transmission range is not isotropic (i.e., a circular shape), where packets are received only within a certain distance from the sender [43]. In fact, the transmission range is defined by three

regions; each with an irregular shape, dynamic bounds (changing over the time), and specific features [8, 28, 18, 29]. These regions are: *(i.)* connected region, where links are often of good quality, stable, and symmetric, *(ii.)* transitional region, where links are of intermediate quality (in long-term assessment), unstable, not correlated with distance, and often asymmetric, and *(iii.)* disconnected region, where links have poor quality and are inadequate for communication. Particularly, the transitional region was subject of several empirical studies because links within this region are extremely unreliable and even unpredictable [4, 8, 28, 18, 29]. These intermediate quality links, referred also as *intermediate links*, are commonly defined as links having an average PRR between 10% and 90%.

*Observation 1: Link quality is not correlated with distance, especially in the transitional region.* To observe the transitional region, most empirical studies conducted measurements of the PRR at different distances from the sender. Figure 1.2(b) is an illustration of the three communication regions through PRR measurements. This figure shows that link quality is *not correlated with distance*, especially in the transitional region. Indeed, two receivers placed at the same distance from the sender can have different PRRs, and a receiver that is farther from the sender can have higher PRR than another receiver nearer to the sender. This observation can be clearly understood from Figure 1.2(a).

*Observation 2: The extent of the transitional region depends on (i.) the environment (e.g., outdoor, indoor, presence of obstacles), and (ii.) the radio hardware characteristics (e.g., the transmission power, the modulation schema, the radio chip) [40].* However, the quantification of this extent by empirical studies shows contradicting observations. Measurements of PRR according to distance, for different environments, radios, and power settings were carried out. In [18], Cerpa et al. performed measurements in indoor (Office) and outdoor (Habitat) environments using Mica 1 and Mica 2 platforms and different power levels, namely -10 dBm, -6 dBm and 1 dBm. They found that the width of the transitional region is significant, ranging from 50% up to 80% of the transmission range. On the other hand, Zhao et al. [8] performed measurements with almost the same settings as of Cerpa et al. [18], but they found the transitional region width smaller, almost one-fifth up to one-third of the transmission range.

*Observation 3: The percentage of intermediate quality links (i.e., located in the transitional region) was found significant in some empirical studies and insignificant in others, which lead to contradicting results.* In [8], Zhao et al. performed experiments with Mica 1 platform in an office building while varying the traffic load. They found that the percentage of intermediate quality links ranges from 35% to 50%. On the other hand, Srinivasan et al. [4] performed experiments with more recent platforms, Micaz and TelosB, in different environments and with varying traffic loads. They found that the number of intermediate links ranges from 5% to 60%. Based on this observation, they claimed that the number of intermediate links observed with recent platforms is lower than that observed with old platforms. This was justified by the fact that recent platforms integrate IEEE 802.15.4 compliant radios (e.g., the CC2420) that have more advanced modulation schemes (e.g., Direct Sequence Spread Spectrum (DSSS)) compared to old platforms. Mottola et al. [44] refuted this

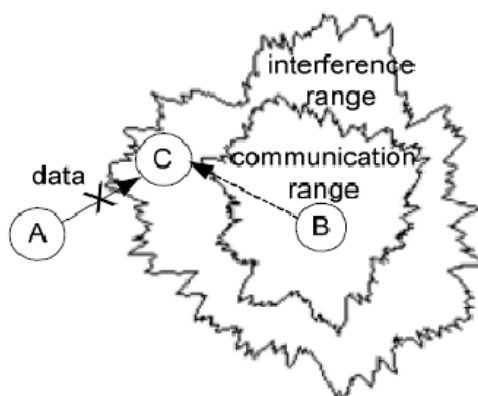


Figure 1.3: Radio irregularity and interference range [1]. Node B cannot communicate with node C as it is out of its communication range. However, B prevents C to communicate with A due to the interference between the signal sent by B and that sent by A.



Figure 1.4: Contour of PRR from a central node: anisotropy of link quality [2].

observation while conducting experiments in road tunnels using nodes having IEEE 802.15.4 compliant radios. They observed a large transitional area in two of their tunnels and found a high number of intermediate quality links due to the constructive/destructive interference. We believe that this aspect remains an open issue and needs to be supported by additional experiments for two reasons. First, intermediate quality links were defined differently, namely “links with PRR less than 50%” in [8] and “links with PRR between 10% and 90%” in [4]. Second, experimental studies that analyzed the percentage of intermediate quality links were based on different network settings (e.g., traffic load, power level, radio type, environment type...) and also different window sizes for PRR calculation, so comparison would not be completely legitimate.

*Observation 4: Link quality is anisotropic.* Empirical studies observed another important spatial characteristic of low-power links often referred as *radio*

*irregularity*, which means that link quality is anisotropic [1, 45, 7, 28, 2]. To demonstrate the existence of radio irregularities, Zhou et al. [7] observed the RSSI and the PRR according to different receiver's directions, but with fixed distance between the transmitter and the receiver. They showed that the radio communication range, assessed by the RSSI, exhibits a non-spherical pattern. They also argued the existence of a non-spherical interference range, located beyond the communication range (refer to Figure 1.3). Within this interference range the receiver cannot interpret correctly the received signal, but this received signal can prevent it from communicating with other transmitters as it causes interference. The existence of the non-spherical radio communication and interference ranges was confirmed by Zhou et al. [45]. They reported that in WSNs, several MAC protocols assume the following: If node B's signal can interfere with node A's signal, preventing A's signal from being received at node C; then node C must be within node B's communication range. Based on experimentation with Mica 2 motes, Zhou et al. showed that this assumption is definitely invalid, since node C may be in the interference range of node B and not in its communication range, as illustrated in Figure 1.3. The communication range assessed by the PRR was also shown to be non-spherical or anisotropic [2], as shown in Figure 3.5. A natural reason for radio irregularity is the anisotropic radiation pattern of the antenna due to the fact that antennas do not have the same gain along all propagation directions [7].

*Observation 5: Sensor nodes that are geographically close to each other may have high spatial correlation in PRRs.* Zhao et al.[8] investigated the spatial correlation in PRRs, measured between a source node and different receiver nodes. They observed that receiver nodes that are geographically close to each other and that are located in the transitional region, have higher coefficient of correlation in their PRRs, compared to nearby receiver nodes located in the connected or disconnected regions. Nevertheless, the coefficient of correlation in the transitional region is not that significant — less than 0.7. Srinivasan et al.[46] introduced the  $\kappa$  Factor, a new metric that captures spatial correlation in PRR between links, using the cross-correlation index. The  $\kappa$  Factor was shown to perform better than existing metrics for the measurement of spatial correlation between links.

*Observation 6: The spatial variation of link quality is due to constructive/destructive interference.* Beyond the connected region, the direct signal is weak due to path loss. Multi-path effects can be either *constructive*, i.e., strengthen the direct signal leading to a good quality link, or *destructive*, i.e., interfere with the direct signal [18], and thus be detrimental to link quality. Being constructive or destructive does not depend on the receiver distance or direction. It rather depends on the nature of the physical path between the sender and the receiver (e.g., presence of obstructions) [47, 48].

### 1.3.2 Temporal characteristics

We showed that link quality varies drastically over space. This section explores link quality variation over time.

*Observation 1: Links with very low or very high average PRRs are more*

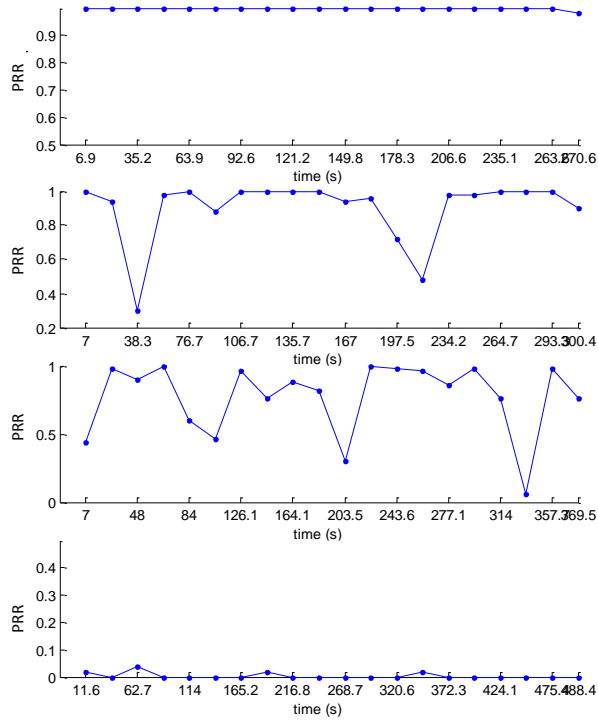


Figure 1.5: Links with very low or very high average PRRs are more stable than links with moderate average PRRs. Outdoor environment, using TelosB sensor motes and -25 dBm as output power (using RadiaLE testbed [3]).

*stable than links with moderate average PRRs.* Several studies [18, 8, 9] claimed that links with very low or very high average PRR, which are mainly located in the connected and disconnected regions respectively, have small variability over time and tend to be stable. In contrast, links with intermediate values of average PRR, which are mainly located in the transitional region, show a very high variability over time, as PRRs vary drastically from 0% to 100% with an average ranging from 20% to 80% [18]. These intermediate links are hence typically unstable. This observation is illustrated in Figure 1.5. The temporal variation of these links can be mitigated by applying an adaptive power control scheme, where transmission power at each node is dynamically adjusted [49].

*Observation 2: Over short time spans, links may experience high temporal correlation in packets reception, which leads to short periods of 0% PRR or 100% PRR.* Srinivasan et al. [4] examined the distribution of PRRs over all links in the test-bed, for different Inter-Packet-Intervals (IPIs). They found that by increasing the IPI, the number of intermediate links increases as well. This finding was justified by the fact that low IPIs correspond to a short-term assessment of the link. In such short-term assessment, most links experience high temporal correlation in packets reception. That means that over these links, packets are either all received or not. Consequently, the measured PRR over most links is either 100% or 0%. For instance, Srinivasan et al. [4] found that for a low

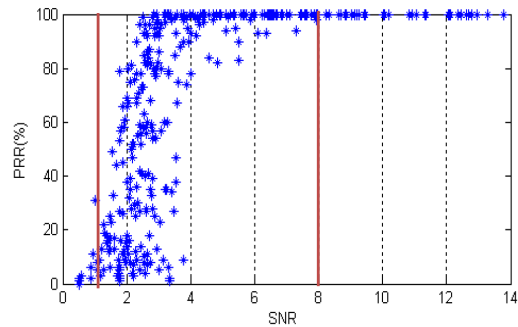


Figure 1.6: The PRR/SNR curve. For  $SNR$  greater than 8 dBm, the  $PRR$  is equal to 100%, and for  $SNR$  less than 1 dBm, the  $PRR$  is less than 25%. In between, a small variation in the  $SNR$  can cause a big difference in the  $PRR$ ; links are typically in the transitional region. Outdoor environment, using TelosB sensor motes and -25 dBm as output power (using the RadiaLE testbed [3]).

IPI equal to 10 milliseconds (PRRs are measured every 2 seconds) 95% of links have either perfect quality (100% PRR) or poor quality (0% PRR), i.e., only 5% of links have intermediate quality. High IPIs corresponds to a long-term assessment of the link. The increase of the IPI leads to the decrease in the temporal correlation in packets reception. That means that links may experience *bursts* (a shift between 0% and 100% PRR) over short periods and the resulting PRR assessed in long-term period is intermediate. This last observation was also made in [6].

Recently, several metrics were introduced for the measurement of link burstiness. Munir et al. [50] define a burst as a period of continuous packet loss. They introduced  $Bmax$ , a metric that computes the maximum burst length for a link, i.e., the maximum number of consecutive transmission failures.  $Bmax$  is computed using an algorithm that takes as input (i.) the data trace of packet successes and failures for each link, and (ii.)  $B'min$ , which is the minimum number of consecutive successful transmissions between two consecutive failure bursts. The authors assume a pre-deployment phase for the determination of  $Bmax$  with respect to each link in the network. However, computed  $Bmax$  values may change during the network operation due to environmental changes. In [51], the authors resolved this problem by introducing BurstProbe, a mechanism for assessing link burstiness through the computation of  $Bmax$  and  $B'min$  during the network operation. The  $\beta$  factor is another metric for assessing link burstiness [52]. It is used to identify bursty links with long bursts of successes or failures. The  $\beta$  factor is computed using conditional probability distribution functions (CPDFs), which determine the probability that the next packet will be received after  $n$  consecutive successes or failures. It requires a large data trace and thus might be inappropriate for online link burstiness assessment.

*Observation 3: The temporal variation of link quality is due to changes in the environment characteristics.* Several studies confirmed that the temporal variation of link quality is due to the changes in the environment characteristics, such as climate conditions (e.g., temperature, humidity), human presence,

interference and obstacles [6, 8, 28, 53, 20, 54]. Particularly, in [20], the authors found that the temporal variation of LQI, RSSI, and Packet Error Rate (PER), in a “clean” environment, (i.e., indoor, with no moving obstacles and well air-conditioned) is not significant. The same observation was made in [44]. Lin et al. [54] distinguished three patterns for link quality temporal variation: small fluctuations, large fluctuations/disturbance, and continuous large fluctuations. The first is mainly caused by multi-path fading of wireless signals; the second is caused by shadowing effect of humans, doors, and other objects; and the last is caused by interference (e.g., Wi-Fi). A deeper analysis of the causes of links temporal variation was presented in [55, 56, 52]. Lal et al. [55] reported that the transitional region can be identified by the PRR/SNR curve using two thresholds (refer to Figure 1.6). Above the first threshold the PRR is consistently high, about 100%, and below the second threshold the PRR is often less than 25%. In between is the transitional region, where a small variation in the SNR can cause a shift between good and bad quality link, which results in a bursty link. In fact, SNR is the ratio of the pure received signal strength to the noise floor. When no interference is present, the noise floor varies with temperature, and so is typically quite stable over time periods of seconds or even minutes [4]. Therefore, what makes the SNR vary according to time leading to link burstiness is mainly the received signal strength variation [52]. The variation of the received signal strength may also be due to the constructive/destructive interference in the deployment environment [44].

### 1.3.3 Link asymmetry

Link asymmetry is an important characteristic of radio links as it has a great impact on the performance of higher layer protocols. Several studies analyzed the asymmetry of low-power links [4, 8, 28, 18, 9, 2, 20, 40]. Link asymmetry is often assessed as the difference in connectivity between the uplink and the downlink. A wireless link is considered as asymmetric when this difference is larger than a certain threshold, e.g., when the difference between the uplink PRR and the downlink PRR is greater than 40% [4, 18].

*Observation 1: Asymmetric links are mainly located at the transitional region.* It was shown that links with very high or very low average PRRs, which are mainly those of the connected and disconnected regions respectively, tend to be symmetric. On the other hand, links with moderate PRRs, those of the transitional regions, tend to be asymmetric [18, 9].

*Observation 2: Link asymmetry is not correlated with distance.* The spatial variation of link asymmetry was the subject of several studies [28, 18, 9, 2]. Ganesan et al. [2] found that the percentage of asymmetric links is negligible at short distances from the transmitter and increases significantly with higher distances. This observation confirms the one made by Cerpa et al. [18, 9], stating that asymmetric links are mainly those in the transitional region. On the other hand, Cerpa et al. found that the percentage of asymmetric links increases as well as decreases as the distance from the transmitter increases. Thus, they argued that link asymmetry is not correlated with distance.

*Observation 3: Link asymmetry may or may not be persistent.* Srinivasan et



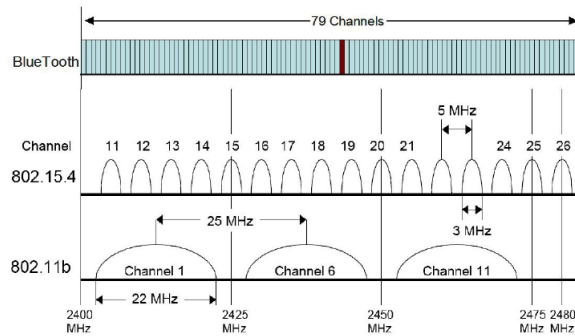


Figure 1.7: IEEE 802.15.1 (Bluetooth), IEEE 802.11b, and IEEE 802.15.4 spectrum usage [4].

al. [4] studied the temporal variation of link asymmetry. They found that very few links (2 of the 16 observed asymmetric links in the testbed) were long-term asymmetric links (i.e., consistently asymmetric) while many links were transiently asymmetric. On the other hand, Mottola et al. [44] found that when links are stable, which is the case in their experiments, link asymmetry also tends to persist. Consequently, link asymmetry might be transient only for unstable links (i.e., their quality varies with time), and ultimately depends on the target environment.

*Observation 4: Hardware asymmetry and radio irregularity constitute the major causes of link asymmetry.* Most studies stated that one of the causes of link asymmetry is hardware asymmetry, i.e., the discrepancy in terms of hardware calibration; namely nodes do not have the same effective transmission power neither the same noise floor (receiver sensitivity) [8, 18, 39, 40]. Ganesan et al. [2] claimed that at large distances from the transmitter, small differences between nodes in hardware calibration may become significant, resulting in asymmetry. The radio irregularity caused by the fact that each antenna has its own radiation pattern that is not uniform, is another major cause of link asymmetry [7, 39].

### 1.3.4 Interference

Interference is a phenomena inherent to wireless transmissions, e.g., because the medium is shared among multiple transmitting nodes. In the following, we provide a bird’s eye view on the current state of the art related to interference in low-power wireless networks. Our goal is not to be exhaustive, but rather to present the essential information to complement the rest of the material in this survey, giving the reader a foundation to understand how interference may affect link quality estimation.

Interference can be either *external* or *internal*. External interference may occur from co-located/co-existing networks that operate in the same frequency band as the WSN; internal interference may occur from concurrent transmission of nodes belonging to the same WSN. In the following, we survey relevant work on both external and internal interference.

#### 1.3.4.1 External interference

WSNs operate on unlicensed ISM bands. Therefore they share the radio spectrum with several other devices. For example, in the 2.4 GHz frequency, WSNs might compete with the communications of Wi-Fi and Bluetooth devices. Furthermore, a set of domestic appliances such as cordless phones and microwave ovens generates electromagnetic noise which can significantly harm the quality of packet receptions [57, 58, 59]. External interference has a strong impact on the performance of WSN communications because it increases packet loss rate, which in turn increases the number of retransmissions and therefore the latency of communications.

*Observation 1: The co-location of 802.15.4 and 802.11b networks affects transmission in both networks due to interference (unless the 802.15.4 network uses channel 26), but the transmission in 802.11b networks is less affected.* Srinivasan et al. [4] observed that 802.11b transmissions (*i.*) can prevent clear channel assessment at 802.15.4 nodes, which increases latencies and (*ii.*) represent high power external noise sources for 802.15.4, which can lead to packet losses. They also observed that 802.11b nodes do not suspend transmission in the presence of 802.15.4 transmission, since 802.11b transmission power is 100 times larger than that of 802.15.4. However, this observation was refuted by Liang et al. [21]. Indeed, they reported that when the 802.15.4 transmitter is close to the 802.11b transmitter, the 802.11b node may suspend its transmission due to elevated channel energy. Furthermore, when this happens, IEEE 802.11b only corrupts the IEEE 802.15.4 packet header, i.e., the remainder of the packet is unaffected. The impact of interference generated by Wi-Fi devices strongly depends also on the traffic pattern. Boano et al. [60] presented experimental results using different Wi-Fi patterns and compared the different PRRs under interference. Srinivasan et al. [4] noticed that only 802.15.4 channel 26 is largely immune to 802.11b interference, as it does not overlap with 802.11b channels (refer to Figure 1.7).

*Observation 2: The co-location of IEEE 802.15.4 and 802.15.1 (Bluetooth) networks affects mostly the transmissions in the IEEE 802.15.4 network.* Bluetooth is based on frequency hopping spread spectrum (FHSS) technology. This technology consists in hopping to a new frequency after transmitting or receiving a packet, using a pseudorandom sequence of frequencies known to both transmitter and receiver. Thanks to this technology, Bluetooth is highly resistant to interference. Consequently, when 802.15.4 and Bluetooth networks coexist, packet losses at Bluetooth devices are not that important as compared to those observed with 802.15.4. The results by Boano et al. [60] show that interference from Bluetooth devices has a much lower impact than the one from Wi-Fi devices or microwave ovens on WSN communications.

*Observation 3: The co-location of IEEE 802.15.4 networks and domestic appliances can significantly affect the transmission in the IEEE 802.15.4 networks.* Using a spectrum analyzer, Zhou et al. [61] showed the impact of interference generated by a microwave oven, which can cover almost half of the 2.4 GHz avail-

able spectrum. Their results were confirmed by Boano et al. [60], who measured the periodic pattern of microwave ovens interference through fast RSSI sampling using off-the-shelf sensor motes. The authors highlighted the periodicity of the generated interference and quantified its impact on the PRR of WSN communications.

*Observation 4: External interference often spreads along several (adjacent) channels [57, 58].* Due to the characteristics of external wide-band interferers such as Wi-Fi devices, interference often spreads throughout spatially nearby channels (refer to Figure 1.7). Another example of the latter are microwave ovens, that spread noise over almost half of the 2.4 GHz available spectrum, as explained earlier.

#### 1.3.4.2 Internal interference

As external interference, internal interference can have a strong impact on the performance of WSN communications.

*Observation 1: In the presence of concurrent transmission, the three reception regions can still be identified by the signal-to-interference-plus-noise-ratio (SINR).* Most studies on low-power link characterization, including those stated previously, were performed using collisions-free scenarios to observe the pure behavior of the channel. In [19], the authors addressed low-power link characterization under concurrent transmissions. They reported that concurrent transmission leads to interference, which has a great impact on link quality. Based on signal-to-interference-plus-noise-ratio (SINR) measurements, conducted with Mica 2 motes equipped with CC1000 radios, the authors found the following key observations: First, when the SINR exceeds a critical threshold, the link is of high quality<sup>1</sup>, i.e., the PRR is greater than 90%, and it belongs to the connected region. Below this threshold, transmission on that link can be successful despite the existence of concurrent transmission, but the resulting PRR is inferior to 90% (transitional and disconnected regions). Second, the identified SINR threshold can vary significantly between different hardware. In fact, this threshold depends on the transmitter hardware and its transmission power level, but it does not depend on its location.

*Observation 2: Concurrent transmissions have a great impact on the link delivery ratio even when nodes are not visible to each other.* In [44], the authors conducted experiments in real road tunnels, with controlled concurrent transmissions. They set up a specific scenario where two nodes communicate and a third node, which is not visible to the first two (i.e., “far from” the two nodes and the PRR to each of them is equal to zero), concurrently transmits its data. They found that the third node was able to create a significant noise for the communicating nodes so that the delivery ratio over that link (assessed by the PRR) was very low, even lower than expected.

---

<sup>1</sup>This is interpreted by the fact that the strength of the received signal is much higher than those of the noise level and the received signal from the interfering node.

*Observation 3: Internal Interference from adjacent channels has a significant influence on the packet delivery rate.* Several work showed that cross-channel interference can cause a significant increase in the packet loss ratio [62, 63, 64, 65]. Wu et al. [64] showed on MicaZ motes that with adjacent channel interference, the PRR decreases 40% compared to when no interference is present on the adjacent channel. The authors also showed that when interference is generated two channels away, the impact on the PRR is minimal. Xing et al. [65] proposed an algorithm that reduces the overhead of multi-channel interference measurements by exploiting the spectral power density of the transmitter.

### 1.3.5 Implication on communication protocols

Previous sections show that low-power links are extremely unreliable as they experience a complex and dynamic behavior. To overcome link unreliability, we believe that three countermeasures should take place.

First, communication protocols should be *designed* under realistic conceptual models. Several communication protocols were designed under simplified conceptual models such as considering the network topology as a graph, where edges represent links and each link is assumed to be symmetric (typically, the assessment of the link in one direction represents the overall quality of the link). Unfortunately, these protocols were found not working well in actual deployments. Therefore, it is mandatory that conceptual models take into consideration low-power links characteristics, such as link asymmetry. In [4], the authors outlined a set of assumptions commonly made by conceptual models and showed that these assumptions are not valid. In [7], the authors discussed the impact of using conceptual models that do not take into account the radio irregularity on the higher layer protocols.

Second, communication protocols should be *validated* under realistic wireless channel models. Network simulators that are based on simplified wireless channel models, such as to abstract the transmission range to a unit disk, lead to misleading protocols validation. A communication protocol that provides excellent performances using such unrealistic simulator may lead to poor performances in real-world scenarios.

Third, communication protocols should rely link quality estimation as a fundamental building block to maintain the correct network operation. For instance, several routing protocols such as [12] rely of link quality estimation to identify poor and intermediate quality links and discard them from the data delivery path. On the other hand, other protocols referred to opportunistic routing protocols such as [66], identify intermediate quality links and use them during the short time periods during which they exhibit good quality. These links are rejected when they turn to poor quality links. Considering the quality of links in routing decisions has been shown to improve the network throughput and lifetime [67].

## 1.4 Fundamentals of link quality estimation

Empirical observations on low-power links raised the need for link quality estimation as a fundamental building block for higher layer protocols. In fact,

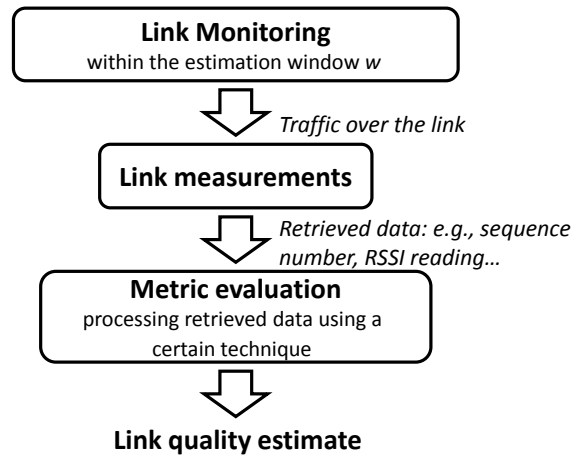


Figure 1.8: Steps for Link Quality Estimation.

link quality estimation enables these protocols to mitigate and overcome low-power link unreliability. For instance, sophisticated routing protocols rely on link quality estimation to improve their efficiency by avoiding bad quality links. Also topology control mechanisms rely on link quality estimation to establish stable topologies that resist to link quality fluctuations.

In this section, we present an overview of different aspects of link quality estimation. First, we define the link quality estimation process and decompose it into different steps. Then, we present requirements for the design of efficient link quality estimators.

### 1.4.1 Steps for link quality estimation

Basically, link quality estimation consists of evaluating a *metric* — a mathematical expression, within an estimation window  $w$  (e.g., at each  $w$  seconds, or based on  $w$  received/sent packets). We refer to this metric as Link Quality Estimator (LQE). The LQE evaluation requires *link measurements*. For example, to evaluate the PRR estimator, link measurements consist of extracting the sequence number from each received packet. *Link monitoring* defines a strategy to have traffic over the link allowing for link measurements. Hence, the link quality estimation process involves three steps: link monitoring, link measurements, and metric evaluation. These steps are described next and illustrated in Figure 1.8.

#### 1.4.1.1 Link monitoring

There are three kinds of link monitoring: (i.) active link monitoring, (ii.) passive link monitoring, and (iii.) hybrid link monitoring. Note that not only link quality estimation relies on link monitoring, but also other mechanisms, such as routing and topology control [12].

*Active link monitoring:* In active link monitoring, a node monitors the links to its neighbors by sending probe packets. Probe packets can be sent either by broadcast such as in [67], or by unicast such as in [68]. Broadcast probe packets

involve no link-level acknowledgments or retransmissions, in contrast to unicast probe packets. Probe packets are generally sent at a certain rate, which yields a tradeoff between energy-efficiency (low rates) and accuracy (high rates). An adaptive beaconing rate, such as the one proposed in [12] might provide a good balance for this tradeoff.

Broadcast-based active link monitoring is simple to implement and incurs a small overhead compared to unicast-based [68]. For that reason, many network protocols and mechanisms rely on it. On the other hand, unicast-based active link monitoring allows for more *accurate* link measurements because of its resemblance to actual data transmission over the link [69]. However, it is still considered as a costly mechanism for WSN due to the communication overhead.

*Passive link monitoring:* Unlike active link monitoring, passive link monitoring exploits existing traffic without incurring additional communication overhead. In fact, a node listens to transmitted packets, even if these packets are not addressed to it (overhearing) [55, 70]. It can also listen to acknowledgments of messages sent by different neighbors [10, 13].

Passive link monitoring has been widely used in WSNs due to its energy-efficiency compared to active link monitoring [6, 13, 55, 71, 70, 72, 73]. However, passive monitoring incurs the overhead of probing idle links [68]. Lal et al. [55] found that overhearing involves expense of significant energy. In addition, when the network operates at low data rate or unbalanced traffic, passive link monitoring may lead to the lack of up-to-date link measurements. Consequently, it leads to inaccurate link quality estimation.

*Hybrid link monitoring:* The use of a hybrid mechanism combining both active and passive monitoring may yield an efficient balance between up-to-date link measurements and energy-efficiency [68]. For instance, in [12], the authors introduced a hybrid link monitoring mechanism for performing both link quality estimation and routing advertisements. Active link monitoring consists in broadcasting beacons with a non-fixed rate. Rather, a specific algorithm is used to adaptively tune the beaconing rate: Initially, the beaconing rate is high and decreases exponentially until it reaches a certain threshold. When the routing layer signals some problems such as loop detection, the beaconing rate resets to its initial value. Active link monitoring is coupled with passive link monitoring, which consists in hearing received acknowledgments from neighbours (that represent next hops).

Finally, it was argued by several recent studies that link quality estimation where link monitoring is based on data traffic is much more accurate than that having link monitoring based on beacon traffic [12, 69, 74, 75]. The reason is that there are several differences between unicast and broadcast link properties [75]. It is thereby difficult to precisely estimate unicast link properties via those of broadcast.

#### 1.4.1.2 Link measurements

Link measurements are performed by retrieving useful information (i.) from received packets/acknowledgments or (ii.) from sent packets. Data retrieved from received packets/acknowledgments, such as sequence numbers, time stamp, RSSI, and LQI, is used to compute *receiver-side* link quality estimators. On the other hand, data retrieved from sent packets, e.g., sequence numbers, time stamp

and packet retransmission count, allows for the computation of *sender-side* link quality estimators.

#### 1.4.1.3 Metric evaluation

Based on link measurements, a metric is evaluated to produce an estimation of the link quality. Generally, this metric is designed according to a certain *estimation technique*, which can be a simple average or a more sophisticated technique such as filtering, learning, regression, Fuzzy Logic, etc. For example, Woo et al. [11] introduced the WMEWMA estimator, which uses the EWMA filter as main estimation technique: based on link measurements, the PRR is computed and then smoothed to the previously computed PRR using EWMA filter. More examples are given in Section 1.5 and Table 1.2.

### 1.4.2 Requirements for link quality estimation

Efficient link quality estimation has several requirements, which are described next.

**Energy efficiency:** As energy may be a major concern in WSNs, LQEs should involve low computation and communication overhead. Consequently, some complex estimation techniques such as learning might be not appropriate in WSNs. Moreover, LQEs should also involve low communication overhead. Typically, an active monitoring with high beaconing rate should be avoided as it is energy consuming.

**Accuracy:** It refers to the ability of the LQE to correctly characterize the link state, i.e., to capture the real behavior of the link. The accuracy of link quality estimation greatly impacts the effectiveness of network protocols. In traditional estimation theory, an estimated process is typically compared to a real known process using a certain statistical figure (e.g., least mean square error or regression analysis). However, such comparison is not possible in link quality estimation, since: (*i.*) there is no metric that is widely considered as the “real” figure to measure link quality; and (*ii.*) link quality is represented by quantities of different nature: some estimators are based on the computation of packet reception ratio, some are based on packet retransmission count, and some are hybrid of these, as described in Section 6. Nevertheless, the accuracy of LQEs can be assessed indirectly, i.e., resorting to a metric that subsume the effect of link quality estimation. For instance, in [76], the authors studied the impact of their four-bit LQE on the performance of CTP (Collection Tree Protocol), a hierarchical routing protocol [12]. They found that four-bit leads to better end-to-end packet delivery ratio, compared with the original version of CTP. Hence, four-bit might be more accurate as it can correctly select routes composed of high quality links. On the other hand, the authors in [3] analyzed the accuracy (referred as reliability) of LQEs by analyzing their statistical properties, namely their temporal behavior and the distribution of link quality estimates.

**Reactivity:** It refers to the ability to quickly react to persistent changes in link quality [77]. For example, a reactive LQE enables routing protocols and topology control mechanisms to quickly adapt to changes in the underlying

connectivity. Reactivity depends on two factors: the estimation window  $w$  and the link monitoring scheme. Low  $w$  and active monitoring with high beaconing rate can lead to reactive LQE. Though, it is important to note that some LQEs are naturally more reactive than others regardless of the  $w$  value or the link monitoring schema. In fact, LQEs that are computed at the sender-side were shown to be more reactive than those computed at the receiver-side [3]. More details are given in Section 6.

**Stability:** It refers to the ability to tolerate transient (short-term) variations in link quality. For instance, routing protocols do not have to recompute information when a link quality shows transient degradation, because rerouting is a very energy and time consuming operation. Lin et al. [54] argued that stability is met through long-term link quality estimation. Long-term link quality estimation was performed by the means of the EWMA filter with a large smoothing factor ( $\alpha = 0.9$ ). Hence, they introduced *Competence* metric that applies the EWMA filter to a binary function indicating whether the current measured link quality is within a desired range. Stability of LQEs can be assessed by the coefficient of variation of link quality estimates, which is computed as the ratio of the standard deviation to the mean [70]. It can also be assessed by studying the impact of the LQE on routing, typically a stable LQE leads to stable topology, e.g., few parent changes in the case of hierarchical routing [25].

As a matter of fact, reactivity and stability are at odds. For instance, consider using PRR as LQE, if we compute the PRR frequently (small  $w$ ), we obtain a reactive LQE as it captures link dynamics at a fine grain. However, this reliability will be at the cost of stability because the PRR will consider some transient link quality fluctuation that might be ignored. Thus, a good LQE is the one that provides a good tradeoff between reactivity and stability. Lin et al. [54] suggest combining their long-term metric *Competence*, considered as a stable but not reactive LQE, with a short-term metric such as ETX, considered as a reactive but unstable LQE, to obtain a good tradeoff. They introduced routing schemes based on this principle. For example, in a tree-based routing scheme, a node selects a potential parent as the neighbour having the best *Competent* link, among all neighbours having low route cost, where route cost is computed based on ETX. The authors argued that such routing scheme selects links that are good in both the short and the long term, and leads to stable network performance. On the other hand, Woo et al. [11] argued that using EWMA filter with convenient smoothing factor would strike balance between reactivity and stability.

Several efforts were carried out for the design of efficient LQEs. In the next section, we survey, classify, and discuss the most relevant LQEs that are suitable for WSNs.

## 1.5 A Survey on link quality estimators

LQEs in WSNs can be classified in two categories: hardware-based and software-based, as illustrated in Figure 1.9. Table 1.2 presents a comparison of LQEs in WSNs.



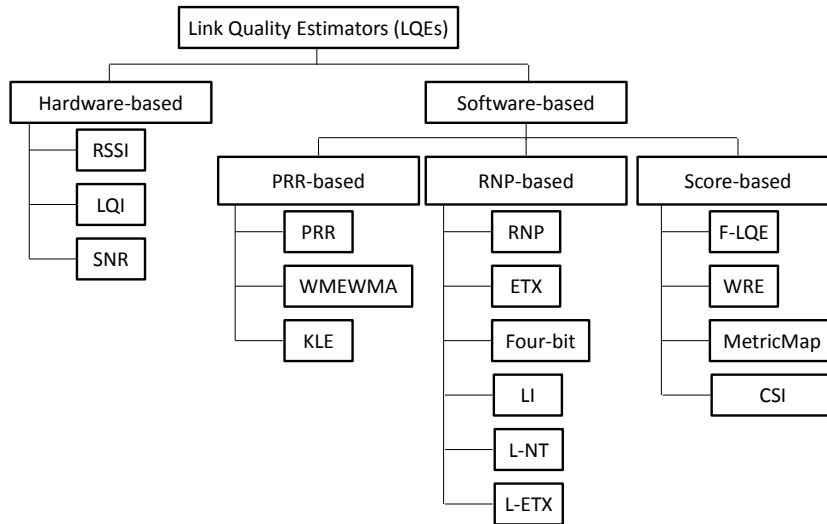
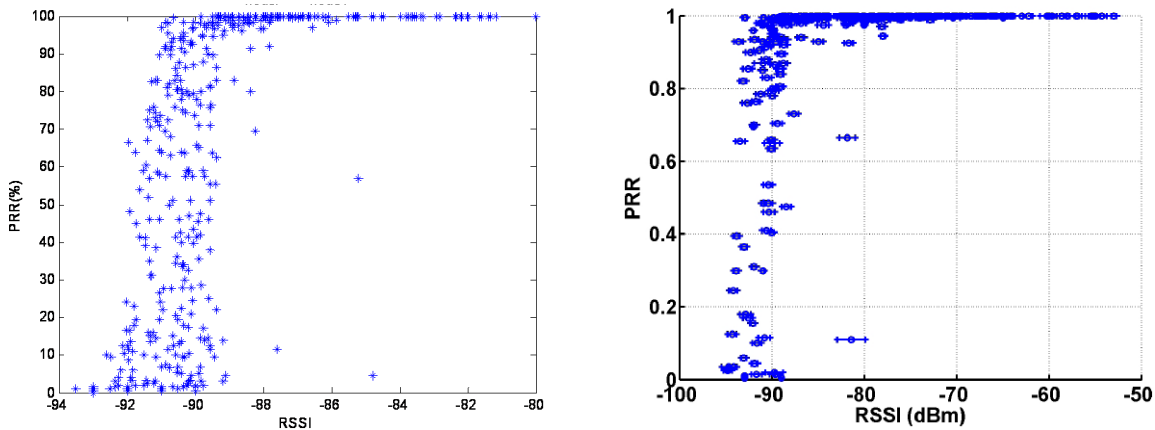


Figure 1.9: Taxonomy of LQEs.



(a) Outdoor environment, using TelosB sensor nodes (using the RadiaLE testbed [3]).

(b) Indoor environment, using MicaZ sensor nodes [80].

Figure 1.10: PRR vs RSSI curve.

### 1.5.1 Hardware-based LQEs

Three LQEs belong to the family of hardware-based LQEs: LQI, RSSI, and SNR. These estimators are directly read from the radio transceiver<sup>2</sup> (e.g., the CC2420). Their advantage is that they do not require any additional computation. However, their adequacy in characterizing links was subject of several research work. We have summarized the literature related to this issue in the following observations:

*Observation 1: RSSI can provide a quick and accurate estimate of whether*

<sup>2</sup>Some radio transceivers do not provide LQI.

Table 1.2: Comparison and classification of LQEs.

			Technique	Link Asymmetry support	Monitoring	Location
<b>Hardware-based</b>	RSSI, LQI and SNR		Read from hardware and can be averaged	No	Passive or Active	Receiver
<b>Software-based</b>	<b>PRR-based</b>	<i>PRR</i>	Average	No	Passive or Active	Receiver
		<i>WMEWMA</i> [70]	Filtering	No	Passive	Receiver
		<i>KLE</i> [78]	Filtering	No	-	Receiver
	<b>RNP-based</b>	<i>RNP</i> [6]	Average	No	Passive	Sender
		<i>LI</i> [55]	Probability	No	Passive	Receiver
		<i>ETX</i> [67]	Average	Yes	Active	Receiver
		<i>four-bit</i> [76]	Filtering	Yes	Active and Passive	Sender and receiver
		<i>L-NT and L-ETX</i> [69]	Filtering	No	-	Sender
		<i>WRE</i> [71]	Regression	No	Passive	Receiver
	<b>Score-based</b>	<i>MetricMap</i> [73]	Training, Classification	No	Passive	Receiver
		<i>CSI</i> [79]	Weighted sum	No	Active	Receiver

a link is of very good quality (connected region). This observation was justified by the following: First, empirical studies such as [80] proved the existence of a RSSI value (-87 dBm [80]) above which the PRR is consistently high (99% [80]), i.e., belong to the connected region. Below this threshold, a shift in the RSSI as small as 2 dBm can change a good link to a bad one and vice versa, which means that the link is in the transitional or disconnected region [4]. This observation is illustrated in Figure 1.10(b) and Figure 1.10(a). Second, RSSI was shown very stable (standard deviation less than 1 dBm) over a short time span (2 s), thereby a single RSSI reading (over a packet reception) is sufficient to determine if the link is in the transitional region or not [4].

*Observation 2: LQI can determine whether the link is of very good quality or not. However, it is not a good indicator of intermediate quality links due to its high variance, unless it is averaged over a certain number of readings.* Srinivasan et al. [4] argued that when the LQI is very high (near 110) the link is of perfect quality (near 100% of PRR). Further, in this situation LQI has low variance so that a single LQI reading would be sufficient to decide if the link is of perfect quality or not. On the other hand, for other LQI values, corresponding to intermediate quality links, the variance of LQI becomes significant and a single LQI reading is not sufficient for accurate link quality estimation. Srinivasan and Levis [81] showed that LQI should be averaged over a large packet window (about 40 up to 120 packets) to provide accurate link quality estimation, but this will be at the cost of agility and responsiveness to link quality changes. The LQI high variance is due to the fact that LQI is a statistical value [80].

Bringing observations 1 and 2 together, it might be reasonable to use a single RSSI or LQI reading to decide if the link is of high quality or not. Such decision is based on RSSI and LQI thresholds, beyond which a link can maintain high quality, e.g., a PRR of at least 95% [53]. Importantly, these thresholds depend on the environment characteristics. For example, Lin et al. [53] found that RSSI threshold is around -90 dBm on a grass field, -91 dBm on a parking lot, and -89 dBm in a corridor. For LQI and RSSI values below these thresholds, neither of these metrics can be used to differentiate links clearly. Nevertheless, an average LQI, with the convenient averaging window, allows a more accurate classification of intermediate links [81]. On the other hand, Mottola et al. [44] claimed that RSSI should not be used to classify intermediate links.

*Observation 3: The variance of LQI can be exploited for link quality estimation.* Empirical studies [81] pointed out that links of intermediate and bad quality have high LQI variance, therefore the LQI needs to be averaged over many samples to give meaningful results. Boano et al. [82] proposed the use of the variance of LQI to distinguish between good links, having very low LQI variance and bad links, having very high LQI variance using as few as 10 samples. However, in that work, the authors did not provide a mapping function or a mathematical expression that exploit the variance of LQI to provide a link quality estimate.

*Observation 4: LQI is a better indicator of the PRR than RSSI.* In [81, 20, 32], it was argued that average LQI shows stronger correlation with PRR, compared to average RSSI. Hence, LQI is a better indicator of PRR than RSSI. On the other hand, in [81] and [20], the authors claimed that RSSI has the advantage of being more stable than LQI (i.e., it shows lower variance), except for multi-path affected links. In fact, which of LQI and RSSI is better for link quality estimation is an unanswered question, reflected by several contradicting statements and results.

*Observation 5: SNR is a good indicator and even predictor of the PRR but it is not accurate, especially for intermediate links.* Theoretically, for a given modulation schema, the SNR leads to an expected bit error rate, which can be extrapolated to packet error rate and then to the PRR [40]. Hence, an analytical expression that gives the PRR as a function of SNR can be derived [40]. Srinivasan et al. [4] justified the observed link characteristics (e.g., link temporal variation and link asymmetry) with SNR behavior. Particularly, they assume that changes in PRR must be due to changes in SNR. However, other studies [72, 78, 83] showed that the theoretical relationship between SNR and PRR reveals many difficulties. These difficulties arise from the fact that mapping between SNR and PRR depends on the actual sensor hardware and environmental effects such as temperature [78]. As a result, these studies concluded that SNR cannot be used as a standalone estimator, but it may help to enhance the accuracy of the PRR estimation. Further, Lal et al. [55] recommended not to use SNR as link quality estimator, when links are inside the transitional region.

*Observation 6: SNR is a better link quality estimator than RSSI.* The RSSI is the sum of the pure received signal and the noise floor at the receiver. On

the other hand, the SNR describes how strong the pure received signal is in comparison with the receiver noise floor. As the noise floor at different nodes can be different, the SNR metric should be better than RSSI [4].

Hardware-based LQEs share some limitations: first, these metrics are only measured for successfully received packets; thus, when a radio link suffers from excessive packet losses, they may overestimate the link quality by not considering the information of lost packets. Second, despite the fact that hardware metrics provide a fast and inexpensive way to classify links as either good or bad, they are incapable of providing a fine grain estimation of link quality [76, 84].

The above limitations of hardware-based LQEs do not mean that this category of LQEs is not useful. In fact, each of these LQEs provides a particular information on the link state, but none of them is able to provide a holistic characterization of the link quality. Currently, there is a growing awareness that the combination of hardware metrics with software metrics can improve the accuracy of the link quality estimation [26, 76, 84, 22, 85]. For example, Fonseca et al. [76] use LQI as a hardware metric to quickly decide whether the link is of good quality. If it is the case, the node is included in the *neighbor table* together with the link quality, assessed using Four-bit as a software metric. Gomez et al. [84] confirm that LQI can accurately identify high quality links, but it fails to accurately classify intermediate links due to its high variance. They exploited this observation to design LETX (LQI-based ETX), a link estimator that is dedicated for routing. The authors first build a piecewise linear model of the PRR as a function of average LQI. This model allows to estimate the PRR given one LQI sample. LETX is then computed as the inverse of the estimated PRR. LETX is used to identify high quality links in route selection process. Rondinone et al. [22] also suggest combining hardware and software metrics through a multiplicative metric between PRR and RSSI, and Boano et al. [85] propose a fast estimator suitable for mobile environments by combining geometrically PRR, SNR, and LQI.

## 1.5.2 Software-based LQEs

Software-based LQEs can be classified into three categories, as illustrated in Figure 1.9: (i.) PRR-based: either count or approximate the PRR, (ii.) RNP-based: either count or approximate the RNP (Required Number of Packet re-transmissions), and (iii.) Score-based: provide a score identifying the link quality. Table 1.2 summarizes the main characteristics of these LQEs.

### 1.5.2.1 PRR-based

PRR is a receiver side estimator that is simple to measure and was widely used in routing protocols [10, 67]. Further, it was often used as an unbiased metric to evaluate the accuracy of hardware-based estimators. In fact, a hardware-based estimator that correlates with PRR is considered as a good metric.

**Discussion:** The efficiency of PRR depends on the adjustment of the time window size. Cerpa et al. [9] showed that for links with very high or very low PRRs, accurate link quality estimation can be achieved within narrow time

windows. On the other hand, links with medium PRRs need much larger time windows to converge to an accurate link quality estimation.

The objective of LQEs that *approximate* the PRR is to provide more efficient link quality estimates than the PRR. In the following, we review the most relevant LQEs in this category.

*The Window Mean with Exponentially Weighted Moving Average* (WMEWMA) [70] is a receiver-side LQE based on passive monitoring. It smoothes PRR estimates using the EWMA filter, which provides more stable but sufficiently agile estimation compared to PRR.

**Discussion:** To assess the performance of WMEWMA, Woo and Culler [70] introduced a set of LQEs that approximate the PRR using filtering techniques other than EWMA. Then, they compared WMEWMA to these filter-based LQEs, in terms of (*i.*) reactivity assessed by the settling time and the crossing time, (*ii.*) accuracy evaluated by the mean square error, (*iii.*) stability assessed by the coefficient of variation, and (*iv.*) efficiency assessed by the memory footprint and computation complexity. WMEWMA was found to outperform the other filter-based LQEs. The work by Woo and Culler [70] laid the foundation for subsequent work on filter-based LQE, although their solution required a more thorough assessment, e.g., based on real-world data traces instead of synthetic ones (i.e., generated analytically).

*The Kalman filter based link quality estimator* (KLE) [78] was proposed to overcome the poor reactivity of average-based LQEs, including PRR. In fact, the objective of KLE is to provide a link quality estimate based on a single received packet rather than waiting for the reception of a certain number of packets within the estimation window and then compute the average. Upon packet reception, RSS (Received Signal Strength) is extracted and injected to a Kalman filter, which produces an estimation of the RSS. Then, an approximation of the SNR is gathered by subtracting the noise floor estimate from the estimated RSS. Using a pre-calibrated PRR-SNR curve at the receiver, the approximated SNR is mapped to an approximated PRR, which represents the KLE link quality estimate.

**Discussion:** Through experiments using a WSN platform of two nodes (a sender and a receiver), Senel et al. [78] proved that KER is able to detect link quality changes faster (i.e., it is more reactive) than PRR. However, the accuracy of KER was not examined. This accuracy is typically related to the accuracy of the PRR-SNR curve, which was considered as constant over time. According to empirical observations on low-power links, this curve varies over time (in dynamic environments) and also from one node to another. Further, it seems that the positive results found by Senel et al. [78] related to the reactivity of KER are due to the steady environment in the experimental evaluation, so that the PRR-SNR curve is constant over time.

### 1.5.2.2 RNP-based

*The Required Number of Packet transmissions* (RNP) [6] is a sender-side estimator that counts the average number of packet transmissions/re-transmissions, required before successful reception. It can be computed as the number of trans-

mitted and retransmitted packets during an estimation window, divided by the number of successfully received packets, minus 1 (to exclude the first packet transmission). RNP assumes an ARQ (Automatic Repeat Request) protocol [86] at the link-layer level, i.e., a node will repeat the transmission of a packet until it is correctly received. Note that a similar metric to the RNP is the Acknowledgment Reception Ratio (ARR). It is computed as the ratio of the number of acknowledged packets to the total number of transmitted packets during a predefined time window.

**Discussion:** Cerpa et al. [6] argued that RNP is better than PRR for characterizing the link quality. In fact, as opposed to RNP, PRR provides a coarse-grain estimation of link quality since it does not take into account the underlying distribution of losses. However, RNP has the disadvantage of being very unstable and can not reliably estimate the link packet delivery, mainly due to link asymmetry [25].

In the following, we review the most relevant LQEs that approximate the RNP using several techniques.

*The Expected Transmission Count (ETX)* [67] is a receiver-side estimator that uses active monitoring. ETX is the inverse of the product of the forward delivery ratio,  $d_f$  and the backward delivery ratio,  $d_b$ , which takes into account link asymmetry.  $d_b$  refers to the PRR (computed based on received packets), while  $d_f$  refers to the ARR (computed based on received ACKs). However, when active monitoring is based on broadcast probe packets,  $d_f$  can also refer to the PRR of the forward link as probe packets are not acknowledged.

**Discussion:** It was shown that routing protocols based on the ETX metric provide high-throughput routes on multi-hop wireless networks, since ETX minimizes the expected total number of packet transmissions required to successfully deliver a packet to the destination [67]. In [73], the authors found that ETX based on passive monitoring fails in overloaded (congested) networks. Indeed, a high traffic load (4 packets/s) leads to a congested network so that packets experience many losses. Consequently, a large number of nodes are not able to compute the ETX because they do not receive packets. Hence, routing is interrupted due to a lack of link quality information. This phenomenon leads to a degradation in the network throughput.

*The Link inefficiency (LI)* proposed by Lal et al. [55] as an approximation of the RNP, is based on passive monitoring and defined as the inverse of the packet success probability (PSP). PSP is an approximated PRR. Lal et al. [55] introduced the PSP metric instead of considering directly the PRR because they assume that accurate PRR measurement requires the reception of several packets, i.e., a large estimation window. This imposes that sensor nodes operate under high duty cycles, which is undesirable for energy-constrained WSNs. PSP is derived by an analytical expression that maps the average SNR to PSP.

**Discussion:** It was shown [83, 72, 78] even by Lal et al. [55], that mapping from average SNR to an approximation of PRR may lead to erratic estimation. Hence, using PSP instead of PRR might be unsuitable for link quality estimation.

*Four-bit* is not only a metric for link quality estimation [76]. It is designed to be used by routing protocols and provides four *bits* of information, compiled

from different layers: the *white bit* is from the physical layer and allows to quickly identify good quality links, based on one packet reading. The *ack bit* is from the link layer and indicates whether an acknowledgment is received for a sent packet. The *pin bit* and the *compare bit* are from the network layer and are used for the neighbor table replacement policy. Four-bit assesses link quality as an approximation of the packet retransmissions count by combining two metrics, through the EWMA filter. The first metric is RNP, computed based on the transmitted data packets and it assesses the quality of the forward link. The second metric is the inverse of WMEWMA minus 1. It is computed based on received beacons and it assesses the quality of the backward link. Four-bit is then both a sender- and received-side LQE and it takes into account link asymmetry. Further, it uses both passive (data packet traffic) and active (beacons traffic) monitoring.

**Discussion:** To evaluate the performance of Four-bit, Fonseca et al. [76] considered the CTP routing protocol [12]. In CTP, routing consists in building and maintaining a tree towards the sink node, based on link quality estimation. Then, the authors compared the original version of CTP that uses ETX as LQE, against a modified version of CTP that uses Four-bit as LQE. They also involved another routing protocol called MultiHopLQI [87], which also builds and maintains a tree toward the sink node, but LQI is used as LQE. Performance comparison was performed using three metrics: (*i.*) cost, which accounts for the total number of transmissions in the network for each unique delivered packet, (*ii.*) average depth of the routing tree, and (*iii.*) delivery rate, which is the fraction of unique messages received at the root. Fonseca et al. [76] found that CTP based on Four-bit provides better performance (e.g., packet delivery) than the original version of CTP and MultiHopLQI.

The *L-NT* and *L-ETX* are two sender-side LQEs that approximate the *RNP* [69]. They are referred as data-driven LQEs because they are based on feedback from unicast data packets. *L-NT* counts the number of transmissions to successfully deliver a packet then applies the EWMA filter. On the other hand, *L-ETX* first computes the ratio of the number of acknowledged packets to the total number of transmitted packets based on a certain estimation window. Then, it applies the EWMA filter and inverts the result.

**Discussion:** Through mathematical analysis and experimental measurements, the authors in [69] demonstrated that *L-ETX* is more accurate in estimating ETX than *L-NT*. It is also more stable. However, this result does not mean that *L-ETX* is accurate at estimating link quality because ETX is not a reference/objective metric. The authors also showed through an experimental study that *L-NT*, when used as a routing metric, achieves better routing performance than *L-ETX*, namely a higher data delivery ratio and energy efficiency. This result might be more convincing than the first as it indeed shows that *L-ETX* is an accurate LQE. Such routing performances can be explained by the fact that *L-ETX* allows to select stable routes with high quality links.

### 1.5.2.3 Score-based

Some LQEs provide a link estimate that does not refer to a physical phenomena (like packet reception or packet retransmission); rather, they provide a score

or a label that is defined within a certain range. In the following, we present an overview on four score-based LQEs: MetricMap [73], WRE [71], and CSI [79].

*MetricMap* is proposed by Wang et al. [73], as an alternative LQE for MintRoute, a hierarchical routing protocol, when the original LQE ETX fails to select routes [11]. Such failure occurs when a node cannot find a route, i.e., a node that can not find a parent (an orphan node) in MintRoute. Wang et al. identified link quality estimation as a classification problem. MetricMap uses a classification algorithm to classify the link among a set of classes (e.g., “Good”, “Bad”). This algorithm has as input a feature vector, which consists of a set of metrics that impact link quality, including RSSI, channel load assessment, and node depth. This classification algorithm relies on a training phase, which is performed using a database of training samples. Each sample consists of a feature vector and a corresponding class label.

**Discussion:** Wang et al. [73] showed that MetricMap combined with ETX improves the network performance in terms of packet delivery rate and fairness. This measures the variability of the delivery rate across all source nodes. However, MetricMap can be used as a back-off metric but not as a sole metric for link quality estimation. This fact is due to the use of learning algorithms, which are greedy algorithms and might be unsuitable to be executed by sensor nodes.

The *Weighted Regression Estimator* (WRE) is proposed by Xu and Lee [71]. They argued that the received signal strength is correlated with distance. This observation was generalized to the fact that a node can determine the quality of the link to its neighbour giving the location of this neighbour. Hence, WRE derives a complex regression function based on an input vector that contains a set of nodes locations together with their links quality known in advance. This function is continuously refined and updated by the knowledge of a new input, i.e., node location and the corresponding link quality. Once derived, this function returns an estimation of the link quality giving the neighbour location.

**Discussion:** The performance of WRE is evaluated by comparing it to WMEWMA using the same evaluation methodology as that of Woo et al. [11], where PRR is considered as the objective metric. Xu and Lee [71] found that WRE is more accurate than WMEWMA. However, we believe that the introduced estimator is complex and involves computation overhead and high memory storage (due to regression weights determination). Moreover, WRE assumes that link quality is correlated with distance, which is not always true, as proved by several empirical studies on low-power links [8, 29, 18, 28].

The *DoUble Cost Field HYbrid* (DUCHY) [79] is a routing metric that allows to select routes with short hops and high quality links. DUCHY is based on two LQEs. The first is receiver-side and uses active monitoring (based on beacon traffic). It is called *Channel State Information* (CSI). CSI is computed by normalizing RSSI and LQI, which are gathered from received beacons and combining the two normalized values into a weighted sum. The second estimator is the RNP. This estimator is used to refine CSI measurements supposed to be inaccurate since they are based on beacon traffic.

**Discussion:** DUCHY was integrated in Arbutus, a hierarchical routing protocol based on link quality estimation [74]. Arbutus is then compared to MultiHopLQI, another hierarchical routing protocol that is based on LQI as LQE



[87]. Performance metrics include packet delivery ratio and the average number of transmissions needed for delivery. It was found that Arbutus outperforms MultiHopLQI and deduce that DUCHY is better than LQI [79]. However, this deduction might be unfair as the two LQEs were compared in different contexts. It would be more reasonable, for example, to integrate LQI in Arbutus and compare DUCHY-based Arbutus to LQI-based Arbutus. Furthermore, it is obvious that DUCHY is better than LQI because DUCHY integrates LQI and other metrics. Hence, it would be interesting to compare DUCHY to other software LQEs to demonstrate its performance.

## 1.6 Conclusion

This chapter addressed the fundamental concepts related to link quality estimation in WSN:

The first part was dedicated for an overview of the most common WSN radio technology and the analysis of low-power link characteristics. We synthesized the vast array of empirical studies on low-power links into a set of high-level observations, some which are contradictory. This is mainly due to the discrepancies in experimental conditions between empirical studies, i.e. they do not have the same environment characteristics, neither the same WSN platform or the same experiment settings. Apart from these contradicting observations, we have identified a set of observations showing how low-power links experience a complex and dynamic behavior. In fact, low-power links are extremely unreliable due to the low-power and low-cost radio hardware typically employed in WSN nodes.

The second part was devoted to link quality estimation, where we described the main related aspects and provided a first taxonomy of LQEs. As discussed in this part, an efficient LQE must be accurate while reflecting the real link state. It must be also reactive to persistent changes in link quality, yet stable by ignoring transient (short-term) variations in link quality. This part demonstrates that research on link quality estimation is challenging and several issues are still unexplored. Especially, we have noticed that although several link quality estimators are available in the literature, none of them has been thoroughly evaluated. The following chapter fills this gap by providing a thorough performance evaluation study of the most representative LQEs in literature.



---

### Performance Evaluation of Link Quality Estimators

---

#### 2.1 Introduction

Link quality estimation is a thorny problem in WSNs, because its accuracy impacts the design and the effectiveness of network protocols. For instance, many routing protocols e.g. [12], rely on link quality estimation to select high quality routes for communication. The more accurate the link quality estimation is, the more correct the decision made by routing protocols in selecting such routes. This is just one example on how important it is to assess the performance of the link quality estimator (LQE) before integrating it into a particular network protocol.

Unfortunately, while several LQEs have been reported in the literature, none has been thoroughly evaluated. One of the reasons is the impossibility, or at least the difficulty, to provide a quantitative evaluation of the accuracy of LQEs. In fact, there is no objective link quality metric to which the link quality estimate can be compared. Furthermore, there are LQEs that are based on the packet reception ratio (PRR), some others are based on packet retransmission count (i.e. RNP) and some others are hybrid and more complex. Thus, comparing their performance becomes challenging as they have different natures. These facts motivated us to study the performance of LQEs.

In this chapter, we conduct an extensive comparative performance study of most of well-known LQEs, based on both simulation and real experimentation. We start by discussing related work and describing LQEs under evaluation. Then, we present our methodology for the performance evaluation of LQEs. The proposed methodology consists in analyzing the statistical properties of LQEs, independently of any external factor, such as collisions and routing. These statistical properties impact the performance of LQEs, in terms of reliability and stability. Next, we present the considered evaluation platforms. We used TOSSIM 2 for the simulation-based performance study. As for the experimental-based performance study, we introduced RadiaLE, a benchmarking testbed that automates the experimental evaluation of LQEs. By comparing simulation re-

sults with experimental results, we examined the realism of TOSSIM 2 channel model. Overall, experimental and simulation results demonstrate that none of the existing LQEs is sufficiently reliable as they either overestimate or underestimate link quality. This is due to the fact that each LQE is only able to assess a single link aspect (e.g. reception ratio, packet retransmissions count) thus providing a partial link characterization.

## 2.2 Related work

To our best knowledge, only [70], [6] and [76] addressed the performance evaluation of LQEs in WSNs.

In [70], the authors compared the performance of WMEWMA, their introduced filter-based LQE, with other filter-based LQEs. Comparison has been carried out in terms of (i.) reactivity assessed by the settling time and the crossing time, (ii.) accuracy evaluated by the mean square error, (iii.) stability assessed by the coefficient of variation, and (iv.) efficiency assessed by the memory footprint and computation complexity. This comparative study was performed analytically, based on a simple generated trace. The trace generator is based on the assumption that packets transmission corresponds to independent Bernoulli trials.

The comparative performance study presented in [70] might be not fairly solid for the following reasons: First, and foremost this study was restricted to filter-based LQEs. Except WMWMA, the involved LQEs are not well referred in the literature. They were introduced in the study to choose the best filter for link quality estimation. Second, the comparison is based on a simple generated trace, which does not take into account some important characteristics of low-power links. Finally, most of the introduced performance metrics are based on PRR as an objective metric (the correct link status). This is not true since PRR is not the ideal metric for link quality estimation as we will discuss next.

In [6], the main goal was to study the temporal characteristics of low-power links, using a real WSN deployment. The authors compared PRR and RNP in order to select the best metric for link characterization, concluding that RNP is better than PRR. To justify their finding the authors observed different links during several hours, by measuring PRR and RNP every one minute. They found that for good-quality and bad-quality links, i.e. according to their definition links having high ( $> 90\%$ ) and low reception rates ( $< 50\%$ ) respectively, PRR follows the same behavior as RNP. However, for intermediate quality links, PRR *overestimates* the link quality because it does not take into account the underlying distribution of packet losses. When the link exhibits short periods during which packets are not received, the PRR can still have high value but the RNP is high so that it indicates the real link state. As a matter of fact, a packet that cannot be delivered may be retransmitted several times before aborting transmission. The authors also analyzed the statistical relationship between RNP and the inverse of PRR by assessing (i.) the cumulative distribution function (CDF) of RNP as a function of  $1/PRR$  and (ii.) the Consistency level between RNP and  $1/PRR$ . They found that RNP and PRR are not directly proportional.

In [76], the authors compared four-bit to ETX by studying their impact on CTP routing protocol. They considered two versions of CTP, the first uses four-

bit as LQE and the second uses ETX as LQE. Then, the authors compared the performances of the two CTP versions. Performance comparison was performed using three metrics: (i.) Cost, which accounts the total number of transmissions in the network for each unique delivered packet, (ii.) average depth of the topology trees, and (iii.) delivery rate, which is the fraction of unique messages received at the root. The authors found that CTP based on four-bit provides better performances than that based on ETX.

## 2.3 LQEs under evaluation

As reported in the previous chapter, LQEs can be classified as either hardware-based or software-based. Hardware-based LQEs, such as LQI, RSSI, and SNR are directly read from the radio transceiver (e.g. the CC2420) upon packet reception. Empirical studies have shown that hardware-based LQEs are not efficient: Despite the fact that they provide a fast and inexpensive way to classify links as either good or bad, they are incapable of providing a fine grain estimation of link quality [76, 84]. Of course, this does not mean that this category of LQEs is useless. Currently, there is a growing awareness that the integration of hardware-based LQEs in software-based LQEs improve the accuracy of the link quality estimation [84, 22, 85].

This study investigates software-based LQEs. Based on the survey presented in the previous chapter, we have selected most representative LQEs. Particularly, we excluded score-based LQEs as they use greedy estimation techniques such as learning and might be inappropriate for energy constrained WSNs. Hence, we have selected the following PRR-based and RNP-based LQEs: PRR, WMEWMA, ETX, RNP, and four-bit. A more detailed overview of these estimator is given next:

**PRR** can be computed as the ratio of the number of successfully received packets to the number of transmitted packets and can be computed at the receiver side, for each window of  $w$  received packets, as:

$$PRR(w) = \frac{\text{Number of received packets}}{\text{Number of sent packets}} \quad (2.1)$$

**WMEWMA** [70] applies EWMA filter on PRR to smooth it, thus providing a metric that resists to transient fluctuation of PRRs, yet is responsive to major link quality changes. WMEWMA is then given by the following:

$$WMEWMA(\alpha, w) = \alpha \times WMEWMA + (1 - \alpha) \times PRR \quad (2.2)$$

where  $\alpha \in [0..1]$  controls the smoothness. This factor enables to give more importance, to the current PRR value (with  $\alpha < 0.5$ ) or to the last computed WMEWMA value (with  $\alpha > 0.5$ ).

**RNP** [6] counts the average number of packet transmissions/re-transmissions required before a successful reception. Based on passive monitoring, this metric is evaluated at the sender side for each  $w$  transmitted and re-transmitted

packets, as follows:

$$RNP(w) = \frac{\text{Number of transmitted and retransmitted packets}}{\text{number of successfully received packets}} - 1 \quad (2.3)$$

Note that the number of successfully received packets is determined by the sender as the number of acknowledged packets.

The aforementioned estimators are not aware of the link asymmetry in the sense that they provide an estimate of the quality of the unidirectional link from the sender to the receiver.

**ETX** [67] is a receiver-initiated estimator that approximates the packet retransmissions count. It uses active monitoring, which means that each node explicitly broadcasts probe packets to collect statistical information. ETX takes into account link asymmetry by estimating the uplink quality from the sender to the receiver, denoted as  $PRR_{forward}$ , as well as the downlink quality from the receiver to the sender, denoted as  $PRR_{backward}$ . The combination of both PRR estimates provides an estimation of the bidirectional link quality, expressed as:

$$ETX(w) = \frac{1}{PRR_{forward} \times PRR_{backward}} \quad (2.4)$$

Note that  $PRR_{forward}$  is simply the PRR of the uplink determined at the receiver, for each  $w$  received probe packets, while  $PRR_{backward}$  is the PRR of the downlink computed at the sender and sent to the receiver in the probe packet.

**four-bit** [76] is a sender-initiated estimator (already implemented in TinyOS) that approximates the packet retransmissions count. Like ETX, four-bit considers link asymmetry property. It combines two metrics (i.)  $estETX_{up}$ , as the quality of the unidirectional link from sender to receiver, and (ii.)  $estETX_{down}$ , as the quality of the unidirectional link from receiver to sender.  $estETX_{up}$  is exactly the RNP metric, computed based on  $w_p$  transmitted/retransmitted data packets.  $estETX_{down}$  approximates RNP as the inverse of WMEWMA, minus 1; and it is computed based on  $w_a$  received beacons. The combination of  $estETX_{up}$  and  $estETX_{down}$  is performed through the EWMA filter as follow:

$$four-bit(w_a, w_p, \alpha) = \alpha \times four-bit + (1 - \alpha) \times estETX \quad (2.5)$$

$estETX$  corresponds to  $estETX_{up}$  or  $estETX_{down}$ : at  $w_a$  received beacons, the node derives four-bit estimate by replacing  $estETX$  in Eq.2.5 for  $estETX_{down}$ . At  $w_p$  transmitted/re-transmitted data packets, the node derives four-bit estimate by replacing  $estETX$  in Eq.2.5 for  $estETX_{up}$ .

Table 4.1 presents the most important characteristics of LQEs under evaluation.

## 2.4 Evaluation methodology

In link quality estimation, there is a lack of a real metric of reference based on which the accuracy of the estimators can be assessed. In fact, in classical estimation theory an estimated process is typically compared to a real known process using a certain statistical tool (e.g. least mean square error or regression analysis). However, such comparison is not possible in link quality estimation,

Table 2.1: Characteristics of link quality estimators under evaluation

	<b>Monitoring type</b>	<b>Location</b>	<b>Direction</b>	<b>Class</b>
PRR	Passive	Receiver	Unidirectional	PRR-based
WMEWMA	Passive	Receiver	Unidirectional	PRR-based
RNP	Passive	Sender	Unidirectional	RNP-based
ETX	Active	Receiver	Bidirectional	RNP-based
four-bit	Hybrid	Sender	Bidirectional	RNP-based

since: (1) there is no metric that is considered as the “real” one to represent link quality; and (2) link quality is represented by quantities with different natures, since some estimators are based on the computation of the packet reception ratio (PRR), some others are based on packet retransmission count (i.e. RNP) and some others would be hybrid and more complex. Therefore, it turns out that the performance evaluation of LQEs is not a trivial problem. In this section, we introduce a unified and holistic methodology for the performance evaluation LQEs, regardless their nature/class.

Basically, our methodology consists in analyzing the statistical properties of LQEs, independently of any external factor, such as collisions (each node transmits its data in an exclusive time slot) and routing (a single-hop network). These statistical properties impact the performance of LQEs, in terms of:

- **Reliability:** It refers to the ability of the LQE to correctly characterize the link state. The reliability of LQEs is assessed *qualitatively*, by analyzing (i.) their temporal behavior, and (ii.) the distribution of their link quality estimates, illustrated by the scatter plot and the empirical cumulative distribution function (CDF).
- **Stability:** It refers to the ability to resist to transient (short-term) variations (also called fluctuations) in link quality. The stability of LQEs is assessed *quantitatively*, by computing the coefficient of variation (CV) of the link quality estimates.

Our evaluation methodology can be established in three steps: links establishment, link measurements collection, and data analysis. These steps are described next.

### 2.4.1 Links establishment

The first step consists in establishing a rich set of links exhibiting different properties, i.e. different qualities. Particularly, it is recommended to have most of links of intermediate quality, i.e., belonging to the transitional region, in order to better evaluate the capability of LQEs. Recall that intermediate quality links are the hardest to assess as they are extremely dynamic and exhibit asymmetric connectivity (refer to Chapter 1 for the description of the three reception regions).

To achieve this goal, we propose to place the sensor nodes according to a radial layout, as shown in Figure 2.1, where nodes  $N_2..N_m$  are placed in

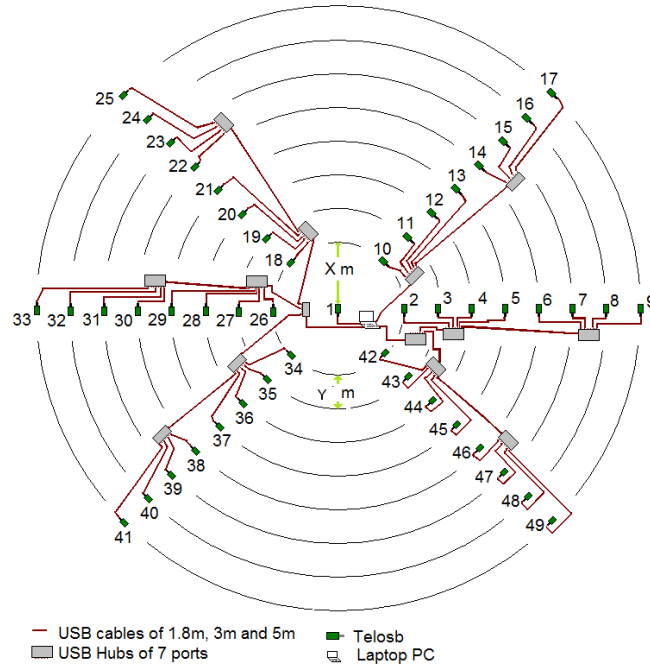


Figure 2.1: Nodes distribution forming a radial topology

different circles around a central node  $N_1$ . The distance (in meters) between two consecutive circles is denoted as  $y$ , and the first circle that is the nearest to  $N_1$  has a radius of  $x$  meters.

Since distance and direction are fundamental factors that affect the link quality, the underlying links  $N_1 \longleftrightarrow N_i$  will have different properties (qualities) by placing nodes  $N_2 \dots N_m$  at different distances and directions from the central node  $N_1$ .  $x$  and  $y$  values should be determined prior to experiments, to have links within the transitional region, which is typically quantified in the literature by means of the PRR.

It is important to note that apart from the network topology (radial topology in our case), network settings also impact the quality of the underlying links. Network settings may include the radio channel, the transmission power, and the environment type (e.g., indoor/outdoor).

## 2.4.2 Link measurements collection

The second step is to create a bidirectional data traffic over each link  $N_1 \longleftrightarrow N_i$ , enabling link measurements through packet-statistics collection. Packet-statistics collection consists of retrieving statistics, such as packet sequence number, from received and sent packets.

We propose two traffic patterns: *Burst*( $N, IPI, P$ ) and *Synch*( $W, IPI$ ). *Burst*( $N, IPI, P$ ) refers to a bursty traffic pattern, where the central node  $N_1$  first sends a burst of packets to a given node  $N_i$ . Then, node  $N_i$  sends its burst of packets back to  $N_1$ . This operation is repeated for  $P$  times, where  $P$  represents the total number of bursts. A burst is defined by two parameters:  $N$ ,



the number of packets in the burst and IPI, the Inter-Packets Interval in ms. On the other hand, *Synch*( $W, IPI$ ) refers to the synchronized traffic, where  $N_1$  and  $N_i$  are synchronized to exchange packets in a round-robin fashion. This traffic is characterized by two parameters: IPI and the total number of sent packets, noted by  $W$ .

In fact, to accurately assess link asymmetry, it is necessary to collect packet-statistics on both link directions at (almost) the same time. Therefore, the synchronized traffic pattern would be more convenient than the bursty traffic pattern (in particular for large bursts) to evaluate link asymmetry. One other reason to support two traffic patterns is that radio channels exhibit different behaviors with respect to these two traffic patterns, as it will be shown later. In [88], it has been observed that the traffic Inter-Packets Interval (IPI) has a noticeable impact on channel characteristics. For that reason, it is important to understand the performance of LQEs for different traffic configurations.

Exchanged traffic over each link allows for link measurements through packet-statistics collection. Some packet-statistics are evaluated at the receiver side (from received packets) such as global sequence number, time stamp, RSSI, LQI, and background noise. Such data is necessary to compute receiver-side LQEs. On the other hand, sender-side LQEs require other statistics collected at the sender side, such as sequence number, time stamp, packet retransmission count.

### 2.4.3 Data analysis

Data analysis comprises two different operations: The first operation is to generate link quality estimates with respect to each LQE, based on packet-statistics collected in the previous step. The second operation corresponds to the statistical analysis of these quality estimates. Concretely, the statistical analysis consist in generating statistical graphics for these LQEs, such as the empirical distribution function and the coefficient of variation, which allows to assess the reliability and the stability of LQEs.

## 2.5 Evaluation platforms

The performance evaluation of LQEs was conducted with both (i.) simulation using TOSSIM 2 simulator and (ii.) real experimentation using RadiaLE, our introduced testbed for benchmarking LQEs. An overview of these evaluation platforms is given next.

### 2.5.1 TOSSIM 2 simulator

TOSSIM 2.x [89] is an event-driven simulation environment for sensor networks. It is used to simulate the code of real sensor nodes that are implemented using the second release of TinyOS (TinyOS 2.x) [90]. TinyOS 2.x is an operating system and a programming framework developed at UC Berkeley and was specifically designed for sensor networks with small resource capacities. It is written in NesC [91], a C-based language that provides a support for the TinyOS component and concurrency model.

One of the main reasons behind the use of TOSSIM 2 is that it provides an accurate wireless channel model, without which it will not be possible to consider the simulation results as valid [56, 40]. Later on in this thesis, we confirm the accuracy of TOSSIM 2 channel model by conducted the study on LQEs statistical properties, with simulation and real experimentation and comparing the results.

### 2.5.1.1 Overview of TOSSIM 2 channel model

In this section, we present a brief overview of this model. The interested readers can refer to [56, 40] for more details on this channel model.

Basically, the wireless channel model of TOSSIM 2 relies on the *Link layer model* [40] and the *Closest-fit Pattern Matching* (CPM) model [56].

The link layer model of Zuniga et al. [40] corresponds to an analytical model of the PRR according to distance:  $PRR(d)$ . For non-coherent FSK modulation and Manchester encoding (used by MICAZ motes), this model is given by the following expression:

$$PRR(d) = (1 - \frac{1}{2} \cdot \exp(-\frac{SNR(d)}{2} \cdot \frac{B_N}{R}))^{8L} \quad (2.6)$$

Where,  $B_N$  is the noise bandwidth,  $R$  is the data rate in bits, and  $L$  is the packet size. These parameters are set to default values.

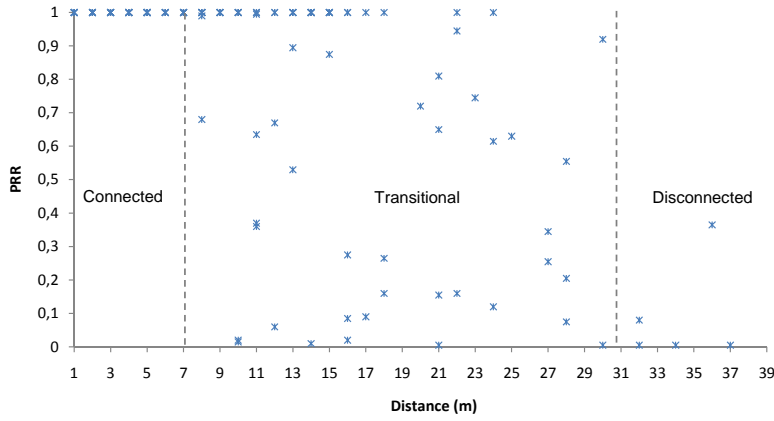
The  $SNR(d)$  is given by:

$$SNR(d) = RSS(d) - P_n \quad (2.7)$$

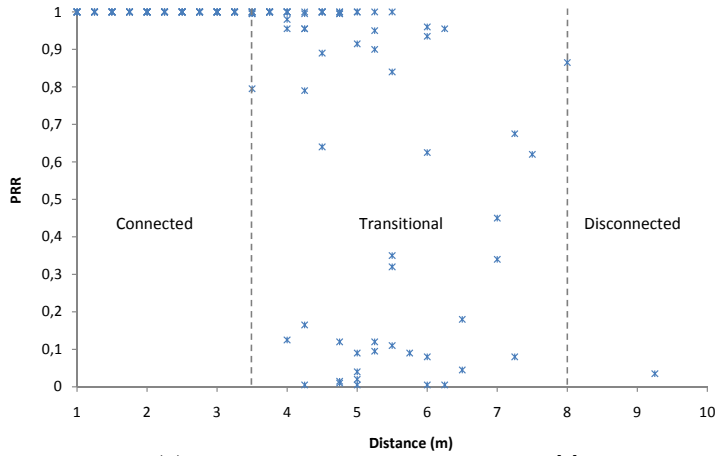
- $RSS(d)$  is the pure (i.e, without noise) received signal strength in dB as a function of distance. It is computed as:  $P_t - PathLoss(d)$ , where  $P_t$  is the transmission power in dB and  $PathLoss(d)$  is the path loss in dB as a function of distance.  $PathLoss(d)$  corresponds to the *log-normal shadowing* path loss model [47, 40].
- $P_n$  is the sampled noise floor in dB. TOSSIM 2 relies on the CPM model [56] to generate noise floor samples for a given link, which captures the temporal variation of the channel. The principal inputs of this model are the average noise floor at the receiver ( $\overline{P_n}$ ) the noise floor variance, and a noise trace file containing 100 readings.

An important feature of the link layer model is the fact that it takes into account the hardware variance, i.e. the variability of the transmission power among different senders and the variability of the noise floor among different receivers. The hardware variance is the main cause of link asymmetry. To model this variance, the transmission power and the noise floor are considered as Gaussian random variables. Given the variances of the noise floor and the transmission power respectively, the link layer model generates two Gaussian distributions for each variable. Thus, it assigns a transmission power  $P_t$  to each simulated sender and a noise floor  $\overline{P_n}$ , to each simulated receiver. For a given link,  $P_t$  is constant over time and  $\overline{P_n}$  is used to generate different noise floor readings (i.e. different  $P_n$ s) to capture the link dynamism.

Now, let's see how TOSSIM 2 uses the channel model presented above: At the beginning of the simulation and based on the channel and radio parameters



(a) Indoor environment: aisle of building [5]



(b) Outdoor environment: football field [5]

Figure 2.2: Illustration of TOSSIM 2 channel model reliability: the three reception regions

as well as the topology specification, determined by the user, TOSSIM 2 generates for each link (sender→receiver) the RSS, and the  $\overline{Pn}$ . TOSSIM 2 models packet reception over a link as a Bernoulli trial with probability equal to PRR. When a packet is received, a simulated receiver samples a noise floor reading ( $Pn$ ) using the CPM model and computes the PRR according the link layer model (Eq.4). Then, the receiver node generates a uniform random number (URN). The packet is received (and eventually acknowledged) if the URN is greater than PRR; otherwise it is considered as lost.

### 2.5.1.2 Advantages and shortcomings of TOSSIM 2 channel model

TOSSIM 2 channel model has the advantage of capturing important low-power links characteristics, namely spatial and temporal characteristics, as well as the asymmetry property. For instance, spatial characteristics are captured by modeling the three reception regions: connected, transitional and disconnected,

using the link layer model [40]. To illustrate this fact, we conducted extensive simulations for two environment settings and plotted the PRR as a function of distance, as shown in Figure 2.2. From this figure, it is possible to observe the three reception regions as observed with real measurements.

On the other hand, TOSSIM 2 presents some shortcomings that result from some assumptions. Indeed, TOSSIM 2 uses the log-normal shadowing model to model the path loss. This model has been shown to provide an accurate multipath channel model. However, it does not take into account the anisotropy property of the radio range, i.e. attenuation of the signal according to the receiver's direction. Therefore, TOSSIM 2 assumes that link quality does not vary according to direction, despite it models the variation according to distance.

Another assumption made by TOSSIM 2 is the fact that  $RSS(d)$ , which concerns a given link having a distance  $d$ , is constant over time. This assumption is justified by the fact that the link layer model is designed for static environments [40]. Nevertheless, the "real" received signal strength, which is the  $RSS(d)$  added to the noise floor ( $RSS + Pn$ ), varies according to time because TOSSIM 2 takes into account the variability of  $Pn$  over time using the CPM model[56]. Therefore, link quality (e.g.  $RSSI$ , PRR,  $SNR$ ) varies over time (for a given link), which captures the link temporal behavior.

## 2.5.2 RadiaLE experimental testbed

Although the performance evaluation of network protocols and mechanisms using network simulators can provide interesting conclusions, there is no guarantee on their validity or trustability level. This fact prompted researchers to build wireless network testbeds for a realistic performance evaluation. In this section, we present RadiaLE, our testbed that automates the experimental assessment of LQEs.

### 2.5.2.1 Existing experimental testbeds

Several testbeds have been designed for the the experimentation of WSNs. They can be classified into *general-purpose* testbeds and *special-purpose* testbeds. Most of existing testbeds, including MoteLab [92], Mirage [93], Twist [94], Kansei [95], and Emulab [96] are general-purpose testbeds. They have been designed and operated to be remotely used by several users having different research objectives. On the other hand, special-purpose testbeds, such as Scale [18] and Swat [88] are designed for a specific research objective.

General-purpose testbeds might be not suitable for benchmarking LQEs. Their tendency to cover multiple research objectives prevent them from satisfying some particular requirements. Namely, the physical topology of sensor nodes as well as the environment conditions cannot be managed by the user. However, to assess the performance of LQEs, it is mandatory to design a network topology, where the underlying links are of different qualities. Especially, it is highly recommended to have links with moderate quality and dynamic behaviour.

Many researchers develop their own tesbeds to achieve *a specific goal*. These belong the category of special-purpose testbeds. To our best knowledge, none of the existing testbeds was devoted for the performance evaluation of LQEs.

Some testbeds have been dedicated for link measurements, such as SCALE [18] and SWAT [88], but they were exploited for analyzing low-power link characteristics rather than the performance evaluation of LQEs. Some well-known WSN testbeds, belonging to this category are described in what follow:

SCALE [18] is a tool for measuring the Packet Reception Ratio (PRR) LQE. It is built using the EmStar programming model. Each sensor node runs a software stack, allowing for sending and receiving probe packets in a round robin fashion, retrieving packet-statistics, and sending them through serial communication. All Sensor nodes are connected to a central PC via serial cables and serial multiplexors. The PC runs different processes - one for each node in the testbed - that perform data collection. Based on the collected data, other processes running on the PC allow for connectivity assessment through the derivation of the PRR of each unidirectional link. Thus, the network connectivity can be visualized during the experiment runtime.

SWAT [88] is a tool for link measurements. The supported link quality metrics (or LQEs) include PRR and hardware-based metrics: *RSSI*, *LQI*, noise floor, and *SNR*. SWAT uses the same infrastructure as SCALE: sensor nodes (MICA2 or TelosB) are connected through serial connections or Ethernet to a central PC. SWAT provides two user-interfaces (UIs), written in HTML and PHP. Through the HTML UI, users can specify the experiment parameters. The interface invokes Python scripts to ensure host-mote communication for performing specific operations, namely sending commands to motes (to control them) and storing raw packet-statistics retrieved from motes into a database. The PHP UI is used to set-up link quality metrics, and to collect some statistics such as PRR over time and correlation between PRR and *RSSI*. Then the UI invokes Python scripts to process the collected data and display reports.

SCALE is compatible with old platforms (MICA 1 and MICA 2 motes) which do not support the *LQI* metric. This metric has been shown as important to understand and analyze channel behavior in WSNs [81]. On the other hand, SWAT is not practical for large-scale experiments, as some configuration tasks are performed manually. Both SWAT and SCALE allow for link measurements through packet-statistics collection but the collected data do not enable to compute various LQEs, namely sender-side LQEs, such as four-bit [76] and RNP [6]. The reason is that SWAT and SCALE do not collect sender-side packet-statistics (e.g. number of packet retransmissions).

Most of the existing testbeds use one-Burst traffic, where each node sends a burst of packets to each of their neighbours then passes the token to the next node to send its burst. This traffic pattern cannot accurately capture the link *Asymmetry* property as the two directions (uplink and downlink) will be assessed in separate time windows. Thus, traffic patterns that improve the accuracy of link Asymmetry assessment are mandatory. In addition, as it has been observed in [88], the traffic Inter-packets Interval has a noticeable impact on channel characteristics. For that reason, it is important to understand the performance of LQEs for different traffic configurations/patterns.

In what follows, we present RadiaLE, our testbed solution that solves the

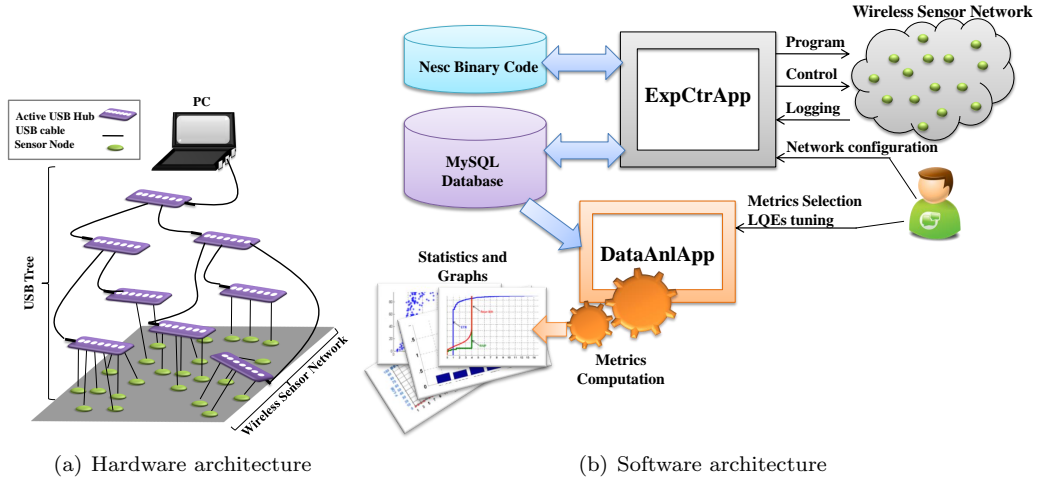


Figure 2.3: Testbed Hardware and Software architectures

above mentioned deficiencies in the existing testbeds. Especially, RadiaLE presents the following advantages/contributions:

- Provides abstractions to the implementation details by enabling its users to configure and control the network, as well as analyzing the collected packet-statistics database, using user-friendly graphical interfaces.
- Due to the flexibility and completeness of the collected database, a wide range of LQEs can be integrated in RadiaLE.
- Supports two traffic patterns, *Bursty* and *Synchronized*, having different parameters that can be tuned by the user in the network configuration step.
- The RadiaLE software is publicly available as an open-source at [24], together with all relevant information and supporting documentation (e.g. installation and user guides).

Note that RadiaLE can be complementary to General-purpose testbeds. In fact, as we have stated above, General-purpose testbeds such as MoteLab provide a remote access to their WSN so that researchers can easily perform experiments at their location. However, users have to provide the necessary code for communication, inter-nodes and between nodes and the remote computer. Hence, the idea is that RadiaLE users that do not have a WSN platform can use our free RadiaLE software tool together with the sensor nodes provided by a General-purpose testbed. As a matter of fact, we have tested RadiaLE software on MoteLab testbed in order to perform large-scale experiments. In these experiments we studied the impact of LQEs on CTP (Collection Tree routing Protocol) [12] (This study is presented in Chapter 4).

### 2.5.2.2 Overview of RadiaLE

RadiaLE allows to evaluate the performance of LQEs based on the general evaluation methodology presented in Section 2.4, basically by analyzing the

statistical properties of LQEs. In what follows, we give some implementation details in what concern RadiaLE hardware and software components as well as traffic patterns.

**2.5.2.2.1 Hardware components** The hardware architecture of RadiaLE, roughly illustrated in Figure 2.3(a), involves three main components: the sensor nodes, the USB tree, and the control station (e.g. laptop PC).

- **Sensor nodes:** The sensor nodes are programmed in nesC [91] over TinyOS 2.x [97]. They do not rely on a particular communicating technology such as Zigbee or 6LowPAN. They also do not use any particular protocol at MAC and network layers. In fact, we have designed traffic patterns that avoid collisions; and we have deployed a single-hop network in order to analyze the statistical properties of LQEs independently any external factor.

In our experiments with RadiaLE, we deployed TelosB motes [32], which are equipped with IEEE 802.15.4 radio compliant chip, namely the CC2420 radio chip [42]. Other platforms (e.g., MICAz) and other radio chip (e.g., CC1000) can also be used with RadiaLE framework. This requires some minor modifications at RadiaLE software tool (specifically, the Experiment Control Application and the nesC application). In fact, if users use platforms other than TelosB but based on the CC2420 radio chip, modifications should only concerns the computation of the sensing measures (e.g., temperature, humidity, and light). On the other hand, if users use different platforms based on other radio chip than the CC2420, additional modifications concerning RSSI and LQI reading, and channel setting should be carried out.

- **USB tree:** The motes are connected to a control station (PC) via a combination of USB cables and *active* USB hubs constituting a USB tree. This USB tree is used as a logging/control reliable channel between the motes and the PC.

Using *passive* USB cables, serial data can only be forwarded over distances that do not exceed 5 meters. RadiaLE uses *active* USB hubs, daisy-chained together, depending on the distance between the sensor node and the PC (refer to Figure 2.3), in order to forward serial data over large distances. Active USB hubs are also useful to connect a set of devices (motes or other USB hubs) as shown in Figure 2.3, and provides motes with power supply.

**2.5.2.2.2 Software components** RadiaLE software tool contains two independent applications: Experiment Control java application (ExpCtrApp), and Data Analysis Matlab application (DataAnlApp).

- **The experiment Control application (ExpCtrApp)** It provides user interfaces to ensure multiple functionalities, namely motes programming/-control, network configuration and data logging into a MySQL database

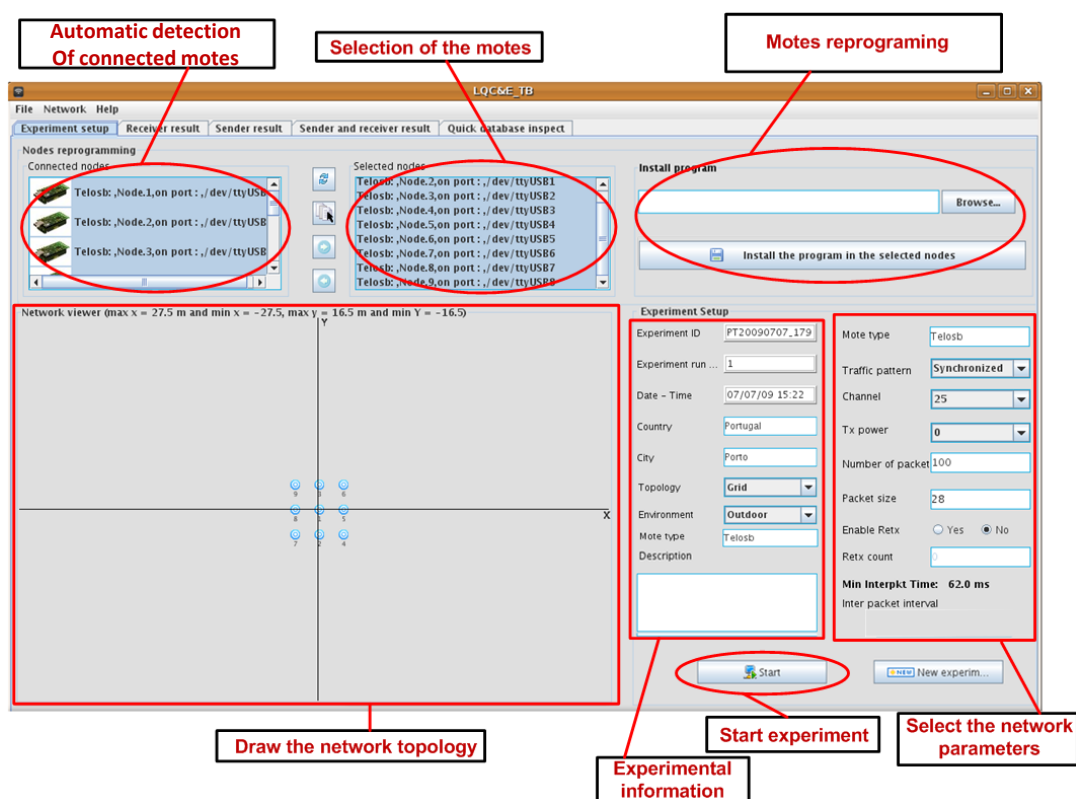


Figure 2.4: ExpCtrApp Java application main functionalities

(Figure 2.4). These functionalities are described next.

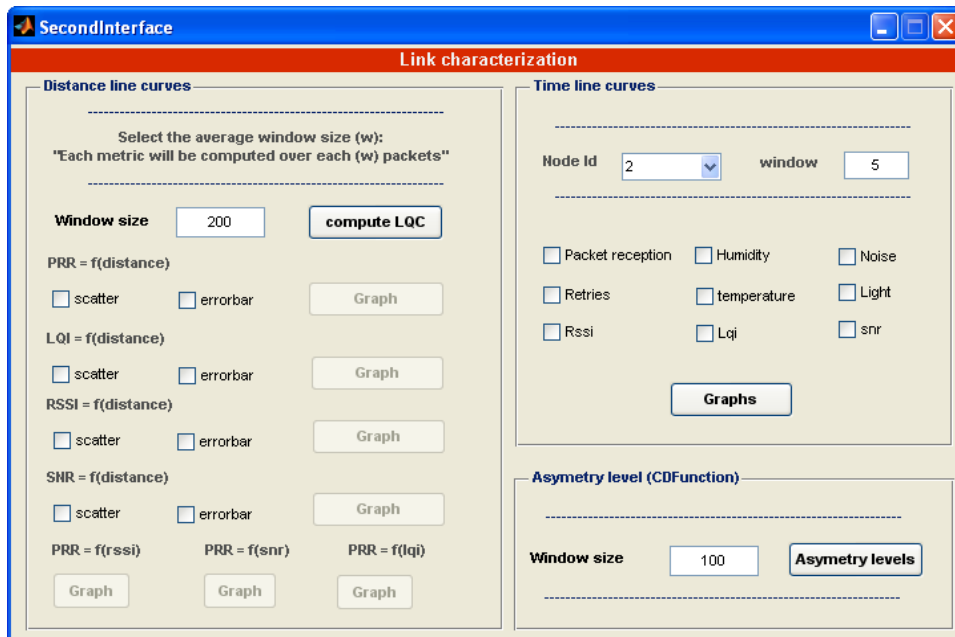
*Motes programming:* A nesC application defines a set of protocols for any bidirectional communication between the motes and between the motes and the ExpCtrApp. The ExpCtrApp automatically detects the motes connected to the PC and programs them by installing the nesC application binary code.

*Network configuration:* The ExpCtrApp enables the user to specify network parameters (e.g. traffic pattern, packets number/size, inter-packet interval, radio channel, transmission power, link layer retransmissions on/off and max. count). These settings are transmitted to the motes to start performing their tasks.

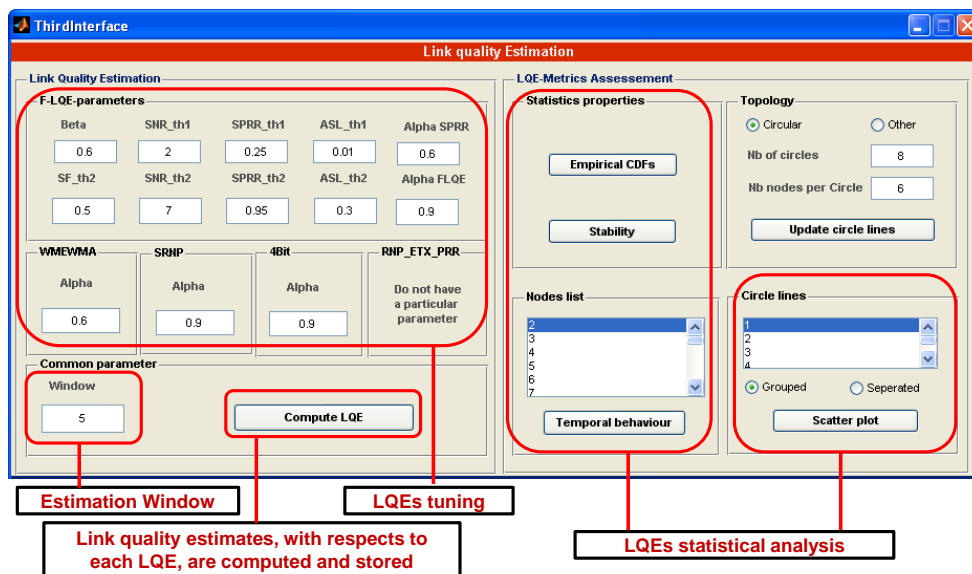
*Link measurements gathering:* Motes exchange data traffic in order to collect packet statistics such as sequence number, *RSSI*, *LQI*, *SNR*, time stamp or background noise, which are sent via USB to the ExpCtrApp in the PC, which stores these log data into a MySQL database.

*Motes control:* ExpCtrApp exchanges commands with the motes to control data transmission according to the traffic pattern set at the network configuration phase. Figure 4.5 illustrates the implementation of the bursty and synchronized traffics. Particularly, this figure shows the interaction between the PC (i.e. ExpCtrApp) and two motes constituting the link  $N_1 \longleftrightarrow N_i$ , through commands exchange. The ExpCtrApp also





(a) Links characterization interface



(b) Link Quality Estimation interface

Figure 2.5: DataAnlApp Matlab application main functionalities

provides: (i.) a *network viewer* to visualize the network map and the link quality metrics (e.g. PRR, RSSI) in real-time; and (ii.) a *database inspector* to view raw data retrieved from the notes in real-time.

- **The data analysis application (DataAnlApp)** The DataAnlApp application provides user interfaces that connects to the database, and process data to ensure two major functionalities (Figure 2.5).

The first functionality provides a set of configurable and customizable graphs that help understanding the channel behaviour, as illustrated in Figure 2.5(a).

The second functionality provides an assistance to RadiaLE users to evaluate the performance of their estimators, as illustrated in Figure 2.5(b). DataAnlApp proposes a set of LQEs that are configured and computed off-line (i.e., after the experiment finishes), based on the collected data available in the MySQL database. In fact, this constitute one of the interesting features of RadiaLE as it enables to perform the statistical analysis of a given LQE under different settings/configurations without the need to repeat experiments. Further, new LQEs can be integrated to the DataAnlApp and also validated without the need to repeat the experiment. Note the integration of any new LQE is possible thanks to the flexibility and completeness of the collected empirical data.

Once LQEs are computed, the DataAnlApp provides pertinent graphs to visualize their statistical properties and deduce their performances in terms of reliability and stability. Currently, DataAnlApp integrates most well-known LQEs (e.g., PRR, WMEWMA, ETX, RNP and four-bit).

**2.5.2.2.3 Traffic patterns** An important feature that distinguishes RadiaLE from existing testbeds is the fact that it provides two traffic patterns: Bursty and Synchronized (refer to Section 2.4 for their description). Figure 4.5 shows some implementation details illustrating the interaction between mote  $N_1$ , mote  $N_i$  and the PC, allowing for a Bursty or Synchronized traffic exchange between the two Motes.

## 2.6 Performance analysis

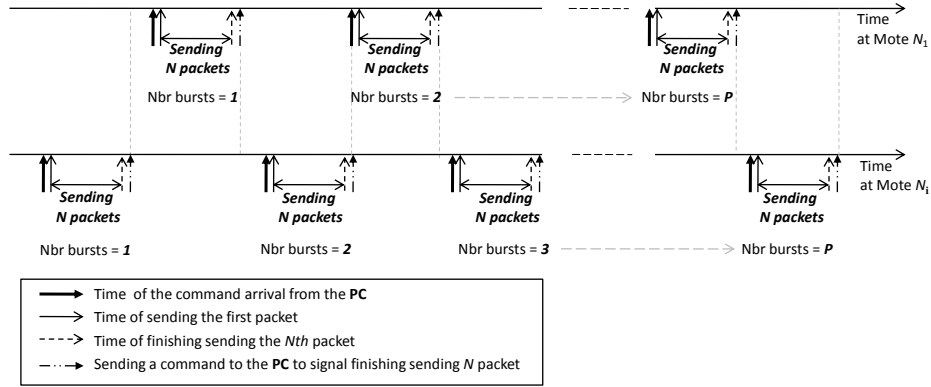
In this section, we conduct a comparative performance evaluation study of the considered LQEs, i.e, PRR, WMEWMA, ETX, RNP and four-bit, based on the evaluation methodology described in Section 2.4 and using TOSSIM 2 and RadiaLE as evaluation platforms. LQEs are set as follow: we have chosen a history control factor  $\alpha = 0.9$  for four-bit, as suggested in [76] and  $\alpha = 0.6$  for WMEWMA, as suggested in [70] and an estimation window  $w = 5$ .

For the fairness and brevity of this section, we start by presenting our experimental study and discussing the related results in detail. Then, we give a brief overview of our simulation study, as most simulation results are shared with experimental results.

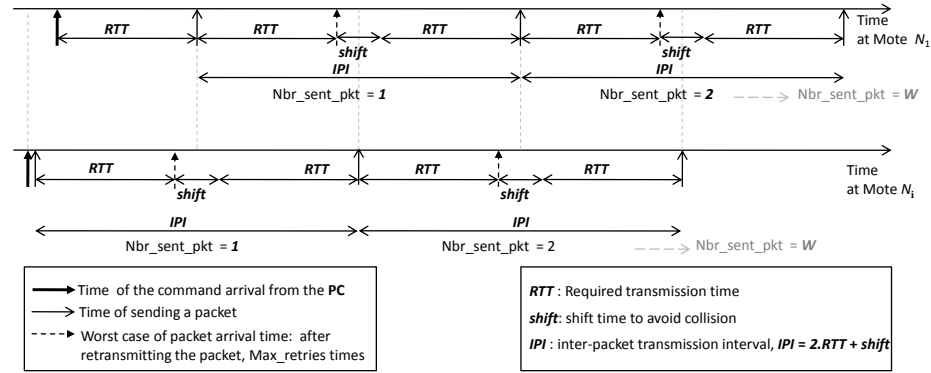
### 2.6.1 Experimental study

#### 2.6.1.1 Experiments description

In our experiments, we have deployed a single-hop network with 49 TelosB motes distributed according to the radial topology (refer to Figure 2.7 and



(a) *Burst*( $N, IPI, P$ ) traffic. After receiving the command from the PC, the mote sends a burst of  $N$  packets to the other mote, with an inter-packet interval equal to  $IPI$  ms. This operation is repeated until reaching a total number of sent bursts equal to  $P$ .



(b) *Synch*( $W, IPI$ ) traffic. After receiving the command from the PC, the mote sends a packet to the other mote each  $IPI$  ms, until reaching a total number of sent packets equal to  $W$ .

Figure 2.6: Interaction between mote  $N_1$ , mote  $N_i$  and the PC, allowing for a Bursty or Synchronized traffic exchange between the two Motes. When  $N_1$  and  $N_i$  finish their transmission, the PC triggers a new Bursty or Synchronized traffic exchange between  $N_1$  and  $N_{i+1}$ .

section 2.4.1), where  $x$  varies in  $\{2, 3\}$  meters and  $y$  is equal to 0.75 meter. Figure 2.7 shows the topology layout of the 49 motes at an outdoor environment (garden in the ISEP/Porto). Note that  $x$  and  $y$  were pre-determined through several experiments, prior to deployment. In each experiment, we set  $x$  and  $y$  to arbitrary values. At the end of the experiment, we measured the average PRR for each link. The chosen  $x$  and  $y$  are retained if the average PRR, with respect to each link, is between 90% and 10%. This means that the underlying links intermediate quality and therefore belong to the *transitional* region. As we have mentioned before, the transitional region is the most relevant context to assess the performance of LQEs. It can be identified by analyzing the average PRR of the link [29, 6]). Note that the average PRR of a given link is the average over different PRR samples. Each PRR sample is computed based on  $w$  received packets, where  $w$  is the estimation window.



Figure 2.7: Deployment of the Radial topology at an outdoor environment

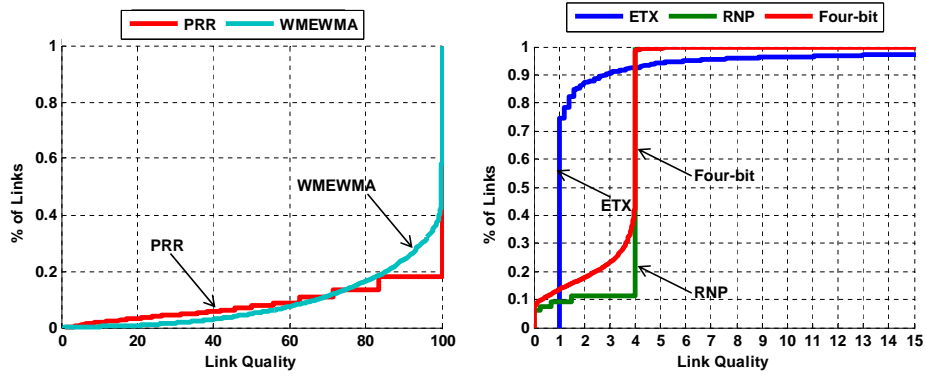


Figure 2.8: Empirical CDFs of LQEs, based on all the links in the network (Default Setting).

Using RadiaLE ExpCtrApp software, we performed extensive experimentations through different sets of experiments. In each experiments set, we varied a certain parameter to study its impact, and for each parameter modification the experiment was repeated. Parameters under consideration were traffic type (3 sorts of bursty traffic and 1 synchronized traffic), packet size (28/114 bytes), channel radio (20/26), and the maximum retransmissions count (0/6). The duration of each experiment was approximately 8 hours. Table 4.2 depicts the different settings for each experiments set. The transmission power was set to the minimum, -25 dBm, in order to reach the transitional region (i.e. have all links with moderate connectivity) at shorter distances. At the end of the experiments, we used DataAnlApp, the RadiaLE data analysis tool, to process packets-statistics retrieved from each bidirectional link  $N_1 \longleftrightarrow N_i$  and stored in a database, which results in LQEs computation and the statistical graphs generation.

### 2.6.1.2 Experimental results

In this section, we present the experimental results related to the performance comparison of PRR, WMEWMA, ETX, RNP, and four-bit, in terms of reliabil-

Table 2.2: Experiment scenarios. Burst(N, IPI, P) and Synch(W, IPI);  
 N: Number of packets per burst, IPI: inter-packets interval, P: number of bursts,  
 W: total number of packets.

	Traffic Type	Pkt Size	Channel	Rtx count
<b>Scenario 1: Impact of Traffic</b>	{Burst(100,100,10), Burst(200,500,4), Burst(100,1000,2), Synch(200,1000)}	28	26	6
<b>Scenario 2: Impact of Pkt Size</b>	Burst(100,100,10)	{28, 114}	26	6
<b>Scenario 3: Impact of Channel</b>	Burst(100,100,10)	28	{20, 26}	6
<b>Scenario 4: Impact of Rtx count</b>	Burst(100,100,10)	28	26	{0, 6}
<b>Scenario 5: Default Settings</b>	Burst(100,100,10)	28	26	6

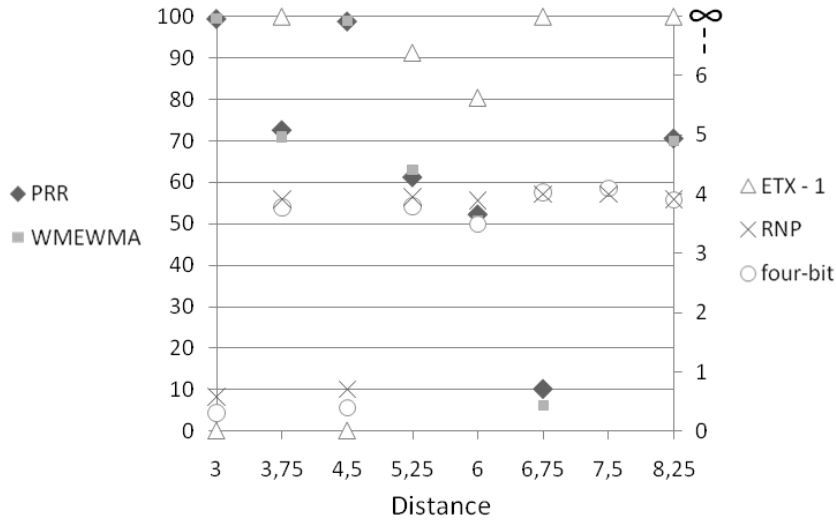


Figure 2.9: Scatter plot of each LQE according to distance in meters (Default Setting). Note we subtract 1 from ETX, to account only for the retransmitted packets.

ity and stability (refer to Section 2.4 for the definition of these criteria).

We point out that we collected empirical data from the 48 links of our Radial topology. Furthermore, we repeated the experiments twice; for  $x = 2$  and  $x = 3$ . In total, we obtained empirical data from  $48 * 2 = 96$  bidirectional links. We have considered all these links to conduct our statistical analysis study, namely the empirical CDF and the CV with respect to each LQE (e.g., in Figure 2.8

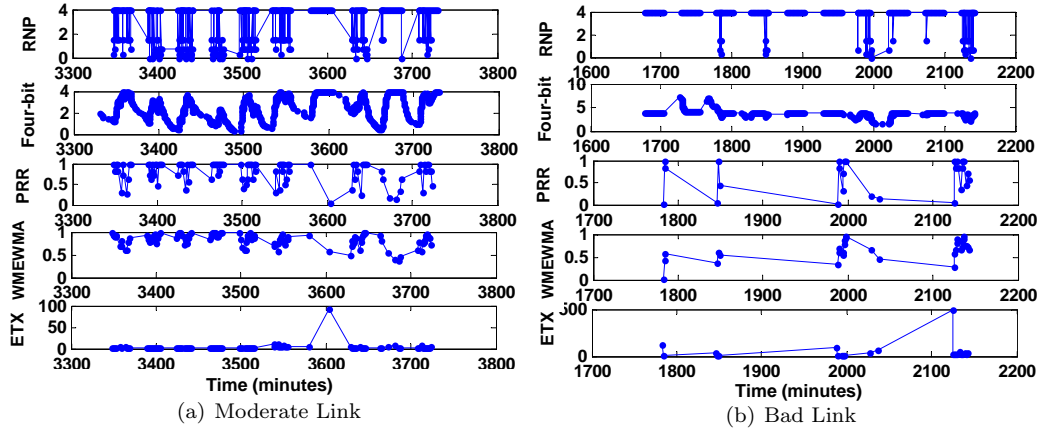


Figure 2.10: Temporal behaviour of LQEs when faced with links with different qualities (Default Setting)

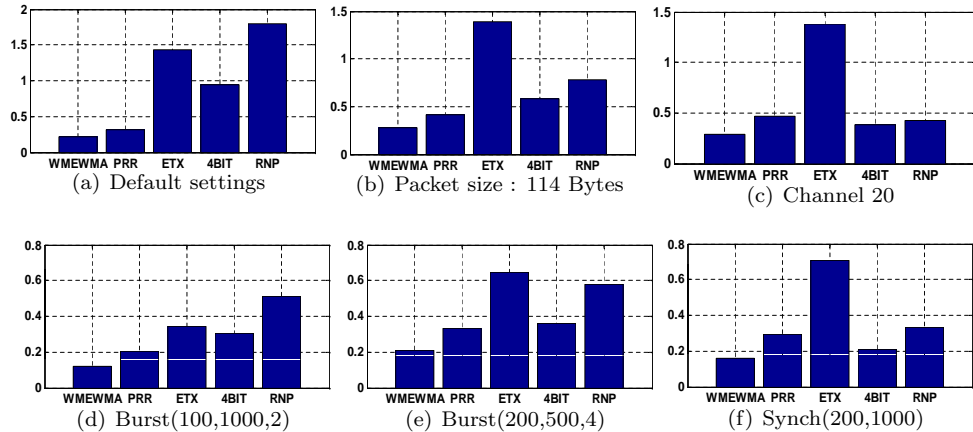


Figure 2.11: Stability of LQEs, for different network settings.

and Figure 2.11). Considering all these links together is important for the following reasons: (i) it improves the accuracy of our statistical analysis by considering a large sample set and (ii) it avoids having the statistical analysis being biased by several factors such as distance and direction, which provides a global understanding of LQEs behavior. In contrast, regarding the evolution of LQEs in space (e.g., in Figure 2.9) or in time (e.g., in Figure 2.10), the observation is made for a particular representative link, because considering all links is not relevant as it was the case with the CDF and CV.

**2.6.1.2.1 Reliability** Figure 2.8 presents the global empirical CDFs of all LQEs. This figure shows that PRR, WMEWMA, and ETX overestimate the link quality. For instance, this figure shows that almost 80% of links in the network have a PRR and WMEWMA greater than 84% (which is considered a high quality value). Also 75% of the links have ETX equal to 1, (i.e. 0 retrans-

missions, which also means high quality). The reason of this overestimation is the fact that the computation of these LQEs is based on PRR (i.e., link delivery). Therefore, these LQEs are only aware of link delivery, and not aware of the number of retransmissions made to deliver a packet. A packet that is lost after one retransmission or after  $n$  retransmissions will produce the same estimate. On the other hand, Figure 2.8 shows that four-bit and RNP underestimate the link quality. For example, Figure 2.8 shows that almost 90% of the links have RNP equal to 4 retransmissions (maximum value for RNP), which means that the link is of very bad quality. We observe that Four-bit provides a more balanced characterization of the link quality than RNP, since its computation also accounts for PRR. This underestimation of RNP and four-bit is due to the fact that they are not able to determine if these packets are received after these retransmissions or not. This discrepancy between PRR, WMEWMA, and ETX; and RNP and four-bit, is justified by the fact that most of the packets transmitted over the link are correctly received (high PRR) but after a certain number of retransmissions (high RNP).

These observations are confirmed by Figure 2.9, and Figure 2.10. Figure 2.9 illustrates the difference in decisions made by LQEs in assessing link quality. For instance, at a distance of 3.75 m, PRR and WMEWMA assess the link to have moderate quality (74% and 72% respectively), whereas RNP and four-bit assess the link to have poor quality (around 3.76 retransmissions). At a distance of 3.75 m, ETX assesses the link to have poor quality (more than 6 retransmissions)—i.e., differently from PRR and WMEWMA despite that each of PRR, WMEWMA and ETX is based on PRR in its computation. The reason is that the PRR in the other direction is low (refer to Eq.2.4).

PRR, WMEWMA, and ETX are computed at the receiver side, whereas RNP and four-bit are computed at the sender side. When the link is of a bad quality, the case of the link in Figure 2.10(b), packets are retransmitted many times without being able to be delivered at the receiver. Consequently, receiver side LQEs can not be updated and they are not responsive to link quality degradation. On the other hand, sender side LQEs are more responsive (i.e., reactive). This observation can be clearly understood from Figure 2.10(b).

**2.6.1.2.2 Stability** A link may show transient link quality fluctuations (Figure 2.10) due to many factors principally related to the environment, and also to the nature of low-power radios, which have been shown to be very prone to noise. LQEs should be robust against these fluctuations and provide stable link quality estimates. This property is of a paramount importance in WSNs. For instance, routing protocols do not have to recompute information when a link quality shows transient degradation, because rerouting is a very energy and time consuming operation.

To reason about this issue, we measured the sensitivity of the LQEs to transient fluctuations through the coefficient of variation of its estimates. Figure 2.11 compares the sensitivity (stability) of LQEs, with respect to different settings (refer to Table 4.2). According to this figure, we retain the following observations. First, WMEWMA is more stable than PRR and four-bit is more stable than RNP. The reason is that WMEWMA and four-bit use filtering to smooth PRR and RNP respectively. Second, except ETX, receiver-side LQEs, i.e. PRR and WMEWMA, are generally more stable than sender-side LQEs,

i.e. RNP and four-bit. ETX is receiver-side, yet it is shown as unstable. The reason is that when the PRR tends to 0 (very bad link) the ETX will tend to infinity, which increases the standard deviation of ETX link estimates.

## 2.6.2 Simulation study

In this section, we examine the statistical properties of LQEs using TOSSIM 2 simulation. Importantly, we compare the simulation results to the experimental results presented in the previous section in order to assess the reliability of TOSSIM 2.

### 2.6.2.1 Simulations description

As reported in Section 2.5.1.2, TOSSIM 2 assumes that link quality varies according to distance, but it does not vary according to direction. To cope with this limitation, we have considered the radial topology while eliminating the *direction* option, which results in a linear topology of nodes  $N_1..N_m$ , where the  $y$  parameter refers to the distance between two consecutive nodes except that between  $N_1$  and  $N_2$ , which corresponds to the  $x$  parameter.

Giving that, we have considered a single-hop network of 10 sensor nodes (i.e.,  $m = 10$ ), where  $y$  is fixed to 1 meter, and  $x$  varies in the set  $\{1, 8, 9.25, 10.5, 11.75, 17, 18.25, 19.5, 19.75, 27\}$ . We have chosen  $x$  values based on a prior study, where we analyzed the three reception regions in both indoor and outdoor environments. The result of this study can be illustrated in Figure 2.2. Hence, these particular values of  $x$  leads to a rich set of links, and copes with the limitation of TOSSIM 2 channel model.

The nodes do not rely on a particular communicating technology such as Zigbee or 6LowPAN. They also do not use any particular protocol at MAC and network layers.

The simulated network is set to an Indoor environment configuration, as described in [5] (The same simulation results have been found for an Outdoor environment configuration). The maximum retransmissions count is set to 6. Other parameters, such as the transmission power are kept to default values as TOSSIM 2 do not permit to tune them. Regarding the traffic pattern, nodes exchange a bursty traffic: Burst(400,720,6). Based on exchanged traffic, nodes perform link measurements through packet-statistic collection. LQEs are implemented at the nodes application level (Source codes are available in [24]) and computed based on the collected link measurements.

At the end of the simulation, we gather a trace file that contains, for each LQE, the different link quality estimates computed at each  $w$ . By processing the simulation trace file using a software tool similar to the DataAnlApp, the different statistical graphs are generated.

### 2.6.2.2 Simulation results

In this section, we present the simulation results related to the performance comparison of PRR, WMEWMA, ETX, RNP, and four-bit, in terms of reliability and stability.



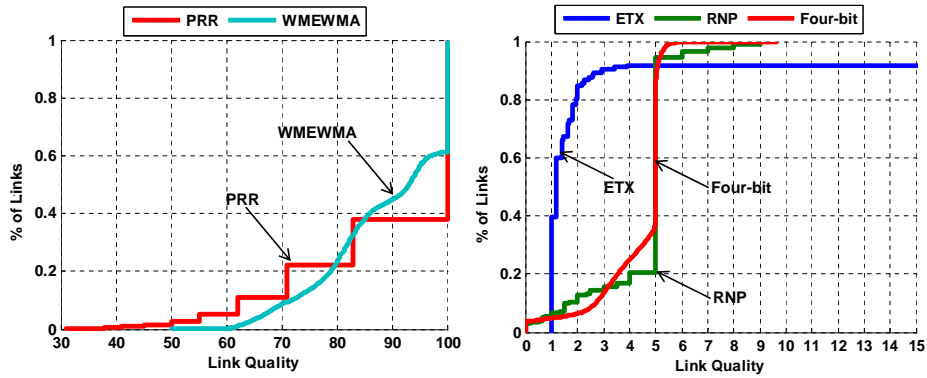


Figure 2.12: Empirical CDFs of LQEs, based on all the links in the simulated network, and observed by Tossim 2 simulation.

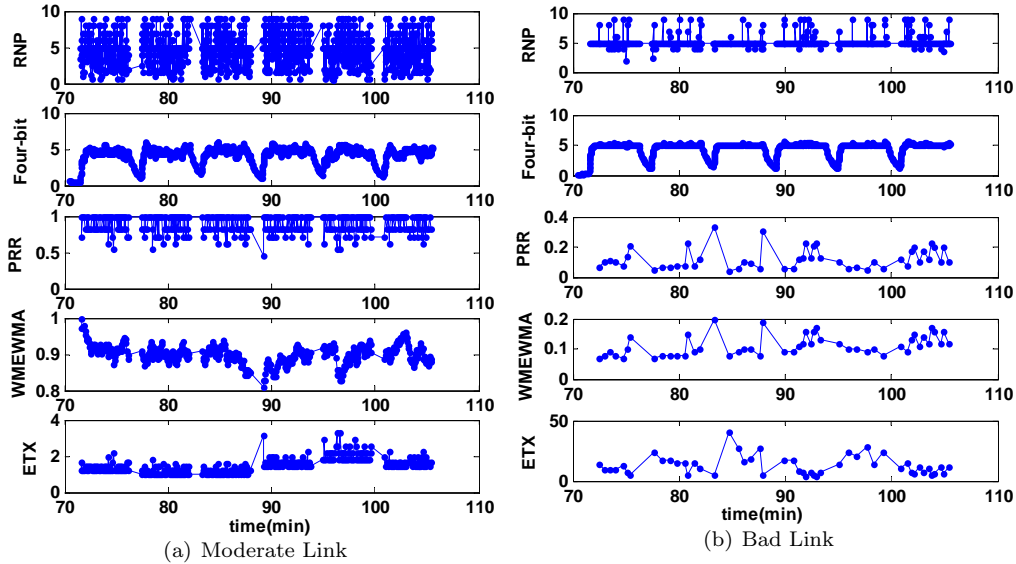


Figure 2.13: Temporal behaviour of LQEs when faced with links with different qualities, observed by Tossim 2 simulation

**2.6.2.2.1 Reliability** It can be clearly observed that the empirical CDF of LQEs, computed based on all links in the simulated networks and illustrated in Figure 2.12 has the same shape as the empirical CDF of LQEs computed based on real experiments (Figure 2.8). Consequently, it can be confirmed, based on these simulation results that PRR, WMEWMA, and ETX over-estimate link quality. On the other hand, RNP and four-bit under-estimate link quality. Moreover, RNP and four-bit are computed at the sender side and are more responsive to link quality degradation. This observation can be understood from the temporal behavior depicted in Figure 2.13.

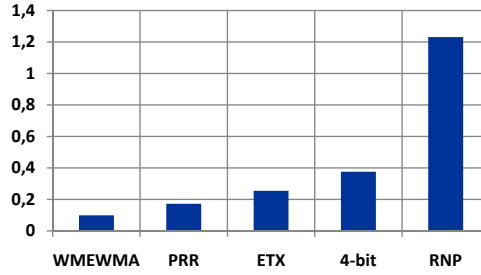


Figure 2.14: Stability of LQEs, observed by Tossim 2 simulation.

**2.6.2.2.2 Stability** Figure 2.14 shows that RNP and four-bit are more unstable than PRR and WMAWMA, as they are more responsive to link quality fluctuations. This finding confirms the results found in the experimental study. However, ETX is shown to be more instable in the experimental study than in simulation. The instability of ETX in the experimental study is due to the presence of very low PRRs (at the range of  $10^{-3}$ ). On the other hand, in simulation, PRR rarely takes low values. This should be due to the assumption that packet reception is a Bernoulli trial, and also to the non-ideality of random number generators. Nevertheless, it is well-known that simulation can not provide very accurate models, as very accurate models will be at the cost of high complexity and poor scalability.

### 2.6.2.3 TOSSIM 2 realism

In the above discussion, we have compared the simulation results to the experimental results. Hence, we can argue that TOSSIM 2 channel model provides a reasonable tradeoff between accuracy and simplicity. Nevertheless, recall that despite that TOSSIM 2 channel model captures important link properties, including spatial and temporal behaviors, and link asymmetry, it does not take into account the variation of the RSS according to the direction. In addition, TOSSIM 2 channel model assumes a static environment. Consequently, the RSS is constant according to time. What makes the channel variability is only the noise floor variation. In our study, these simplifications had not a great impact on the validity of the results, but they could be for other link-layer dependant studies.

## 2.7 Summary of the results

We have thoroughly analyzed and compared several well-know LQEs, namely PRR, WMEWMA, ETX, RNP and four-bit, by analyzing their statistical properties independently from higher layer protocols. The results of this study are summarized in Table 2.3. In particular, we retain the following general lessons:

- All the selected LQEs are not highly reliable, as they either overestimate or underestimate link quality. This is due to the fact that each LQE is only able to assess a single link aspect (e.g. reception ratio, packet retransmissions count) thus providing a partial link characterization.

Table 2.3: Comparison of considered LQEs

	Stability	Over-estimation	Under-estimation	Reactivity
<i>ETX</i>	☹	☹	-	☹
<i>four-bit</i>	☹	-	☹	☺
<i>PRR</i>	☺	☹	-	☹
<i>RNP</i>	☹	-	☹	☺
<b>WMEWMA</b>	☺	☹	-	☹

- Sender side LQEs, namely RNP and four-bit are more reactive to link quality degradation than receiver side LQEs, i.e. PRR, WMEWMA, and ETX.
- Reactivity and stability are at odds. A LQE can be either reactive or stable. However, being reactive is not very dramatic as the non stability can be repaired by higher layer protocols. Using the EWMA filter allows to provide a good tradeoff between stability and reactivity as seen with four-bit.

## 2.8 Conclusion

In this chapter, we performed an extensive comparative performance study of most well-known link quality estimators. This chapter presents four different contributions:

- An evaluation methodology that allows (i.) to properly set different types of links and different types of traffic, (ii.) to collect rich link measurements, and (iii.) to validate LQEs using a holistic and unified approach.
- RadiaLE testbed that automates the assessment of LQEs according to the introduced evaluation methodology. It comprises (i.) the hardware components of the WSN testbed and (ii.) a software tool for setting up and controlling the experiments, automating link measurements gathering through packets-statistics collection, and analyzing the collected data, allowing for LQEs evaluation.
- A thorough performance analysis of five representative LQEs, namely PRR, WMEWMA, ETX, RNP and four-bit, using both TOSSIM 2 simulator and RadiaLE experimental testbed.
- The assessment of the accuracy of TOSSIM 2 wireless channel model by comparing simulation results with empirical results obtained with RadiaLE.

The results of our study demonstrate that there is a need to design a new LQE that overcomes the limitations of existing LQEs. This estimator should combine several link quality metrics rather than considering a single metric, in

order to capture the different link aspects. However, “how to derive appropriate metrics ?” and “how to combine these metrics, giving that they have not necessarily the same magnitude order?” are just inevitable questions that are going to be answered in the next chapter.

## CHAPTER 3

---

# F-LQE: A Fuzzy Link Quality Estimator for Wireless Sensor Networks

---

### 3.1 Introduction

In previous chapters, we have classified LQEs to hardware-based and software-based. Hardware-based LQEs such as *SNR* and *LQI*, have been shown inaccurate, though their integration to software-based LQEs can enhance the accuracy of link quality estimation. Among software-based LQEs, we have selected a set of representative and well-known LQEs, and extensively analyzed their performance. Roughly, we found that none of these LQEs is highly reliable. This is due to the fact that they base their estimation on a single link property. However, other properties contribute to link quality, e.g. stability and asymmetry.

In order to better estimate link quality, we advocate combining several important link properties, to get a holistic characterization of the link. In this chapter, we propose a LQE that combines multiple metrics in order to achieve this goal. Link quality is affected by several aspects that are usually *imprecisely* measured. Fuzzy logic provides a convenient language to express and combine such imprecise knowledge. Thus, we resort to fuzzy logic to estimate link quality. Individual link properties are stated in linguistic terms and combined in a fuzzy rule whose evaluation gives the degree of membership of the link in the fuzzy subset of good quality links. An extensive performance analysis based on both simulation and real experimentation shows that F-LQE outperforms existing estimators.

### 3.2 Related work

Most of existing LQEs (hardware or software) rely on on a single link quality metric such as *PRR*, *LQI* or *RNP* and thus provide a partial characterization of the link. The design of composite LQEs that combine several metrics encompassing the different link aspects is a recent research problem. It arises two

major design challenges: The first is how to derive appropriate metrics that capture important link properties. The second challenge is how to combine these metrics, giving that they have not necessarily the same nature. Few research works addressed this problem [76, 22, 85]:

four-bit estimator combines RNP and the inverse of WMEWMA through EWMA filter [76]. However, as we have shown in the previous chapter, four-bit is not highly reliable as it has the limitation of evaluating a single link aspect: the number of packet retransmissions. Further, four-bit combines two metrics having different nature, using EWMA filter. Although filtering has been shown to be efficient to smooth the link quality estimates and provides a metric that resists to transient link quality changes [70], exploiting it for combining different metrics can lead to unstable link quality estimation (refer to previous chapter).

Rondinone et al. [22] suggest combining PRR and RSSI metrics in order to overcome the shortcomings of single metric LQEs, especially in what concern accuracy and stability. The combination is performed through the multiplication of PRR by the normalized average RSSI. To validate their estimator, the authors considered 10 different links and a bursty traffic over each link. PRR and average RSSI are computed based on each burst, where the burst length is equal to 250 packets. Then, by observing the temporal behavior of their LQE and that of PRR, the authors conclude that their estimator is able to classify links better than PRR, which implies of its accuracy. They also observed that their estimator is more stable than PRR. However, the introduced LQE has two limitations: First, its accuracy and stability are conditioned by a large estimation window (250 packets), which means that it can not quickly react to link quality changes. This observation has been partially confirmed by the authors. Second, the estimator does not provide a holistic characterization of the link as it ignores important link properties such as link asymmetry.

Boano et al. [85] propose the Triangle Metric that combines geometrically PRR, LQI, and SNR. The authors argued that each single metric has its own limitations and strengths. For example, Boano et al observed that LQI is useful to estimate bad links but does not perform well for other kinds of links. The PRR is good for intermediate links, while it often misclassifies good links as intermediate. Hence, the Triangle Metric merges the strength of each individual metric into a more accurate metric. To validate their estimator, the authors considered a static and a mobile scenarios. In both scenarios, different pairs of nodes periodically transmit packets at a rate of 64 packets per second. In the mobile scenario, the transmitter nodes are placed on moving humans. PRR, LQI, SNR, and Triangle Metric are computed based on each 10 received packets. Based on specific thresholds with respect to each metric, links are classified into Very Good, Good, Intermediate, and Bad. Then the authors tested the prediction capability of PRR, LQI, SNR, and Triangle Metric by comparing the classification provided by each of these metrics to future and long-term based (250 packets) classification. Hence, it has been found that in both mobile and static scenarios, the Triangle Metric provides more accurate prediction than PRR, LQI, SNR. The idea behind the Triangle Metric seems promising but again, this LQE does not provide a holistic characterization of the link as it ignores important link properties such as link asymmetry or stability.

### 3.3 Fuzzy logic for link quality estimation

The assessment of the quality of a radio link is a function of a number of metrics that are usually imprecisely estimated. Fuzzy logic provides a rigorous algebra for dealing with imprecise information. It is a mathematical discipline invented to express human reasoning in a rigorous mathematical notation. Unlike classical logic where a proposition is either true or false, fuzzy logic establishes the approximate truth value of a proposition based on linguistic variables and inference rules. Furthermore, fuzzy logic is a convenient method of combining conflicting objectives and expert human knowledge.

A linguistic variable is a variable whose values are words or sentences in natural or artificial language [98]. By using hedges like 'more', 'many', 'few', etc., and connectors like AND, OR, and NOT with linguistic variables, an expert can form rules, which will govern the approximate reasoning. In ordinary set theory, an element is either in a set or not in a set. In contrast, in fuzzy set theory, an element may partially belong to a set. A fuzzy set is defined as a class of objects with a continuum of grades of membership [99]. Formally, a fuzzy set  $A$  of a universe of discourse  $X = \{x\}$  is defined as  $A = \{x; \mu_A(x) \mid \forall x \in X\}$ , where  $X$  is a space of points and  $\mu_A(x)$  is a membership function of  $x \in X$  being an element of  $A$ . In general, the membership function  $\mu_A(\cdot)$  is a mapping from  $X$  to the interval  $[0,1]$ . If  $\mu_A(x) = 1$  or  $0$ ,  $\forall x \in X$ , then the fuzzy set  $A$  becomes an ordinary set [99].

**Example:** Packet delivery is an important link property whose goodness is highly correlated with the overall goodness of the link. It can be evaluated by the PRR link quality metric. Let PRR be the Packet Reception Ratio across a given link. According to classical logic, a link is declared good when its PRR is greater than a given threshold, say 0.95, and bad otherwise. For instance, given two different links, the first has a PRR equal to 95% and the second has a PRR equal to 94%. Classical logic declares only the first link as good. This example illustrates how PRR can only be imprecisely evaluated and classical reasoning fails to deal with such knowledge. Fuzzy Logic has been developed to handle this type of imprecise knowledge.

Let  $x \in [0..1]$  be a particular value of PRR and  $H$  be the fuzzy subset of links with high PRR. Then, for each  $x$  in the interval  $[0..1]$ ,  $\mu_H(x)$  indicates the extent to which the link is considered having a high PRR, and  $\mu_H(\cdot)$  is the membership function of the fuzzy subset of links with high PRR. Packet delivery is considered as a fuzzy variable, which is expressed in linguistic terms such as low packet delivery and high packet delivery. The membership of the link in the Fuzzy set of high packet delivery links, is a matter of degree rather than a yes-no situation. It ranges in the interval  $[0..1]$ . By recalling the previous example, the first link with PRR equal to 95%, can have a degree of membership in the fuzzy subset of high delivery links, equal to 1, whereas the second link with PRR equal to 94%, can have a degree of membership of 0.9. A possible membership function of high packet delivery links is illustrated in Figure 3.3 (refer to  $\mu_{SPRR}(\cdot)$ ).

During the lifetime of a WSN, the quality of a wireless channel is usually a function of several imprecisely measured channel properties, as packet delivery, asymmetry, and stability. Because of their imprecise nature, each such property can be conveniently expressed in linguistic terms. E.g., a channel can be unstable, stable, and highly stable. Each such term is a linguistic value for

the linguistic variable channel stability. The numerical interpretation of each linguistic value is defined in the form of a fuzzy subset, characterized by a particular fuzzy membership function. Now, suppose that we want to combine multiple link properties to properly assess the link quality, each such combination is performed by a Fuzzy IF-THEN Rule. A fuzzy rule combines the linguistic variables using connectors (operators) such as AND and OR. The evaluation of the rule using a fuzzy operator (e.g. Yager operator [100]) returns a membership degree that represents the link quality estimate.

We resort to Fuzzy Logic to estimate link quality and we propose F-LQE, which stands for Fuzzy logic-Link Quality Estimator. The goodness of the link depends on the goodness of its individual properties. Thus, the proposed LQE combines important link properties, expressed in linguistic terms, in a fuzzy rule. The evaluation of the fuzzy rule returns the degree of membership of the link in the fuzzy subset of good quality links. In the next section we first identify the most important properties that greatly impact the overall quality of the link. Then, we present a Fuzzy Rule that combines these properties to better estimate link quality.

## 3.4 Overview of F-LQE

### 3.4.1 Link quality metrics

In this section, we identify four link quality metrics to be considered in the design of F-LQE. Each metric describes an important link property. Selected link properties will be used in the next section to express the goodness of a given link.

Empirical studies such as [8, 28, 18, 29] have shown that the transmission range is defined by three regions (refer to Section 1.3.1):

- The connected region, where links are often (1) of high packet delivery, i.e. PRR is greater than 90%, (2) stable, and (3) symmetric.
- The transitional region, where links are (1) of moderate packet delivery, i.e. PRR (in long-term assessment, e.g., based on 200 packets) is between 10% and 90%, (2) unstable, i.e. PRR (in short-term assessment e.g., based 5 packets) fluctuates between 0% and 100%, and (3) often asymmetric.
- The disconnected region, where links (1) have low packet delivery, i.e. PRR is less than 10%, and (2) are overall inadequate for communication.

From these observations, it can be easily inferred that three main properties characterize a link in WSNs: *Packet Delivery*, *Asymmetry*, and *Stability*. These properties can be assessed by software-based metrics such as PRR. On the other hand, *Channel Quality* is another important link property that is complementary to previous ones. It is assessed by hardware-based metrics and impacted by channel characteristics (interference, multi-path effects, etc.). Here, we make a difference between “channel quality” and “link quality”. We define channel quality as a particular property of the communication link, which can be assessed by hardware-based metrics such as LQI and SNR. Link quality represents the overall quality of the communication link, as it takes into account all (or a



set of) link properties, including channel quality property.

Next, we derive four link quality metrics for the evaluation of selected link properties, namely packet delivery, asymmetry, stability, and channel quality.

#### 3.4.1.1 Packet delivery

Link packet delivery represents the capacity of the link to successfully deliver data. This property is captured by some existing LQEs such as PRR, WMEWMA, and ETX, but not by others, such as RNP. F-LQE accounts for the packet delivery of the link by a measure of SPRR, which stands for Smoothed PRR. The SPRR is exactly the WMEWMA [70]. It applies EWMA filter on PRR to smooth it, thus providing a metric that resists to transient fluctuation of PRRs, yet is responsive to major link quality changes. SPRR is then given by the following expression:

$$SPRR(\alpha, w) = \alpha \times SPRR + (1 - \alpha) \times PRR \quad (3.1)$$

where  $\alpha \in [0..1]$  controls the smoothness and  $w$  is the estimation window.

Although SPRR can accurately assess the link packet delivery property, it is not able to differentiate between a high delivery stable link, and a high delivery unstable link. Both links may have the same high delivery value, say 100%, but the first should be significantly better than the second. The first link is resilient to external effects and it typically belongs to the connected region. On the other hand, the second might be within the transitional region, where the received signal strength is weak so that any minor environmental change such as shadowing or interference can significantly change the link packet delivery. This example shows how it is important to assess link stability besides link packet delivery, in order to provide a more accurate link quality estimation. Next, we introduce the metric considered by F-LQE, for the assessment of link stability.

#### 3.4.1.2 Stability

Link stability (or variability) is of a paramount importance for network protocols that preferably forward data over stable links in order to minimize retransmissions and topological changes. F-LQE assesses the stability of the link by the measure of the coefficient-of-variation of PRR, noted as SF (Stability Factor):

$$SF = \frac{\sigma_{PRR}}{\mu_{PRR}} \quad (3.2)$$

where  $\sigma_{PRR}$  is the standard deviation of  $n$  measured  $PRRs$ , and  $\mu_{PRR}$  is the mean of  $n$  measured  $PRRs$ .

The algorithm of SF metric computation is illustrated in Figure 3.1: SF is basically computed based on a history of 30  $PRRs$ . We adopt the idea of “sliding window”, for the update of the  $PRRs$  history at a new measure of PRR. We choose 30 as the history length to ensure a certain confidence for the computation of the coefficient of variation. Nevertheless, at network startup, we anticipate the computation of SF by considering only a history of 5  $PRRs$  and as long as packets are received, the  $PRRs$  history is feeded back at every new measure of PRR, until collecting the 30  $PRRs$  values.

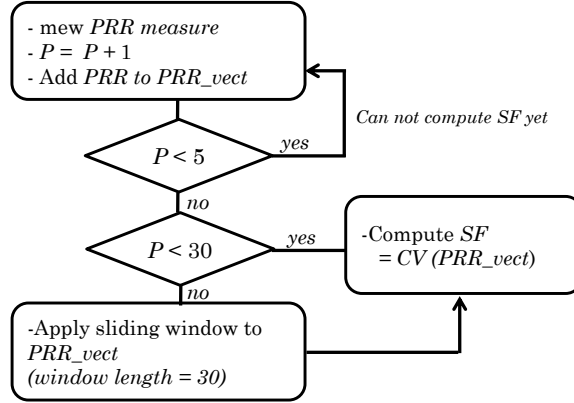


Figure 3.1: Algorithm of SF computation.  $P$  is the number of computed  $PRRs$ , initially  $P = 0$  and  $PRR\_vect$  is an array that contains a set of measured  $PRRs$ .

The combination of SF and SPRR allows to assess the link packet delivery while taking into account its stability level. Now, let's consider two links, both having high delivery and high stability level. Further, the first link has low asymmetry level while the second has high asymmetry level which makes some acknowledgment packets not reaching the transmitter. Consequently, the second link involves more MAC retransmissions for packet delivery. Hence, it is clear that although both links have high delivery and high stability, the second link appears better than the second due to its low asymmetry. This example illustrates how packet delivery and stability are not sufficient to accurately identify good links. Next, we introduce the metric considered by F-LQE, for the assessment of link asymmetry level.

### 3.4.1.3 Asymmetry

Link asymmetry is the difference in connectivity between the forward link and the backward link. Communication between sensor nodes is usually bidirectional. Empirical studies such as [8] have shown that links asymmetry is due to the discrepancy in terms of hardware calibration, i.e. nodes do not have the same effective transmission power, reception sensitivity and noise floor. Therefore, it is not sufficient to estimate the link quality as the quality of the link in one direction. While some LQEs, such as ETX and four-bit, take into account link asymmetry, other estimators including PRR, *WMAWMA* and RNP, do not. F-LQE takes into account link asymmetry by measuring the difference between PRR of the forward link ( $PRR_{forward}$ ) and the PRR of backward link ( $PRR_{backward}$ ), noted as ASL (ASymmetry Level):

$$ASL(w) = | PRR_{forward} - PRR_{backward} | \quad (3.3)$$

The ASL metric gives an idea on whether a transmitted packet can be acknowledged or not. In fact, for a given sender, when the forward is of high PRR and the backward is of bad PRR, a correctly received packet would not be acknowledged or at least acknowledged after a certain number of retransmissions. The ASL captures this effect, which cannot be detected by the PRR or SPRR

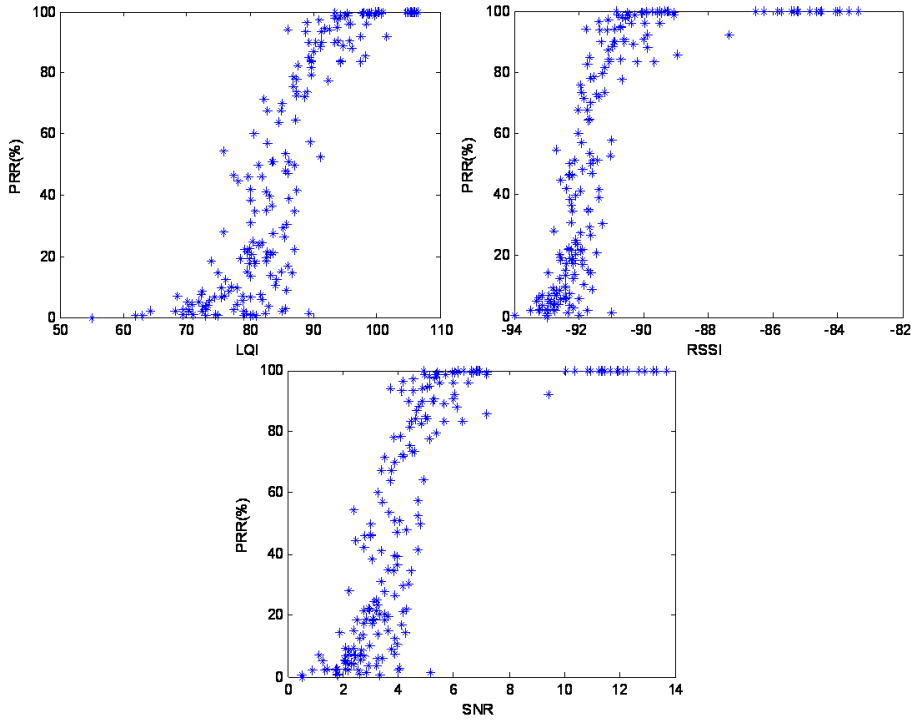


Figure 3.2: Hardware-based metrics as a function of PRR. These curves are obtained from experimentation with RadiaLE (refer to Table 2.2 — Default Setting).

alone.

ASL, SF, and SPRR represent software-based metrics. Several studies such as [72] and [55], argued that hardware-based metrics, such as SNR, RSSI, and LQI, are inaccurate when used individually, but their integration to software-based metrics improve their accuracy. In other words, hardware-based and software-based metrics are complementary. Particularly, hardware-based metrics are convenient to evaluate the channel quality.

To illustrate this fact, we have analyzed the curves in Figure 3.2. These curves illustrate hardware-based metrics, namely LQI, RSSI, and SNR as a function of PRR. Each measure of LQI, RSSI, or SNR is an average over  $w$  values, where  $w$  is also the estimation window of PRR, set to 200 packets. Figure 3.2 show that PRR metric can not differentiate between “good” and “very good” links. On the other hand, hardware-based metrics, especially SNR and RSSI can only differentiate between “very good” links and the rest. For example, consider tow links having perfect packet delivery, i.e., PRR equal to 100%. The first link has SNR equal to 13 dB and the second has SNR equal to 6 dB. According to PRR, both links are of ”very good” quality. This classification is not correct if we take into consideration the SNR: The fist link should be of ”very good” quality as it belongs to the connected region, while the second link is of ”Good” quality as it is in the border of the transitional region (refer to

Section 1.3.2/ Observation 3). A link in the transitional region is susceptible to drop considerably with a small change in the noise floor.

#### 3.4.1.4 Channel quality

F-LQE assesses channel quality through the measure of the SNR. In fact, as reported in Section 1.5.1 /Observation 6, SNR is better than RSSI. It is also better than LQI as it can better identify very good quality links as depicted in Figure 3.2.

The SNR metric can be derived by subtracting the noise floor ( $N$ ) from the received signal ( $S$ ), both in dBm. The  $S$  can be deduced by sampling the RSSI at the packet reception, and  $N$  can be derived from the RSSI sample just after the packet reception. In our proposed LQE, we average SNR, over  $w$  received packets to get ASNR (Average SNR): the link quality metric for the channel assessment.

### 3.4.2 Combination of link quality metrics

#### 3.4.2.1 Fuzzy rule

F-LQE considers each of the link properties mentioned in the previous section as a different fuzzy variable. The goodness (i.e. high quality) of a link is characterized by the following rule:

**IF** the link has *high packet delivery* AND *low asymmetry* AND *high stability* AND *high channel quality* **THEN** it has *high quality*.

Here, *high packet delivery*, *low asymmetry*, *high stability*, *high channel quality*, and *high goodness* are linguistic values for the fuzzy variables packet delivery, asymmetry level, stability, channel quality, and quality (refers to link quality). Using and-like compensatory operator of [100], the above rule translates to the following equation of the fuzzy measure of the link  $i$  high quality.

$$\mu(i) = \beta \cdot \min(\mu_{SPRR}(i), \mu_{ASL}(i), \mu_{SF}(i), \mu_{ASNR}(i)) + (1 - \beta) \cdot \text{mean}(\mu_{SPRR}(i), \mu_{ASL}(i), \mu_{SF}(i), \mu_{ASNR}(i)) \quad (3.4)$$

$\mu(i)$  is the membership in the fuzzy subset of high quality links. The parameter  $\beta$  is a constant in [0..1]. Recommended values for  $\beta$  are in the range [0.5..0.8] where 0.6 usually gives the best results [101], which is also confirmed in this work (see Section 3.5.2.1).  $\mu_{SPRR}$ ,  $\mu_{ASL}$ ,  $\mu_{SF}$ , and  $\mu_{ASNR}$  represent membership functions in the fuzzy subsets of high packet delivery, low asymmetry, low stability, and high channel quality, respectively.

#### 3.4.2.2 Membership functions

All membership functions have piecewise linear forms and then have low computation complexity. They are determined by two thresholds, as it is shown by Figure 3.3.

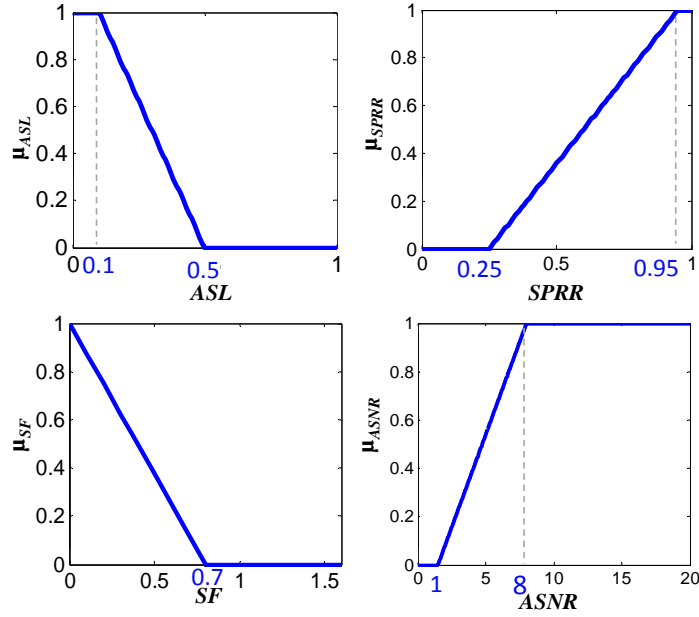


Figure 3.3: Definition of membership functions

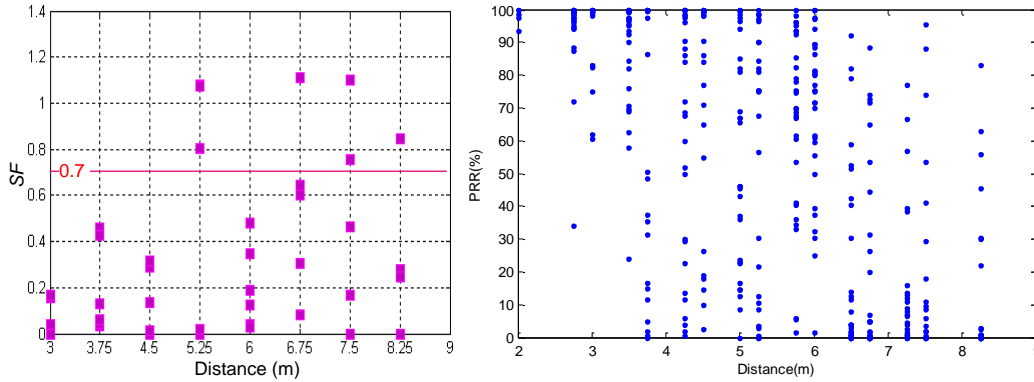


Figure 3.4: SF threshold determination based on curves obtained from real experimentation with RadiaLE (refer to Table 2.2 — Default Setting)).

The choice of the two thresholds, for the membership functions  $\mu_{SPRR}$  and  $\mu_{ASL}$  can be tuned according the application requirements. We have chosen reasonable values of these thresholds, with respect to each membership function. For  $\mu_{SPRR}$ , for values of SPRR below 25%, the link is considered totally out of the fuzzy subset of links with high packet delivery. Starting from 95%, the membership to the fuzzy subset of links with high packet delivery is of 1. For values of SPRR between 25% and 95%, the membership increases linearly from 0 to 1. The same reasoning holds for  $\mu_{ASL}$ .

The membership function  $\mu_{SF}$  differs slightly from the other ones as the two thresholds are superposed. A link has 1 as membership to the fuzzy subset of links with high stability, only when the measured SF is equal to 0. For SF

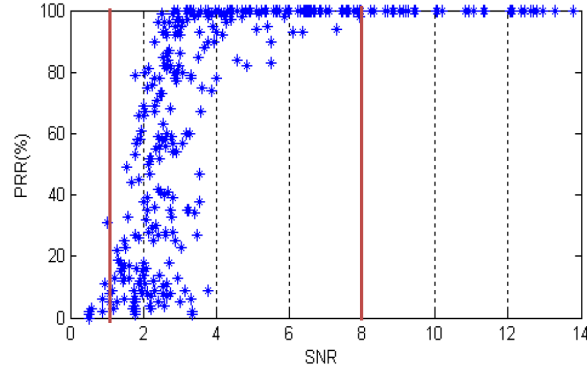


Figure 3.5: PRR/SNR curve obtained from real experimentation with RadiaLE (refer to Table 2.2 — Default Setting)). For ASNR greater than 8dBm, the PRR is equal to 100%, and for ASNR less than 1 dBm, the PRR is less than 25%. In between, a small variation in the ASNR can cause a big difference in the PRR; links are typically in the transitional region.

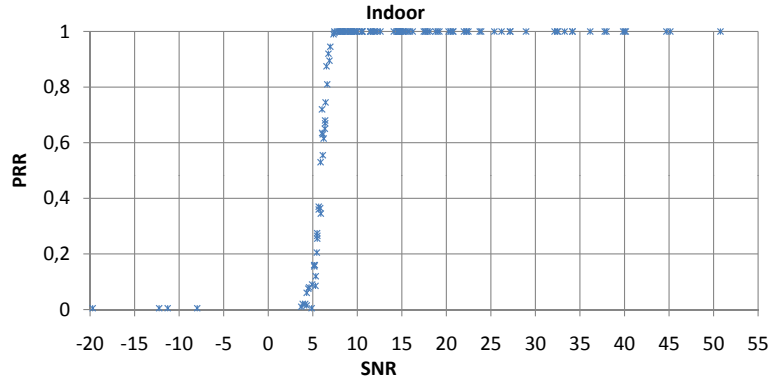


Figure 3.6: PRR/SNR curve obtained from simulation with TOSSIM 2 (indoor environment[5]). For ASNR greater than 9dBm, the PRR is equal to 100%, and for ASNR less than 5 dBm, the PRR is less than 25%. In between, a small variation in the ASNR can cause a big difference in the PRR; links are typically in the transitional region.

values greater than 0, the link membership decreases linearly to achieves 0 when SF is equal to 0.7. The value 0.7 has been chosen by analyzing the SF of all experienced links in our experimental study. Experiments were conducted under different network conditions (refer to Table 2.2). We generate the SF/*Distance* and PRR/*Distance* curves for each network setting. Figure 3.4 shows these curves for the default setting. The SF/*Distance* curve shows that when SF is equal to 0.7, the corresponding distance between the transmitter and the receiver is around 7 meters. PRR/*Distance* curve shows that for this distance (i.e., 7 meters), the link is in the middle of transitional region and thus might be very unstable.

The choice of the two thresholds for the membership function  $\mu_{ASNR}$  depends

on the environment and the hardware characteristics. In what follow, we present a detailed analysis for an efficient determination of these two thresholds.

In previous empirical studies, such as [55], based on the PRR/SNR curve, the existence of two SNR thresholds has been proven. When SNR is larger than the first threshold, the PRR is greater than 95% almost all the time, which implies good channel quality. If SNR is less than the second threshold, the PRR is lower than 25 % most of the time and the channel quality is bad. These thresholds are determined from the PRR/SNR curve, which is in turn determined experimentally. In fact, each measure of SNR in the PRR/SNR curve is an average over  $w$  values, where  $w$  is also the estimation window of PRR. In the rest of this section we note this SNR measure as ASNR. In order to gather the this curve, we carried out a set of experiments, using our RadiaLE testbed. Experiments were conducted under different network conditions (refer to Table 2.2). We generate the PRR/SNR curve for each network setting and we set  $w$  to 200 packets.

Figure 3.5 depicts the PRR/SNR curve for the default setting. The convenient choice of the two ASNR thresholds can be easily inferred from this curve (1 dBm and 8 dBm). Notice that these thresholds are the same for all PRR/SNR curves (settings), as we found that the curves have similar shapes. We have also conducted extensive simulation to gather the PRR/SNR curve shown in Figure 3.6 and infer the two ASNR thresholds (5 dBm and 8 dBm). We use these thresholds to tune F-LQE for our simulation study that will be presented later on.

### 3.4.2.3 F-LQE expression

The final step toward F-LQE computation is detailed in this section. We consider the following link quality metric (LQ):

$$LQ(w) = 100 \cdot \mu(i) \quad (3.5)$$

$LQ$  combines SPRR, ASL, SF and ASL to provide a comprehensive assessment of the link. It attributes a score to the link, ranging in  $[0..100]$ , where 100 is the best link quality and 0 is the worst. Using EWMA filter, we smooth  $LQ$  to get the F-LQE metric:

$$FLQE(\alpha, w) = \alpha \cdot FLQE + (1 - \alpha) \cdot LQ \quad (3.6)$$

where,  $\alpha = 0.9$ , to provide stable link quality estimates. Notice that  $w$  is the estimation window, meaning that a node estimates link quality, i.e. computes F-LQE, based on each  $w$  received packets.

Eq.3.4 assumes that the mote has available data to compute the SF and the ASL. However, SF can be computed only when the mote has at least 5 measures of PRR (refer to Figure 3.1) and ASL can be computed only when the mote has both forward and backward  $PRRs$  (refer to Eq.3.3). Therefore, we introduced a simple mechanism that consists in the following: a node wishes to estimate link quality by considering different link properties, evaluated by the SPRR, ASNR, ASL, and SF. When one or both ASL and SF can not be computed due to the lack of some data, the node ignores the corresponding metric(s) in the computation of the membership function  $\mu(i)$  in Eq.3.4. For instance, when the node is not able to compute both ASL and SF,  $\mu(i)$  in Eq.3.4 becomes:

$$\mu(i) = \beta \cdot \min(\mu_{SPRR}(i), \mu_{ASNR}(i)) + (1 - \beta) \cdot \text{mean}(\mu_{SPRR}(i), \mu_{ASNR}(i)) \quad (3.7)$$

## 3.5 Performance analysis

### 3.5.1 Methodology

To validate F-LQE, we have extended the comparative performance study of LQEs presented in Chapter 2, while including F-LQE in the set of LQEs under-evaluation. Recall that our evaluation methodology consists in analyzing and understanding the statistical properties of LQEs, independently of any external factor, such as collisions and routing. These statistical properties impact their performance, mainly in terms of reliability and stability. As for the evaluation platforms, we use TOSSIM 2 simulator as well as RadiaLE testbed for real experimentation.

Hence, we implemented and integrated F-LQE to TOSSIM 2 and RadiaLE and performed a set of simulations and experimentations using the same settings and scenarios as in the previous study presented in chapter 2 (refer to Section 2.6.1.1 and Section 2.6.2.1 for the experiment and simulation settings respectively).

### 3.5.2 Experimental results

#### 3.5.2.1 Reliability

The reliability of F-LQE is tested by studying (*i.*) the temporal behavior (Figure 3.7), and (*ii.*) the distribution of link quality estimates, illustrated by the a scatter plot (Figure 3.8) and the empirical cumulative distribution function, CDF, (Figure 3.9).

**3.5.2.1.1 Temporal behavior** Figure 3.7 uses four different links to show the temporal behaviour of each individual metric that constitutes F-LQE and its overall behavior. It also presents the results from other existing LQEs. From this figure, it can be observed that all LQEs agree that the first link (Figure 3.7(a)) is of very good quality. This is expected since links of good quality are easy to estimate as they tend to be stable and symmetric [6, 8]. On the other hand, moderate and bad links which are typically those of the transitional region and the disconnected region respectively, are more difficult to characterize.

Figure 3.7(b) shows how F-LQE outperforms existing LQEs because they are not able to distinguish between links, especially good links and very good links. In fact, let's observe the temporal behaviour of the link in Figure 3.7(b), until the time *3660 min* (just before the link quality fluctuation). PRR, SPRR, and ETX are based on PRR in their computation. They account for only one property: link delivery for PRR and SPRR; and packet retransmissions count for ETX. These LQEs declare the link as of very good quality. The same link quality state is declared by RNP and four-bit, which also account for a unique link property: packet retransmissions count. However, our link should not have a very good quality due to the low ASNR value. In fact, the measured ASNR values are close to the receiver sensitivity. Consequently, the channel is of moderate quality, which prevents the link of being declared as "very good". In addition, the good properties that the link have are likely due to the constructive interference effect. On the other hand, F-LQE detects the real link state by considering different link properties. Indeed the link shown in Figure 3.7(b)



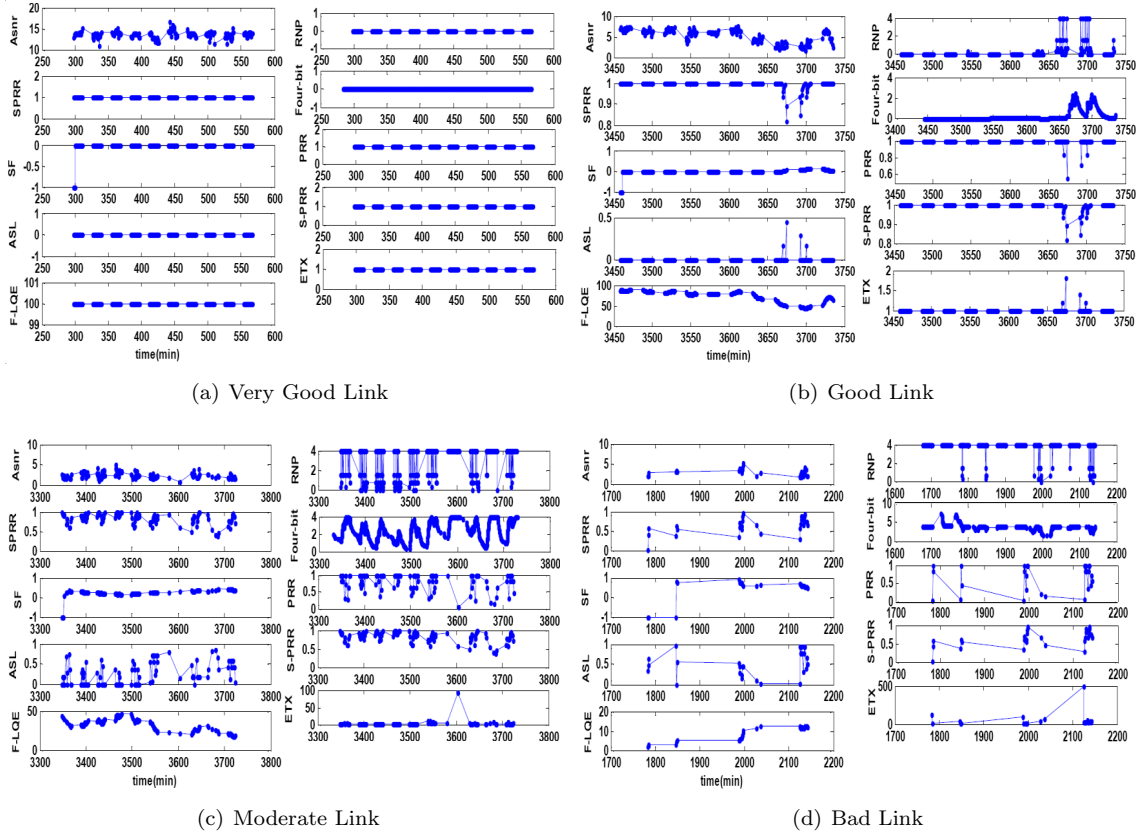


Figure 3.7: Temporal behaviour of LQEs when faced with links with different qualities (Default Setting)

has some very good properties, including the delivery, the asymmetry and the stability, yet it has an ASNR of moderate quality which make of it a good link but not a very good link.

From Figure 3.7(c), we can observe how PRR, ETX and SPRR can overestimate link quality as they provide relatively high link quality estimates. On the other hand, RNP and four-bit, can underestimate link quality by providing low link quality estimates. More importantly, each of these LQEs assess a single and different link property. F-LQE estimates the link not as good as PRR, ETX and SPRR do, and not as bad as RNP and four-bit do. It takes into account different link properties to provide a holistic characterization of the real link state.

Figure 3.7(d) gives a preliminary idea on the stability of F-LQE as well as the other LQEs (a detailed analysis of the stability of F-LQE is given in section 3.5.2.2). Indeed, the link shown in Figure 3.7(d) is generally of bad quality. Furthermore, this link is a *bursty* link, as its quality can turn to good (e.g. PRR equal to 1 and RNP equal to 0), yet in the short term. F-LQE is a stable LQE as it resists to these short-term link quality fluctuation whereas the other LQEs are not stable as their link quality estimates switch temporarily to very

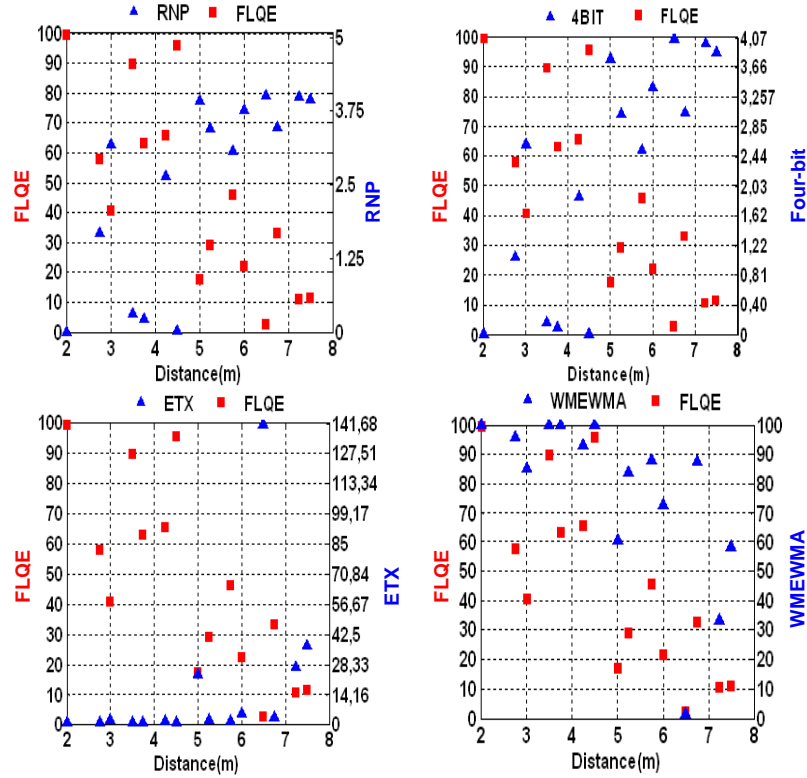


Figure 3.8: Scatter plot of each LQE according to distance (Default Setting).

good estimates.

Now, let us see more arguments for F-LQE reliability by analyzing the distribution of link quality estimates.

**3.5.2.1.2 Link quality estimates distribution** Form the scatter plot of Figure 3.8, we can see that F-LQE estimates are more scattered than those of the other link estimators. For example, the RNP estimates are mostly aggregated to 4 retransmissions (the maximum). That means that two links assumed to have different qualities, may be aggregated to have almost the same qualities when using RNP as LQE; and they would have different qualities when using F-LQE as LQE. The same thing holds for the rest of LQEs. This observation shows that F-LQE would surely perform better than the existing LQEs. Hence again, we show the reliability of F-LQE as it is able to provide a fine grain classification of links.

The above observations can be confirmed if we look into the CDF plot in Figure 3.9. This plot is obtained based on all the links and the default setting (refer to Table 2.2). Notice that we did not include the CDF plots for the other settings, as they have similar shape as the CDF plot based on the default setting. Figure 3.9 shows that PRR, SPRR and ETX overestimate link quality as they estimate most of the links to have good quality. In contrast, RNP, and four-bit underestimate link quality as they consider most of the links having bad

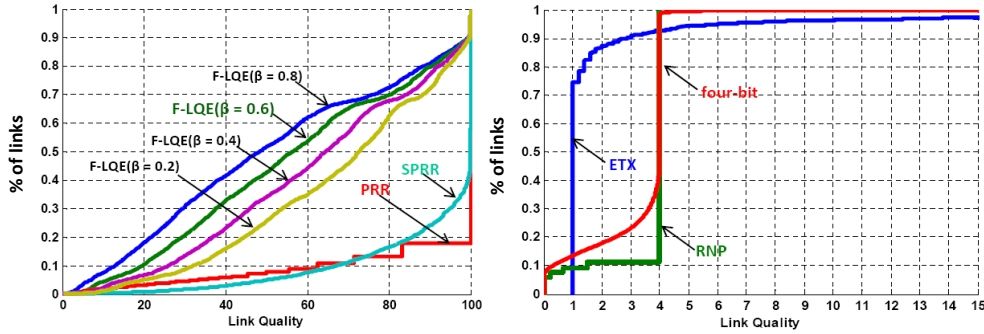


Figure 3.9: Empirical CDFs of LQEs (Default Setting).

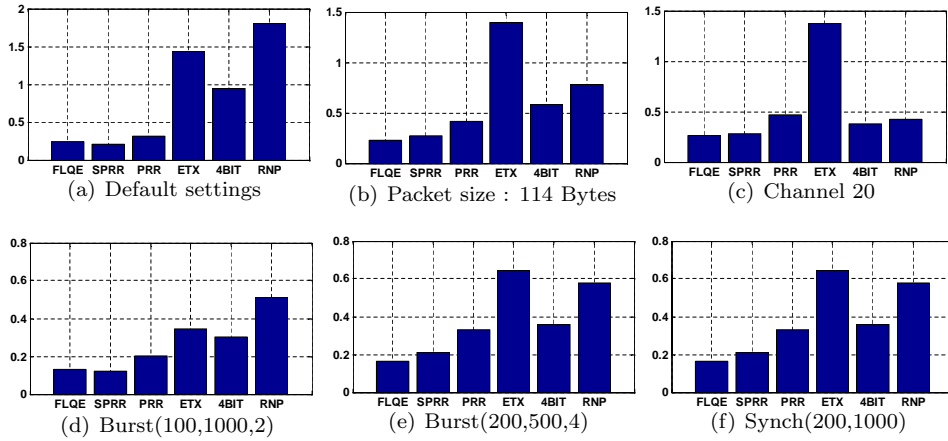


Figure 3.10: Sensitivity to transient fluctuation in link quality, for different network settings.

quality. In between, F-LQE provides reasonable link quality estimates (neither overestimate nor underestimate link quality). Furthermore, the distribution of link quality estimates is nearly an uniform distribution, which means that F-LQE is able to distinguish between links having different link qualities. These observations confirm the reliability of F-LQE.

In our study, we have set  $\beta$  (refer to Eq.3.4) to 0.6. In the following, we justify this choice by studying the impact of  $\beta$  on the reliability of F-LQE. Figure 3.9 shows the effect of  $\beta$  on the CDF. From this figure, we retain two important findings: First, the higher  $\beta$  is, the more pessimistic F-LQE is. This is completely reasonable, since by increasing  $\beta$ , we give more importance to the *min* (refer to Eq.3.4). Second and more importantly, by choosing  $\beta$  equal to 0.6, we get the nearest distribution to the uniform distribution, which justify the choice of  $\beta$ .

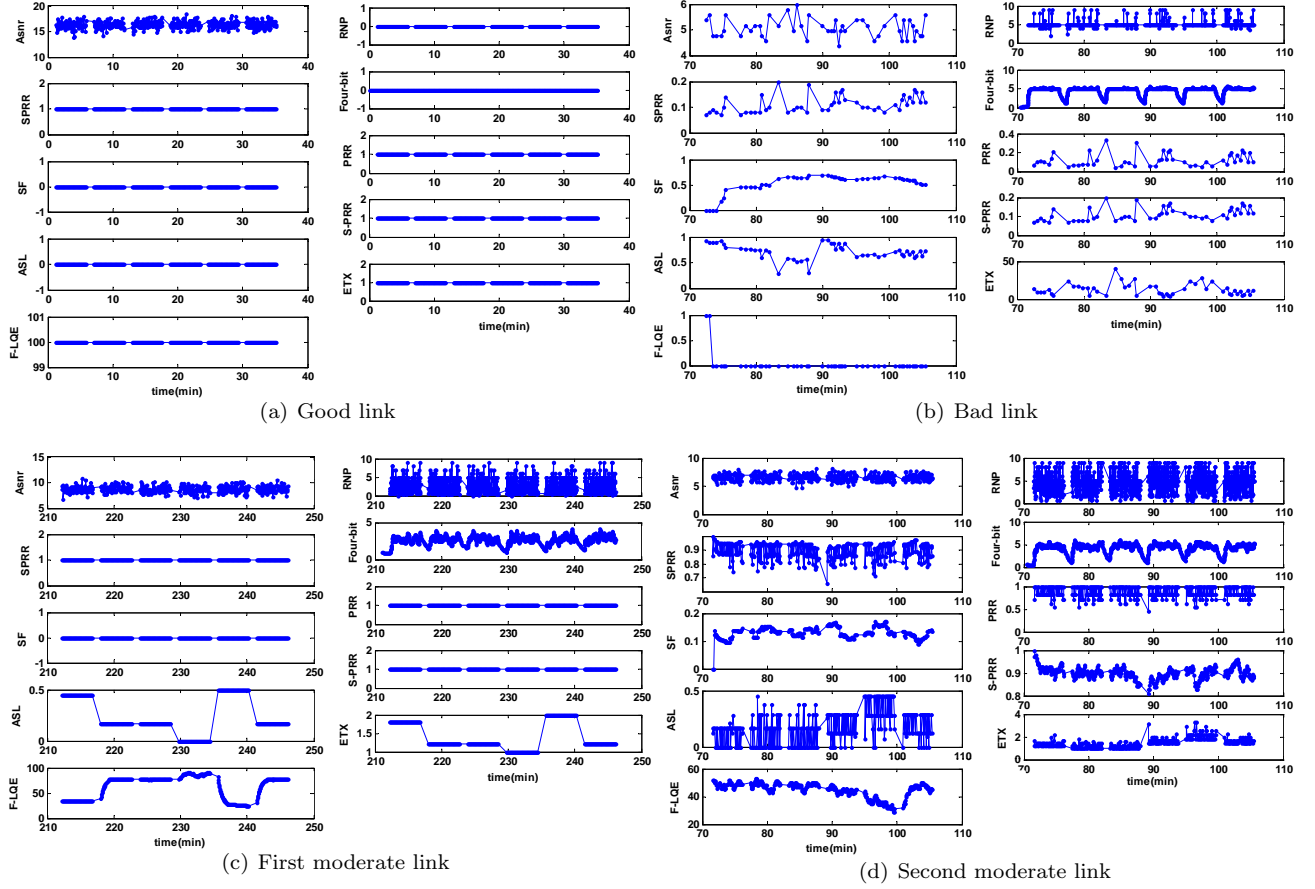


Figure 3.11: Temporal behaviour of link quality estimators when faced to links with different qualities, observed by Tossim 2 simulation.

### 3.5.2.2 Stability

We measure the sensitivity of the LQEs to transient fluctuations by the coefficient of variation of its estimates. Figure 3.10 compares the sensitivity (stability) of F-LQE with that of PRR, ETX, SPRR, RNP, and four-bit, with respect to different setting (refer to Table 2.2). According this figure, we retain two observations: First, generally, F-LQE is the most stable LQE. Second, except ETX, receiver-side LQEs, i.e. PRR and SPRR, are more stable than sender-side LQEs, i.e. RNP and four-bit. ETX is receiver-side, yet it is shown as unstable. The reason is that when the PRR tends to 0 (very bad link) the ETX will tend to infinity, which increase the standard deviation of ETX link estimates.

## 3.5.3 Simulation results

### 3.5.3.1 Reliability

As in the experimental study, we examine the reliability of F-LQE studying (*i.*) the temporal behavior (Figure 3.11), and (*ii.*) the distribution of link quality

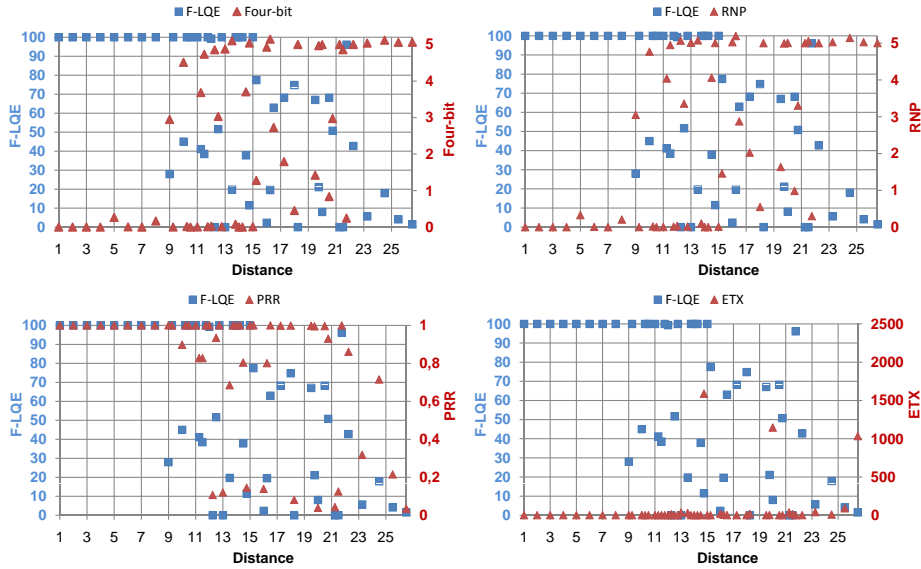


Figure 3.12: Scatter plot of each link quality estimator according to distance, observed by Tossim 2 simulation.

estimates, illustrated by the by the a scatter plot (Figure 3.12) and the empirical cumulative distribution function, CDF, (Figure 3.13).

**3.5.3.1.1 Temporal behavior** Figure 3.7 shows the temporal behaviour of F-LQE, its related link quality metrics, and the other conventional link quality estimators, with respect to four different links. From this figure, it can be observed that all link quality estimators agree that the first link (Figure 3.11(a)) is roughly good and the second is roughly bad (Figure 3.7(b)).

Figure 3.11(c) and Figure 3.11(d) deal with two links of moderate qualities. These figures show that RNP and four-bit underestimate link quality, and PRR, SPRR, and ETX overestimate link quality, whereas F-LQE provides reasonable link quality estimates. Indeed, PRR, SPRR and ETX estimate the two links (Figure 3.11(c) and Figure 3.11(d)), to have very good quality or overestimate link quality: Average PRR and SPRR is 1 in Figure 3.11(c) and almost 0.9 in Figure 3.11(d) and average ETX is almost 1.5 transmission/retransmissions (i.e. 0.5 retransmissions) for both links. On the other hand, four-bit and RNP estimators, estimate both links in Figure 3.11(c) and Figure 3.11(d), to have less goodness, as the average RNP and four-bit is about 3 retransmissions in Figure 3.11(c) and 5 retransmissions in Figure 3.11(d), shifting from 0 to 9 for RNP, which underestimate link quality. F-LQE estimates the link not as good as PRR, WMEWMA, and ETX estimators do, and not as bad as RNP and four-bit do. In the following we show how F-LQE provides reasonable link quality estimates, which make of it more reliable than conventional link quality estimators, namely PRR, ETX, SPRR, RNP, and four-bit.

In fact, the link depicted in Figure 3.11(c) has some positive features: (1) good packet delivery and (2) high stability, but it has also some negative features: (3)

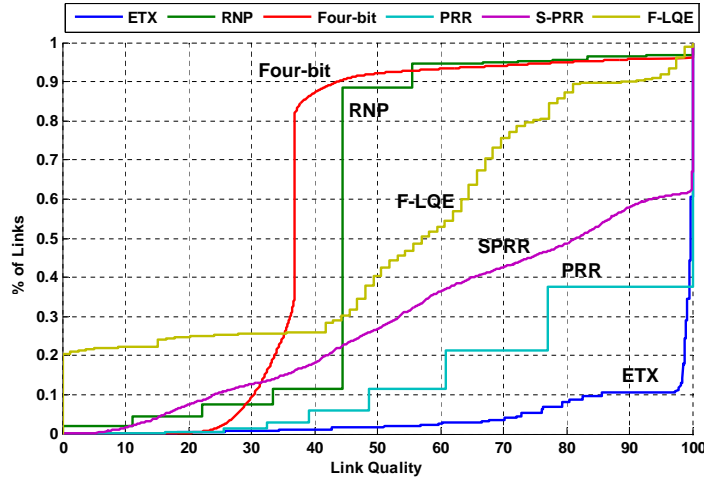


Figure 3.13: Empirical CDFs of link quality estimators, observed by Tossim 2 simulation.

medium channel quality and (4) high asymmetry. The last two features justify the high number of packet retransmissions. As a result, the average F-LQE link quality estimate is 62 (out of 100), which is a reasonable link quality estimate, given the above link properties. The link shown in Figure 3.11(d) is also of moderate quality. The difference with the first link is mainly (1) the channel quality is worse, which justifies a higher number of packet retransmissions, and (2) the link is much more unstable. These properties make this link (Figure 3.11(d)) having worse quality compared to the first (Figure 3.11(c)): the average F-LQE is 45 for the second moderate link against 62 for the first.

Now, let us see more arguments for F-LQE reliability by analyzing the distribution of link quality estimates.

**3.5.3.1.2 Link quality estimates distribution** The above observations can be confirmed if we look into the CDF plot in Figure 3.13. The CDF presented in this figure is obtained based on all the links of one simulation scenario. Further, link quality estimates with respect to link quality estimators have been normalized and transformed to be in the range  $[0..100]$ , where 0 is the worst link quality and 100 is the best. The aim of this transformation is to better visualize the different link quality estimates having different ranges, in the same X-axis. Figure 3.13 shows that PRR, SPRR and ETX overestimate link quality as they estimate most of the links to have good quality. In contrast, RNP and four-bit underestimate link quality as they consider most of the links having bad quality. In between F-LQE provides reasonable link quality estimates (neither overestimate nor underestimate link quality). Furthermore, the distribution of link quality estimates is near to uniform distribution which means that F-LQE is able to distinguish between links having different link qualities. These observations confirm the reliability of F-LQE.

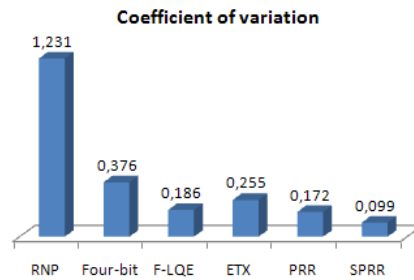


Figure 3.14: Sensitivity to transient fluctuation in link quality, observed by Tossim 2 simulation.

### 3.5.3.2 Stability

Figure 3.14 compares the stability of F-LQE with that of PRR, ETX, SPRR, RNP and four-bit. According this figure, we retain two observations: First, receiver-side link quality estimators, including PRR, SPRR, and ETX are the most stable, and sender-side link quality estimators, including RNP and four-bit are the most instable. Second F-LQE is not the most stable link quality estimator, but its stability is in between receiver-side and sender-side LQEs, which makes a good balance. We can not blame F-LQE on that because a very stable estimator trend to be less responsive to the major changes in link quality. Finally, we believe that F-LQE provides a good balance between sensitivity to transient changes and responsiveness to major changes, in link quality.

## 3.6 Conclusion

In this chapter, we have presented a novel link quality estimator (F-LQE) for wireless sensor networks (WSNs). In contrast to existing LQEs, which only assess one single link property thus providing a partial view on the link, F-LQE combines four link metrics (SPRR, ASNR, ASL, and SF) using Fuzzy Logic, since we believed (and proved) to be an appropriate strategy to fuse different and imprecise metrics. The overall quality of the link is then specified as a Fuzzy IF-THEN rule, which combines the four metrics, viewed as linguistic variables. The evaluation of the fuzzy rule returns the membership of the link in the fuzzy subset of good links. *F-LQE* has been evaluated extensively both by simulation and experimentation, demonstrating greater performance over existing solutions, in terms of reliability and stability.

Link quality estimation in WSNs has a fundamental impact on the network performance and affects as well the design and performance of higher layer protocols — specifically routing protocols. In the following chapter, we demonstrate the efficiency of F-LQE by assessing its impact on routing performance.





---

## Boosting Collection Tree Routing Protocols Through Fuzzy Link Quality Estimation

---

### 4.1 Introduction

The design of efficient routing protocols is a key issue to ensure reliable end-to-end delivery in Wireless Sensor Networks (WSNs). However, the unreliability of WSN links — namely their quality fluctuation over time [6] as well as space [7, 28], and their asymmetric connectivity [7, 9], makes it challenging for routing protocols to maintain their correct operation. Therefore, considering the quality of links in routing decisions is a prerequisite to overcome link unreliability and maintain acceptable network performance. Delivering data over high quality links (i.) reduces the number of packet retransmissions in the network, (ii.) increases its throughput and (iii.) ensures a stable topology. This implies that efficient routing metrics should integrate not only the path length criterion, in terms of hops or communication delay, but also the path *global quality*. Path quality is evaluated based on the assessment of links that compose it.

Most existing link quality based routing metrics are based on traditional and not sufficiently accurate LQEs such as PRR. The accuracy of link quality estimation is essential as it impacts the effectiveness of routing metrics and thus routing performance. In the previous Chapter, we have shown that accurate link quality estimation is performed by the combination of several link quality metrics that capture the different link aspects, rather than considering a single metric. Thus, we have introduced and validated a new link estimator, called F-LQE, that combines four important link quality metrics using Fuzzy logic.

This chapter focuses on the design of a routing metric based on accurate link estimation using F-LQE — we call it FLQE-RM. In other words, it examines the question of how to use link quality estimates provided by F-LQE to select the optimum path in terms of global quality as well as length, i.e. hop-count. To answer this question, we first describe design requirements for an efficient F-LQE based routing metric. Then, we propose four potential solutions. Each

solution evaluates the path cost based on link F-LQE estimates but using a different expression. Based on extensive simulations, we evaluate the performance of potential solutions by analyzing their impact on the performance of CTP (Collection Tree Protocol) [12] tree routing. Our simulation study allowed us to select the most efficient solution among proposed F-LQE based routing metrics. We call this solution FLQE-RM. Simulation results also show that FLQE-RM establishes and maintain the routing tree better than four-bit, the default routing metric of CTP. In order to validate FLQE-RM metric, we extended the simulation study to a large scale experimental study, using real WSN platforms. In this experimental study, we compare the impact of FLQE-RM on CTP performance with that of four-bit and ETX, which are two representative routing metrics in WSN community. Experimental results show that our routing metric outperforms four-bit and ETX: It improves the end-to-end-delivery by up to 16%, reduces the number of packet retransmissions by up to 32%, reduces the Hop count by up to 4%, and improves the topology stability by up to 47%. These results indeed demonstrate the applicability and the usefulness of F-LQE for routing protocols — specifically, collection tree routing protocols.

## 4.2 Related work

### 4.2.1 Collection tree routing protocols

Many routing protocols have been proposed for WSNs and various classifications and taxonomies of these protocols have emerged [102, 103]. However, a few of them have been implemented and tested on real sensor nodes [103]. The most experimentally tested and deployed routing protocols are collection tree-based, which are characterized by the many-to-one paradigm. This fact is justified by the nature of WSNs applications that generally consist in collecting information from the physical world and relaying it to the sink node using multi-hop wireless communication.

Several collection tree routing protocols have been reported in the recent literature [11, 87, 12, 74, 104]. Particularly, MintRoute [11] is a collection tree routing protocol that formed the core of the TinyOS network layer over the past years. It has led to Multi-HopLQI [87] followed by the Collection Tree Protocol (CTP) [12]. CTP is the reference protocol of TinyOS 2.x. network layer. It was shown to work well with different WSN platforms. Typically, CTP establishes a *routing tree* towards the sink node, on the basis of a link quality based routing metric. This metric is the sum of quality estimates of links constituting the path. Link quality estimation is performed using four-bit estimator. In our study, we consider CTP as a benchmark for analyzing the impact of different link-quality based routing metrics on routing performance (more details about CTP will be given in Section 4.3).

### 4.2.2 Link quality based routing metrics

Link quality-based routing metrics consider the criteria of path global quality in path selection. They may also integrate other criteria such as path length in terms of hops or communication delay, and nodes energy, depending on the application requirements.

Path quality is determined through the assessment of links composing the path. Depending on the link quality estimator category, the path quality can be the sum (e.g., for RNP-based LQEs), the product (e.g., PRR-based LQEs) or the max/min (e.g., Hardware-based LQEs and score-based LQEs) of link quality estimates over the path. Next we overview a set of representative routing metrics to illustrate this statement.

The DoUble Cost Field HYbrid (DUCHY) [74] and SP( $t$ ) [11] are two routing metrics that allow to select routes with minimum hops and high quality links. For DUCHY, each node maintains a set of neighbors that are nearer, in terms of hops, to the tree root. Then, the parent node is selected among the maintained set of neighbors as the one that has the best link quality. Link quality estimation is performed using both CSI (Channel State Information) and RNP. As for SP( $t$ ), each node maintains a set of neighbors that have link quality exceeding a threshold  $t$ . Link quality estimation is performed using WMEWMA. Then, the parent node is selected among the maintained set of neighbors as the nearest one, in terms of hops, to the tree root.

ETX [67] and four-bit [76] are two link quality estimators that have been extensively used as routing metrics. Both approximate the RNP (RNP-based category). Using ETX or four-bit, the path cost is the the sum of quality estimates of its links. This can be generalized to any RNP-based link estimator as the number of packet retransmissions over the path is typically the sum of packet retransmissions of each link composing the path.

MAX-LQI and Path-DR metrics [105] aims to select the most reliable path, regardless its hop count. MAX-LQI selects the path having the highest minimum LQI over the links that compose the path. Path-DR approximates the link PRR using LQI measurements and then evaluates path cost as the product of link PRRs. Path-DR selects paths having the maximum of this product. The product of link estimates can be generalized to any PRR-based LQE.

Existing link quality based routing metrics use traditional LQEs, such as PRR, RNP, four-bit, and LQI. These LQEs are not sufficiently accurate as they either rely on a single-link-quality metric, or use not sophisticated techniques for the combination of link quality metrics such as filtering through the EWMA. Further, these metrics can only capture one link aspect such as link delivery or the number of packet retransmissions over the link (refer to chapter 2 for more details on the limitation of these LQEs). Our introduced estimator F-LQE combines four important link quality metrics using Fuzzy logic. We have shown using both simulation and real experimentation, that F-LQE provides accurate estimation as it takes into account several important link aspects (refer to Chapter 3). The accuracy of link quality estimation greatly affects the effectiveness of link quality based routing metrics. In this chapter, we design a new routing metric based on F-LQE and we demonstrate its effectiveness by investigating its impact on the CTP routing performance.

### 4.3 Overview of CTP (Collection Tree Protocol)

As data collection is one of the most popular WSN applications, CTP has gained a lot of interest during the last years. CTP establishes and maintains a routing tree, where the tree root is the ultimate sink node of the collected data. Hence, three types of nodes can be identified:

- *The sink node:* One node in the network advertises itself as a sink node (generally the node of id 0). It is the root of the routing tree. All other nodes join the tree on the basis of link quality estimation.
- *The parent node:* Except the sink node, each node has a parent, which represents the next hop towards the tree root. Each parent node has a certain number of child nodes.
- *The child node:* It is associated to a single parent node and can be in turn the parent of other child nodes situated below in the tree hierarchy. Notice that data traffic flow is from child node to parent node.

CTP is the reference protocol of TinyOS 2.x. network layer [106]. Due to its modularity, and also the fact that it relies on a link quality based routing metric, we use it as a benchmark for analyzing the impact of different link quality based routing metrics on routing performance.

CTP implementation contains three basic components: link estimator, routing engine and forwarding engine. These components are shortly described next.

### 4.3.1 Link estimator

This component is based on the Link Estimation Exchange Protocol (LEEP) [107] and four-bit [76]. Note that the implementation of four-bit in Link estimator component is slightly different from its specification [76], which was described in Chapter 2. According to this implementation, four-bit combines beacon-driven estimate (estETX) and data-driven estimate (RNP) using the EWMA filter. RNP is computed based on  $DLQ$  transmitted/retransmitted data packets and estETX is given by the following expression:

$$ETX(BLQ, \alpha) = \frac{1}{SPRR_{in} \times SPRR_{out}} - 1 \quad (4.1)$$

Where  $SPRR_{in}$  is the PRR of the inbound link, smoothed using EWMA. It is computed based on  $BLQ$  received beacons.  $SPRR_{out}$  is the PRR of the outbound link, smoothed using EWMA. It is gathered from a received beacon or data packet.

Each node maintains a *neighbour table*, where each entry contains useful information for estimating the quality of the link to a particular neighbor. These information include (i.) the neighbour address; (ii.) the sequence number of the last received beacon, the number of received beacons and the number of missed beacons (these are used for  $SPRR_{in}$  computation); (iii.) the inbound link quality ( $SPRR_{in}$ ) and the outbound link quality ( $SPRR_{out}$ ); (iv.) the number of acknowledged packets and the total number of transmitted/retransmitted data packets (these are used to compute  $estETX_{up}$ ); (v.) link cost (four-bit estimate); and (vi.) different flags that describe the state of the entry.

The replacement policy in the neighbour table is governed by the use of *compare bit* and *pin bit*. The pin bit applies to neighbour table entries. When the pin bit is set on a particular entry, it cannot be removed from the table until the pin bit is cleared. The compare bit is checked when a beacon is received. It indicates whether the route provided by the beacon sender is better than the route provided by one or more of the entries in the neighbour table.

### 4.3.2 Routing engine

This component is responsible for the establishment and maintaining of the routing tree for data collection. Each node maintains a *routing table*, where each entry contains the neighbour address, the parent of this neighbour address, the neighbour cost, and an indicator on whether the neighbour is congested. The neighbour cost refers to the route cost from this neighbour to the sink. Generally, a node cost is computed as the cost of its parent plus the cost of its link to its parent. The link cost corresponds to four-bit estimate. Hence, the cost of a route is the sum of four-bit estimates of its links. Lower route costs are better. Note that the sink node has a cost equal to zero.

A node updates its route to the sink, which corresponds to the update of its parent, periodically. Parent update consists in searching in the routing table for a neighbour that provides a route cost better than that provided by current parent. To compute the route cost through a given neighbour, the node gets the neighbour cost from the routing table, and the link cost to the neighbour from the neighbour table and then sums the two values. To avoid frequent parent changes leading to unstable topology, a node changes its parent only when a number of conditions are satisfied. For example, the new parent should provide a route cost lower than the current route cost by *ParentChTh*, which is a constant parameter defined by CTP.

The tree is maintained by beacons sent by each node according to an adaptive beaconing rate, to ensure a minimum sent beacons along with a consistent tree. When a node sends a beacon, it includes the address of its parent as well as its cost, i.e., the route cost from the node to the sink, in the beacon header. It also includes a list of *neighbour entries* in the beacon footer. A neighbour entry is composed of the neighbour address and the SPRR of the inbound link,  $SPRR_{in}$ . When a node receives a beacon, it seeks for its address in the list of neighbour entries. When found, it extracts the  $SPRR_{in}$ , and updates the SPRR of the outbound link,  $SPRR_{out}$ , in its neighbour table.

### 4.3.3 Forwarding engine

This component is responsible for queueing and scheduling outgoing data packets. Each node, maintains a forwarding queue that adopts a set of rules to process data packets. For example, a data packet is ejected from the queue if it has been acknowledged or has reached the maximum retransmission count. When a node receives a data packet from a neighbour with cost less than its cost, it drops the packet and signals an inconsistency in the network (a loop detection). Data packets are automatically forwarded to the next hop in the tree, which corresponds to the parent node. When a node sends a data packet, it includes its cost in the packet header. As with beacons, the node includes a list of *neighbour entries* in the packet footer.

## 4.4 Towards an efficient F-LQE based Routing Metric (FLQE-RM) for tree routing

This section examines the question of how to use link quality estimates provided by F-LQE to select the optimum routing path. To answer this question, we

first describe design requirements for an efficient F-LQE based routing metric (FLQE-RM). Then, we propose four potential solutions. Each solution evaluates the path cost based on link F-LQE estimates but using a different expression.

#### 4.4.1 Design requirements

Routing metrics design is critical for the performance of routing protocols. Our goal is to design a routing metric based on accurate link quality estimation, using F-LQE. Such design has three main requirements:

- Firstly, our routing metric should correctly evaluate the path cost based on individual link costs, i.e., F-LQE link quality estimates. This requirement should be carefully addressed as F-LQE can be efficient on a link basis, but inadequate at the path level due to inadequate path cost evaluation. This situation may result to dramatic routing performance.
- Secondly, path cost evaluation should take into account not only the path global quality but also the weakest quality link in the path. In fact, a path may have highest global quality among candidate paths; yet contains a weak quality link. This situation leads to several packet losses over this link, which negatively affects routing performance, such as the end-to-end packet delivery.
- Thirdly, our routing metric should favor the selection of short paths. In fact, selecting short paths reduces the number of transmissions over the path and also the number of nodes involved for packet delivery, which conserves nodes energy and thus extends the network lifetime.

#### 4.4.2 Potential solutions

F-LQE is a score-based LQE. Hence, the most intuitive solution for a routing metric based on F-LQE, that we denote as  $FLQE-RM_{Min}$  is the following:

$$FLQE-RM_{Min} = \text{Min}_{i \in Path} FLQE_i \quad (4.2)$$

Where,  $FLQE_i$  is the cost of the link  $i$  through F-LQE computation.  $FLQE-RM_{Min}$  represents the the weakest quality link in the current path. Hence, the path having the highest  $FLQE-RM_{Min}$  is selected for data delivery.  $FLQE-RM_{Min}$  might be not convenient as a link quality based routing metric, since it does not consider the quality of the rest of links other than the weakest quality link. Further, it does not take into account the path hop count. Generally, link quality based routing metrics that evaluate the path cost as the quality estimate of the weakest quality link (e.g., MAX-LQI metric [105]) should be avoided [84]. Hence, we have proposed three other possible routing metrics based on F-LQE, denoted as  $FLQE-RM_{MinAvg}$ ,  $FLQE-RM_{Sum}$ , and  $FLQE-RM_{SumInv}$ . These are described next.

$FLQE-RM_{MinAvg}$  evaluates the link  $i$  cost as  $FLQE_i$  and the path cost by the following expression:

$$FLQE-RM_{MinAvg} = \beta.AFLQE + (1 - \beta). \text{Min}_{i \in Path} FLQE_i \quad (4.3)$$

Where,  $AFLQE$  is the average path quality. It is computed as the sum of F-LQE estimates of links composing the path, divided by the path hop count.  $\beta$  is a parameter between 0 and 1. The larger the  $\beta$  value, the smaller the influence of the weakest quality link (i.e.,  $Min_{i \in Path} FLQE_i$ ) on path selection. The path having highest  $FLQE-RM_{MinAvg}$  is selected.  $FLQE-RM_{MinAvg}$  considers both the path global quality and the path weakest quality link, which are combined through a weighted sum. We choose  $\beta$  equal to 0.7 to increase the influence of path global quality on path selection.

$FLQE-RM_{Sum}$  evaluates the link  $i$  cost as  $1 - FLQE_i$  and the path cost as the sum of the link costs:

$$FLQE\_RM_{Sum} = \sum_{i \in Path} (1 - FLQE_i) \quad (4.4)$$

The path having minimal  $FLQE-RM_{Sum}$  is selected.  $FLQE-RM_{Sum}$  takes into account the path global quality. It also implicitly favors the selection of short paths. By defining the link cost as  $1 - FLQE_i$  instead of  $FLQE_i$ , path selection is a minimization of the path cost instead of a maximization. Hence, the more the path is long, the more it has high cost and thus the less chance it has to be selected.

$FLQE-RM_{SumInv}$  evaluates the link  $i$  cost as  $\frac{1}{FLQE_i}$  and the path cost as the sum of the link costs:

$$FLQE\_RM_{SumInv} = \sum_{i \in Path} \frac{1}{FLQE_i} \quad (4.5)$$

The path having minimal  $FLQE-RM_{SumInv}$  is selected. Like  $FLQE-RM_{Sum}$ ,  $FLQE-RM_{SumInv}$  takes into account the path global quality and implicitly favors the selection of short paths thanks to the link cost definition. The difference between  $FLQE-RM_{Sum}$  and  $FLQE-RM_{SumInv}$  is in the definition of the link cost. In fact, this difference makes much sense as it improves the effectiveness of  $FLQE-RM_{SumInv}$  routing metric by avoiding paths having weak quality links. The more the link is of poor quality, the more it has a high link cost, which impacts the overall path cost and increases the probability that the path is rejected.

Table 4.1 summarizes the main characteristics of proposed F-LQE based routing metrics. From this table, it can be inferred that  $FLQE-RM_{SumInv}$  is the best metric as it takes into account the three criterion for efficient path selection. However, this observation should be supported by experimental results.

Next, we conduct a comparative simulation study of  $FLQE-RM_{MinAvg}$ ,  $FLQE-RM_{Sum}$ , and  $FLQE-RM_{SumInv}$  by analyzing their impact on the performance of CTP routing. We exclude  $FLQE-RM_{Min}$  from our study as we have argued (in the beginning of this section) that it is not an appropriate solution. Beforehand, we show how we have integrated these F-LQE based routing metrics in CTP.

#### 4.4.3 Integration of potential solutions in CTP

To integrate proposed F-LQE based routing metrics in CTP, we have implemented F-LQE in the Link Estimator component, as replacement of four-bit

Table 4.1: Characteristics of F-LQE based routing metrics

Path selection criterion	Global quality	Weakest quality link	Path length
FLQE-RM <sub>Min</sub>	No	Yes	No
FLQE-RM <sub>MinAvg</sub>	Yes	Yes	No
FLQE-RM <sub>Sum</sub>	Yes	No	Yes
FLQE-RM <sub>SumInv</sub>	Yes	Yes	Yes

estimator.

#### 4.4.3.1 Beacon-driven link quality estimation

F-LQE combines four metrics, SPRR, ASL, SF, and ASNR, which are computed at the receiver side, i.e., based on received traffic. Our implementation of F-LQE leverages on broadcast control traffic (i.e., beacons), which is initiated by CTP routing engine for the topology control. F-LQE can be also implemented based on data traffic, which requires the overhearing of incoming packets.

CTP uses an adaptive beaconing rate that changes according to the topology consistency. In our implementation, we disabled this mechanism and we used a constant beaconing rate of 1 beacon/s.

#### 4.4.3.2 LQI for channel quality assessment

we have slightly modified the original version of FLQE by considering ALQI (average LQI) for channel quality assessment instead of ASNR (Average SNR). In fact, both LQI and SNR are hardware-based estimators and reflect channel quality. However, ASNR involves more memory overhead than ALQI: 34642 bytes in ROM for FLQE based on ASNR, vs 28054 bytes in ROM a for FLQE based on ALQI. Further, SNR computation is more complex and time consuming than LQI: The SNR is derived by subtracting the noise floor (N) from the received signal (S). The S is deduced by sampling the RSSI at the packet reception, and N can be derived from the RSSI sample just after the packet reception. On the other hand, LQI is derived in one operation, just by sampling the LQI at the packet reception.

#### 4.4.3.3 Link direction

In CTP tree routing, data travel from child to parent. In order to select their parents, child nodes need to assess direct links, i.e., *child* → *parent* links. Although F-LQE takes into consideration link asymmetry through ASL metric, it evaluates the reverse link, i.e., *parent* → *child* link (because each of SPRR, SF, and ASNR provides reverse link estimate). Considering the reverse link estimate to decide about the direct link for parent selection leads to misleading routing decisions. Therefore, we define two F-LQE estimates: F-LQE<sub>in</sub> and F-LQE<sub>out</sub>. F-LQE<sub>in</sub> is the F-LQE for the reverse link, (i.e., inbound link). It is computed by each node, based on incoming beacons. F-LQE<sub>out</sub> is the F-LQE for the direct link, (i.e., outbound link) and it is gathered from received packets. F-LQE<sub>in</sub>



and  $F\text{-LQE}_{out}$  are stored in the neighbor table, with respect to each neighbour node. As reported in Section 4.3, CTP defines a list of neighbour entries, that is included in the footer of each sent packet. In our implementation, a neighbour entry is composed of the neighbour address,  $PRR_{in}$ , and  $F\text{-LQE}_{in}$ . When a node receives a packet, it extracts  $PRR_{in}$ , and  $F\text{-LQE}_{in}$  and stores them in its neighbour table, specifically in  $PRR_{out}$ , and the  $F\text{-LQE}_{out}$  fields.

Link Estimator component is used by the Routing engine to get the link cost. For  $FLQE\text{-RM}_{MinAvg}$ , the link cost corresponds to  $F\text{-LQE}_{out}$  (F-LQE of the direct link:  $child \rightarrow parent$ ). As for  $FLQE\text{-RM}_{Sum}$  and  $FLQE\text{-RM}_{SumInv}$ , the link cost is  $1 - F\text{-LQE}_{out}$  and  $\frac{1}{F\text{-LQE}_{out}}$  respectively.

#### 4.4.3.4 Parent update

Nodes update their parents, when the new parent is better than the current one by  $ParentChTh$ . This constant parameter depends on the routing metric. We set it to 4 for F-LQE based routing metrics. The  $ParentChTh$  for four-bit is equal to 1.5 (default value).

#### 4.4.3.5 Routing engine

Like four-bit,  $FLQE\text{-RM}_{Sum}$  and  $FLQE\text{-RM}_{SumInv}$  select parents that lead to minimal path costs, where a path cost is the sum of its link costs. Hence, the implementation of  $FLQE\text{-RM}_{Sum}$  and  $FLQE\text{-RM}_{SumInv}$  does not require major modifications in the Routing Engine component. On the other hand, the implementation of  $FLQE\text{-RM}_{MinAvg}$  requires some modifications in the Routing Engine component, which are as follow: First, some extra-fields are included the beacon header as well as the routing table entry, allowing for the path cost evaluation through a particular neighbour (refer to to Eq.4.3). These fields are the path hop count  $HopCount$ , the sum of F-LQE estimates of path links  $SF\text{-LQE}$ , and the minimum F-LQE value in the path  $MinF\text{-LQE}$  (worst quality link). Second, the route cost field is deleted from the beacon header and the routing table entry as it can be deduced from the three added fields. Finally, parent selection leverages on the maximization of the route cost instead of its minimization.

### 4.4.4 Simulation study of the potential solutions

We have proposed three potential routing metrics based on F-LQE:  $FLQE\text{-RM}_{MinAvg}$ ,  $FLQE\text{-RM}_{Sum}$ , and  $FLQE\text{-RM}_{SumInv}$ . The goal of this simulation study is to evaluate the performance of these potential solutions, in order to identify the most efficient one.

#### 4.4.4.1 Evaluation methodology

To achieve the above goal, we analyzed the impact of proposed routing metrics on the performance of CTP routing. Hence, we implemented different versions of CTP; in each version, we replaced the default four-bit based routing metric by one of the proposed F-LQE based routing metrics. Then, we conducted different simulations with each CTP version, including the original version of CTP. In each simulation we assessed several performance metrics that allows to compare the contribution of each routing metric, i.e., four-bit,  $FLQE\text{-RM}_{MinAvg}$ ,

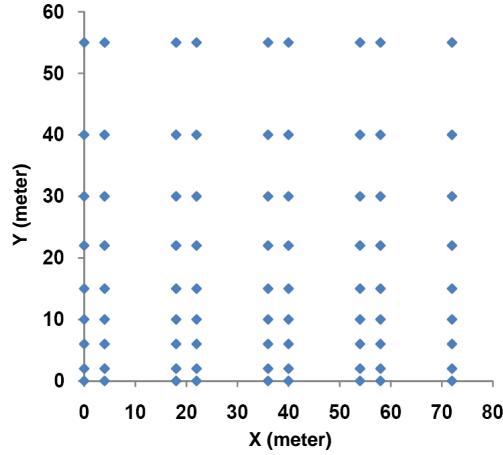


Figure 4.1: Distribution pattern of 80 sensor nodes and a single sink node, in a non-uniform grid topology.

FLQE-RM<sub>Sum</sub>, and FLQE-RM<sub>SumInv</sub> in enhancing CTP routing. Considered performance metrics are the following:

- Packet Delivery Ratio (PDR). It is computed as the total number of delivered packets (at the sink node, i.e., the root) over the the total number of sent packets (by all source nodes). This metric indicates the end-to-end reliability of routing protocols.
- Average number of retransmissions across the network per delivered packet. (RTX). This metric is of paramount importance for WSNs as it greatly affects the network lifetime. In fact, communication is the most energy consuming operation for a sensor node. Therefore, efficient routing protocols try to minimize packet retransmissions by delivering data over high quality links, which extend the network lifetime.
- Average number of parent changes per node (ParentCh). This metric is an indicator of topology stability. The number parent changes depends on tow factors: the *ParentChTh* parameter of CTP, and also the agility of the LQE allowing for detecting link quality changes. Too many parent changes leads to instable topology, but improves the quality of routes and thus improves routing performance (e.g., PDR and RTX). On the other hand, few parent changes leads to stable topology but also worse quality routes. Hence, an agile LQE, along with a good *ParentChTh* choice would lead to a good tradeoff between topology stability and route qualities.
- Average path lengths, i.e., average hop count (Hop Count). It is important that link quality aware routing protocols minimize route lengths in order to reduce (i.) the number of packet transmissions to deliver a packet, (ii.) the number of involved nodes for data delivery, and possibly (iii.) the end-to-end latency (in case the involved nodes are not overloaded).

#### 4.4.4.2 Simulation description

Our simulation study is based on TOSSIM 2 simulator [89]. An overview of TOSSIM 2 channel model was presented in Chapter 2 (refer to Section 2.5.1.1). Recall that TOSSIM 2 channel model has the advantage of capturing important low-power link characteristics, namely spatial and temporal characteristics, as well as the asymmetry property. However, it presents some shortcomings that result from some assumptions. For example, it assumes that that link quality does not vary according to direction. In chapter 2, we have shown that TOSSIM 2 has a realistic channel model, as simulation results confirmed experimental results (refer to Section 2.6.2). In other other words, the simplifications made by TOSSIM 2 channel model had not a great impact on the validity of the results.

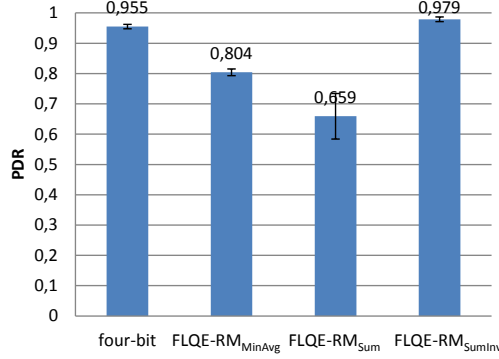
In our simulation study, we considered a 81-node multi-hop network, where nodes use the default MAC protocol in TinyOS: Berkley-MAC (B-MAC) [108], and CTP as routing protocol. Nodes generate a Poisson traffic with a mean rate of 0.125 packets/s. They begin their transmission after a delay of 10 min (to enable the topology establishment). The total simulation time is 40 min. Each simulation is repeated 30 times and each performance metric is estimated with a 95% confidence interval.

To establish a rich set of links with different qualities, over this multi-hop network, we have considered a non-uniform grid topology layout, as shown Figure 4.1. The sink node is located at coordinates (0,0). The grid unit varies in {4,14} meters. The choice of the these grid units is based on a prior study on receptions regions analysis (refer to Figure 2.2), so that we have a mixture of link qualities: good, intermediate and bad. This way, we make sure that the integrated LQE in a given routing metric operates in extreme conditions. The simulated network is set to an Indoor environment configuration, as described in [5].

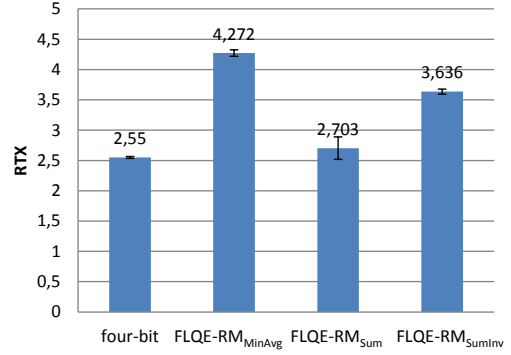
#### 4.4.4.3 Simulation results

Figure 4.2 compares the effectiveness of the considered link quality based routing metrics, while investigating their impact on the performance of CTP tree routing. From this figure, two relevant observations can be drawn.

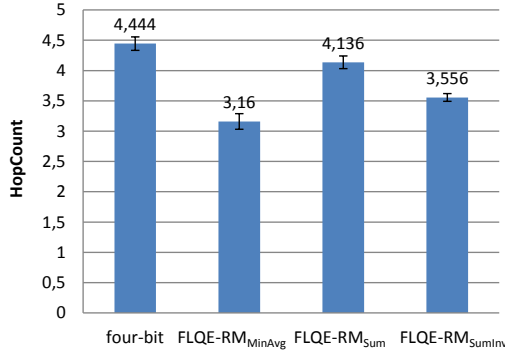
*Observation 1:* Overall,  $FLQE-RM_{SumInv}$  presents better performance than  $FLQE-RM_{MinAvg}$  and  $FLQE-RM_{Sum}$ , and thus appears as the best candidate for an efficient F-LQE based routing metric: Figure 4.2(a) shows that  $FLQE-RM_{SumInv}$  provides significantly better PDR compared with  $FLQE-RM_{MinAvg}$  and  $FLQE-RM_{Sum}$ . RTX (Figure 4.2(b)) and Hop Count (Figure 4.2(c)) indicate respectively the number of packet retransmissions, and the number of packet transmissions, to deliver of packet. By observing the RTX and Hop count together, it can be observed that (i.)  $FLQE-RM_{SumInv}$  have nearly the same performance as  $FLQE-RM_{Sum}$  (one has better RTX but worst Hop Count and the other has worst Hop Count and better RTX), and (ii.) it is slightly better than  $FLQE-RM_{MinAvg}$  (it reduces the RTX and provides almost the same Hop count). Figure 4.2(d) shows that  $FLQE-RM_{SumInv}$  leads to higher ParentCh compared with  $FLQE-RM_{MinAvg}$  and  $FLQE-RM_{Sum}$ . In fact, this observation can be interpreted by the fact that  $FLQE-RM_{SumInv}$  is more responsive to the



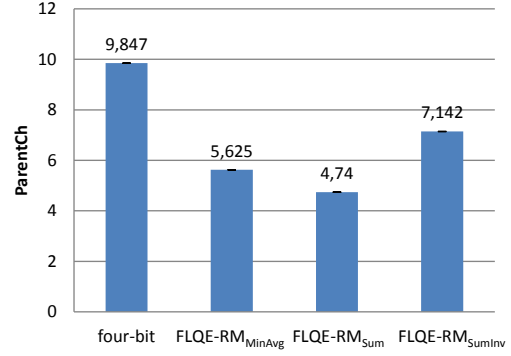
(a) Impact of routing metrics on the packet delivery ratio (PDR)



(b) Impact of routing metrics on the average number of packet retransmissions (RTX)



(c) Impact of routing metrics on the average routes hop count (Hop Count)



(d) Impact of routing metrics on the average number of parent changes (ParentCh)

Figure 4.2: Impact of routing metrics on CTP performance (Tossim 2 simulation results)

route quality degradation than FLQE-RM<sub>MinAvg</sub> and FLQE-RM<sub>Sum</sub>.

*Observation 2:* FLQE-RM<sub>SumInv</sub> slightly outperforms four-bit, the default routing metric of CTP. Figure 4.2(a) and Figure 4.2(d) show that FLQE-RM<sub>SumInv</sub> provides better PDR than four-bit, while performing less ParentCh. By observing the RTX and the Hop count together (Figure 4.2(a) and Figure 4.2(d)), FLQE-RM<sub>SumInv</sub> and four-bit have nearly equal performance.

Based on simulation results, we retain FLQE-RM<sub>SumInv</sub> as an efficient FLQE based routing metric. In the reminder of this dissertation, we call this metric *FLQE-RM*. We have shown through TOSSIM 2 simulation that FLQE-RM slightly outperforms four-bit, which is a representative routing metric in the WSN community. However, to better validate FLQE-RM, especially guaranteeing its effectiveness in real word deployments, it is important to evaluate its performance using real WSN platforms. This constitutes the objective of the next section.

## 4.5 Experimental performance evaluation of FLQE-RM

The objective of this section is to demonstrate the effectiveness of FLQE-RM metric through large scale real experimentation.

### 4.5.1 Evaluation methodology

We adopt the same evaluation methodology as our simulation study, presented in Section 4.4.4.1, i.e., we investigate the impact of FLQE-RM on CTP routing performance, namely PDR, RTX, ParentCh, and Hop Count. We compare the impact of FLQE-RM to that of four-bit, the default metric of CTP, as well as ETX [67]. Both four-bit and ETX are considered by the WSN community as representative and reference metrics.

In our experimental study, we resort to remote testbeds (i.e., general-purpose testbeds) for large scale experiments. Examples of remote testbeds include MoteLab [92], Indriya [109], Twist [94], Kansei [95], and Emulab [96].

Remote testbeds are designed to be remotely used by several users over the world. Roughly, they are composed of four building blocks: (*i.*) the underlying WSN (i.e., a set of sensor nodes), (*ii.*) a network backbone providing reliable channels to remotely control sensor nodes, (*iii.*) a server that handles sensor nodes reprogramming and data logging into a database, and (*iv.*) a web-interface coupled with a scheduling policy to allow the testbed sharing among several users. The testbed users must be experts on the programming environment supported by the testbeds (e.g. TinyOS, Emstar), to be able to provide executable files for motes programming. They must also create their own software tool to analyze the experimental data and produce results.

Our experimental study is carried out on both MoteLab [92] and Indriya [109] testbeds. MoteLab consists of 190 TMote Sky motes, deployed over 3 floors of Harvard university building, and Indriya consists of 127 TelosB motes, deployed over 3 floors of National University of Singapore (NUS) building. In both testbeds, node placement is very irregular. Node programming is performed using TinyOS.

In contrast to Indriya, which is a recently released testbed, MoteLab is serving the WSN community for six years. Hence, around 100 nodes in MoteLab are not working mostly due to aged hardware. Further, the number of working nodes in both testbeds varies according to time due to many reasons such as hardware failure and human activity. Our experiments were conducted within April-July 2011, where 72 nodes from MoteLab and 121 nodes from Indriya were available.

Using low transmission powers for sensor nodes allows to have more intermediate quality links, and thus better evaluate link quality based routing metrics. However, this may lead to a partitioned network, as some of nodes will not be able to join the network due to poor connectivity. Hence, the transmission power should be correctly set to have as much as possible a rich set of links (i.e., having different qualities), while preserving the network connectivity. To this end, we set the transmission power to -25 dBm for Indriya experiments and to 0 dBm for MoteLab experiments. These values were determined through several experiments. In each experiment, we set the transmission power to arbitrary values and check the connectivity of the network through the graphical interface provided by the testbed software.

Table 4.2: Experiment sets.

	<b>Testbed</b>	<b>Traffic load</b> (in pkts/s)	<b>Num. of source nodes</b>	<b>Topology</b> (root ID)
<b>Set 1: Impact of testbed</b>	{Indriya, MoteLab}	0.125	120	1
<b>Set 2: Impact of traffic load</b>	Indriya	{0.125, 0.25, 0.5, 1, 2}	120	1
<b>Set 3: Impact of source nodes</b>	Indriya	0.125	{120, 84, 60, 42, 29}	1
<b>Set 4: Impact of topology</b>	Indriya	0.125	120	{1, 15, 58, 113}

### 4.5.2 Experiments description

Our experiments consist of a many-to-one application scenario where nodes generate traffic at a fixed rate, destined to the sink node. Data collection is performed using CTP, with a fixed beacon rate (1 packet/s). Nodes use the default MAC protocol in TinyOS, B-MAC. Recall that we set the transmit power to -25 dBm for Indriya experiments and to 0 dBm for MoteLb experiments. The radio channel is set to 26 to avoid interference with co-existing networks such as Wi-Fi. Most of experiments were conducted with Indriya as it provides more active nodes (121 nodes) than MoteLab (72 nodes). Each experiment lasts 60 minutes. Nodes begin their transmission after a delay of 10 minutes to enable the topology establishment.

Experiments are divided into different sets. In each experiment set, we varied a certain parameter to study its impact, and the experiment was repeated for each parameter modification. Parameters under-consideration were the testbed under use, traffic load, topology, and number of source nodes. Table 4.2 depicts the different settings for each experiments set.

### 4.5.3 Experimental results

#### 4.5.3.1 Performance for different testbeds

We begin by assessing the overall impact of FLQE-RM, four-bit and ETX on CTP routing performance, using Indriya testbed (refer to Table 4.2 — Set 1 of experiments). Each experiment is repeated 5 times. Experimental results are illustrated in Figure 4.3.

Figure 4.3 shows that FLQE-RM provides better routing performance, compared to four-bit and ETX as it is capable to deliver more packets (Figure 4.3(a)), with less retransmissions (Figure 4.3(b)), less parent changes (Figure 4.3(d)), and through shorter routes (Figure 4.3(c)).

Figure 4.3(a) shows that ETX presents very low PDR compared with FLQE-RM and four-bit. This can be interpreted by the fact that ETX is not able to identify high quality routes for data delivery. One of the reasons is the unreliability of ETX as a LQE, i.e., ETX is not an accurate metric for link quality estimation. Further, ETX is unstable as it leads to frequent parent changes

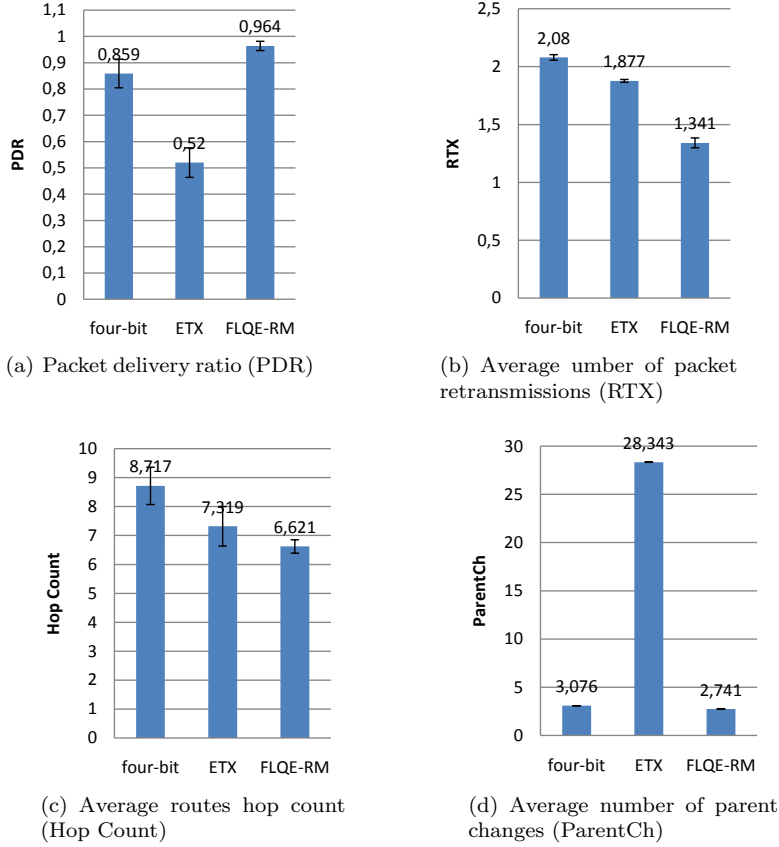


Figure 4.3: Impact of FLQE-RM, four-bit, and ETX on CTP performance, using Indriya testbed (refer to Table 4.2 — Set 1).

(Figure 4.3(d)). Parent changes may lead to several packet losses. The unreliability and instability of ETX was confirmed in Chapter 2, when we analyzed the statistical properties of different LQEs, including ETX, independently of higher layer protocols, especially routing.

Network conditions, especially the nature of the surrounding environment (e.g., indoor/outdoor, static/mobile obstacles, the geography of the environment), the type of the WSN platform, and even the climate conditions (e.g., temperature, humidity), affects the quality of the underlying links, and thus impacts the network performance. For this reason, we have investigated the performance of FLQE-RM, four-bit, and ETX, using a different testbed from Indriya. Experimental results carried out with MoteLab (refer to Table 4.2 — Set 1 of experiments) are depicted in Figure 4.4. From this figure two main observations can be made: First, by examining the PDR in Figure 4.4(a), it can be inferred that links in MoteLab have worse quality, than those in Indriya, as the maximum achieved PDR (by FLQE-RM) is equal to 75%. Second, MoteLab experimental results confirm that FLQE-RM leads to the best routing performance and ETX leads to the worst. This observation can be interpreted by

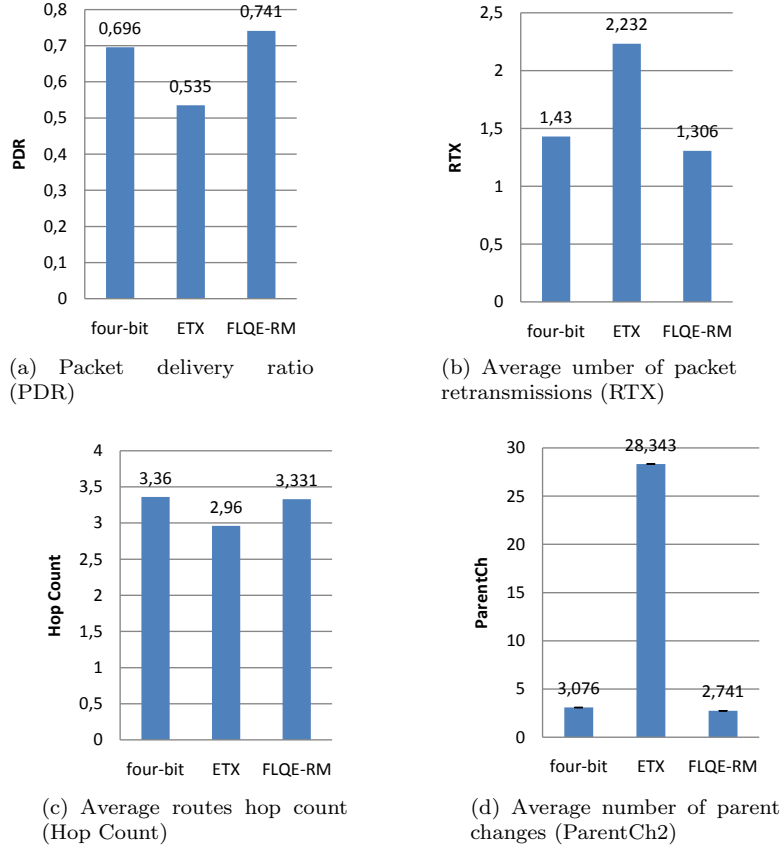


Figure 4.4: Impact of FLQE-RM, four-bit and ETX, on CTP performance, using MoteLab testbed (refer to Table 4.2 — Set 1).

F-LQE reliability. Indeed, we have shown in Chapter 3 that F-LQE provides a fine grain classification of links, especially intermediate links, better than four-bit and ETX.

#### 4.5.3.2 Performance as a function of the traffic load

We have assessed the impact of FLQE-RM, four-bit and ETX on CTP routing performance for different traffic loads. Experiment settings are presented in Table 4.2 — Set 2 and Figure 4.5 illustrates the experimental results. With the increase of the traffic load, the congestion level of the network increases, which leads to packet loss induced by buffer overflow as well as MAC collisions.

For traffic load less than or equal to 1 pkt/s, Figure 4.5 shows that FLQE-RM performs better than four-bit and ETX: It improves the PDR and reduces the number of parent changes. If we observe RTX and Hop count together, it can be inferred that FLQE-RM reduces the global number of packet transmissions (i.e., Hop count) and retransmissions (i.e., RTX), compared with ETX and four-bit. For example, for traffic load equal to 1 pkt/s, FLQE-RM has RTX equal to 1.27 and Hop count equal to 4.56, while ETX has RTX equal to 1.123 and Hop



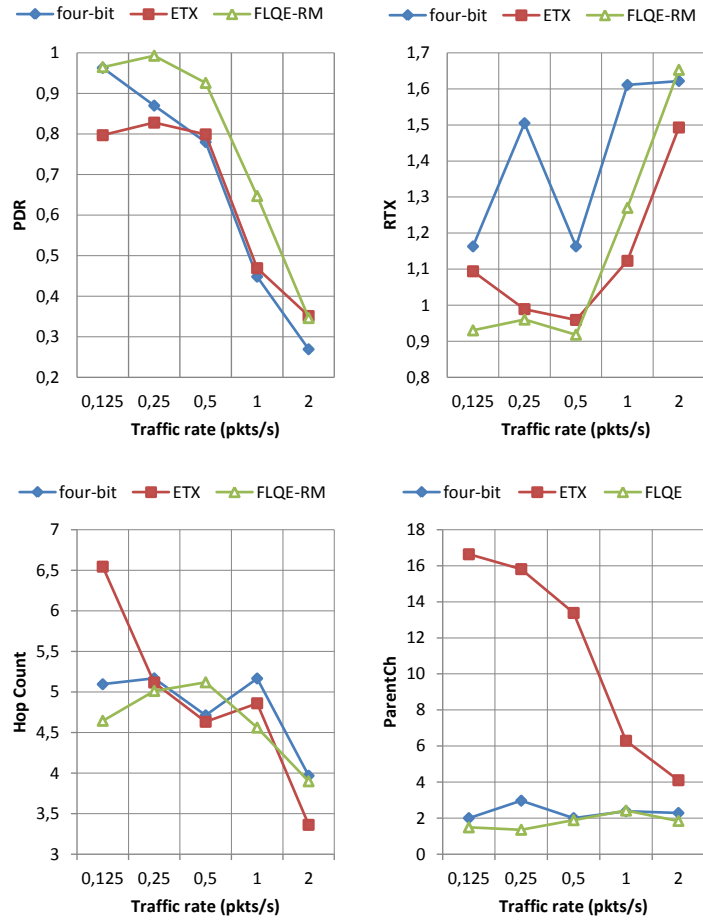


Figure 4.5: Performance as a function of the traffic load (refer to Table 4.2 — Set 2).

count equal to 4.86. Thus, overall, FLQE-RM reduces the number of packet transmissions and retransmissions (5.83) compared with ETX (5.98).

For traffic load equal to 2 pkts/s, Figure 4.5 shows that FLQE-RM provides slightly better (or nearly equal) performance than four-bit. This might be due to the fact that four-bit has more information on links status as the data rate (2 pkts/s) is the double of the beacon rate (1 packet/s). Recall that four-bit uses both beacon traffic and data traffic for link quality estimation, while FLQE-RM and ETX perform link quality estimation based on beacon traffic only. Figure 4.5 also shows that for traffic load equal to 2 pkts/s, ETX outperforms FLQE-RM and four-bit in terms of all performance metrics, except the parent changes. This observation would pertain to CTP, which does not contain any explicit congestion control mechanism, as it is designed for low data-rate applications.

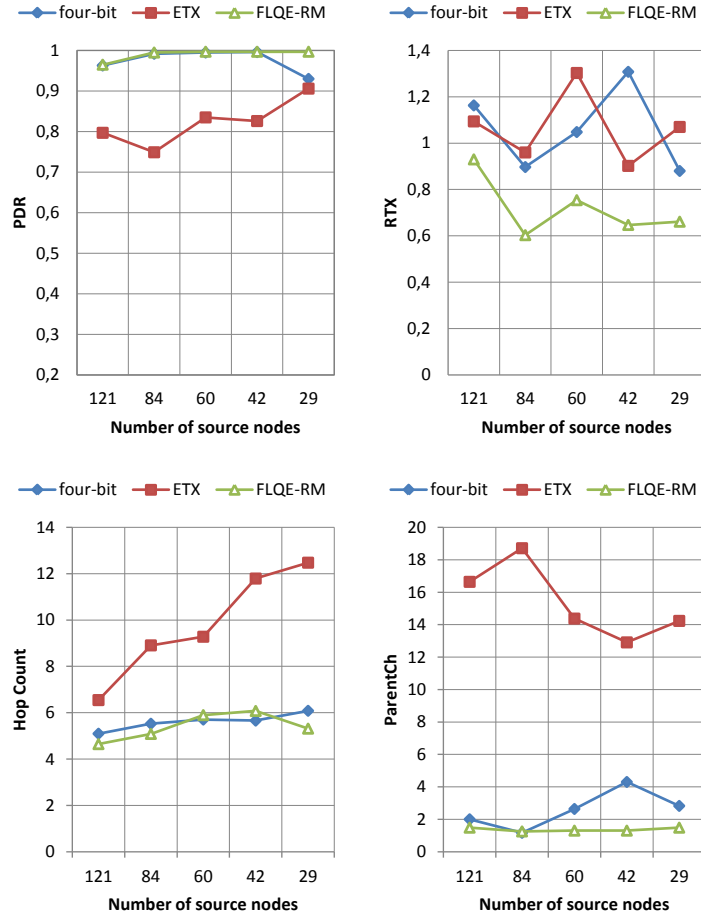


Figure 4.6: Performance as a function of the number of source nodes (refer to Table 4.2 — Set 3).

#### 4.5.3.3 Performance as a function of the number of source nodes

We have analyzed the impact of FLQE-RM, four-bit and ETX on CTP routing performance while varying the number of source nodes. Experiment settings are presented in Table 4.2 — Set 3 and experimental results are illustrated in Figure 4.6. By default, all nodes except the root node (i.e., 121 nodes) are data sources (refer to Table 4.2). By decreasing the number of source nodes, the congestion level of the network decreases, which reduces the number of packet losses induced by collisions or buffer overflow.

Figure 4.6 shows that overall, FLQE-RM leads to the best performance and ETX leads to the worst. By observing Figure 4.6 and Figure 4.5, it can be observed that generally, in terms of PDR, routing metrics are more sensitive to the traffic load variation than the number of source nodes variation. This is due to the considered data traffic rate (0.125 pkt/s), which is low enough to avoid network congestion for any number of source nodes.

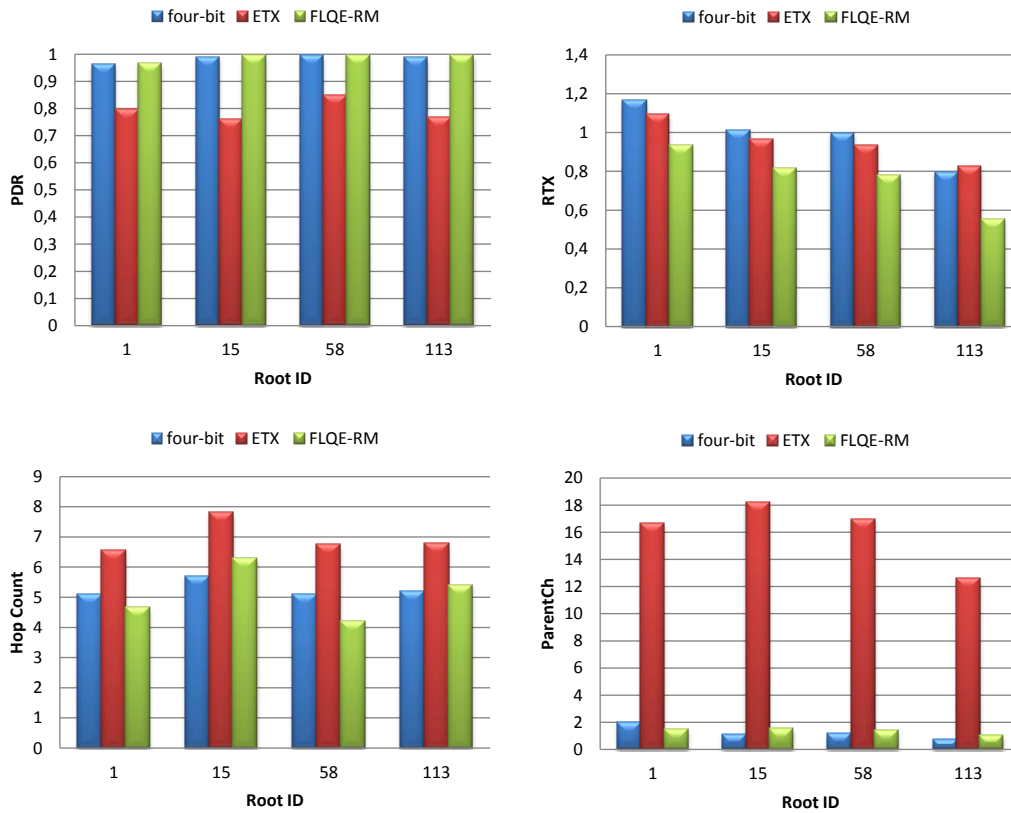


Figure 4.7: Performance as a function of the topology (refer to Table 4.2 — Set 4).

#### 4.5.3.4 Performance as a function of the topology

The network topology has a significant impact on routing performance [110]. To examine the impact of topology on CTP tree routing, we considered different sink (Root node) placements. Hence, for each CTP version, based on a particular routing metric (FLQE-RM, four-bit or ETX), we carried out a set of experiments, while varying the sink node assignment, i.e., varying the Root ID (refer to Table 4.2 — Set 4).

Figure 4.7 illustrates routing performance, with respect to each routing metric as a function of the root ID assignment. This figure confirms the impact of the topology on routing performance. Further, it shows that again, FLQE-RM leads to the best performance and ETX leads to the worst, for all considered sink assignments.

#### 4.5.3.5 Results review

This section provides a review of our experimental results with the 122-node Indriya testbed, as illustrated in Table 4.3, Table 4.4, and Table 4.5. These tables show that overall, FLQE-RM improves the end to end packet delivery (PDR) by up to 16% over four-bit (Table 4.3) and up to 24% over ETX (Table

Table 4.3: Overall results for Indriya experiments, where 121 nodes are data sources and the node with ID equal to 1 is selected as root, averaged over all considered traffic loads.

<b>Performance indicator</b>	<b>four-bit</b>	<b>ETX</b>	<b>FLQE-RM</b>
<b>Packet delivery ratio (PDR)</b>	0.666 ± 0.26	0.647 ± 0.19	0.775 ± 0.24
<b>Number of retransmissions for packet delivery (RTX)</b>	1.412 ± 0.2	1.131 ± 0.19	1.146 ± 0.28
<b>Hop count</b>	4.821 ± 0.45	4.902 ± 1.01	4.646 ± 0.43
<b>Number of parent changes (ParentCh)</b>	2.326 ± 0.35	11.246 ± 5.1	1.794 ± 0.37

Table 4.4: Overall results for Indriya experiments, where the traffic load is fixed to 0.125 pkt/s and the node with ID equal to 1 is selected as root, averaged over all considered number of source nodes.

<b>Performance indicator</b>	<b>four-bit</b>	<b>ETX</b>	<b>FLQE-RM</b>
<b>Packet delivery ratio (PDR)</b>	0.975 ± 0.02	0.822 ± 0.05	0.99 ± 0.01
<b>Number of retransmissions for packet delivery (RTX)</b>	1.059 ± 0.16	1.065 ± 0.13	0.719 ± 0.11
<b>Hop count</b>	5.613 ± 0.31	9.8 ± 2.13	5.402 ± 0.52
<b>Number of parent changes (ParentCh)</b>	2.585 ± 1.03	15.374 ± 2.05	1.363 ± 0.09

Table 4.5: Overall results for Indriya experiments, where 121 nodes are data sources and the traffic load is fixed to 0.125 pkt/s, averaged over all considered Root ID assignments.

<b>Performance indicator</b>	<b>four-bit</b>	<b>ETX</b>	<b>FLQE-RM</b>
<b>Packet delivery ratio (PDR)</b>	0.982 ± 0.01	0.793 ± 0.03	0.987 ± 0.01
<b>Number of retransmissions for packet delivery (RTX)</b>	0.991 ± 0.13	0.954 ± 0.09	0.769 ± 0.13
<b>Hop count</b>	5.268 ± 0.24	6.963 ± 0.48	5.129 ± 0.8
<b>Number of parent changes (ParentCh)</b>	1.247 ± 0.46	16.083 ± 2.1	1.354 ± 0.19

4.5). It also reduces the number of retransmissions per delivered packet by up to 32% over four-bit and also ETX (Table 4.4). The Hop count metric can be interpreted by the average route lengths as well as the average number of packet transmissions to deliver a packet. FLQE-RM reduces the Hop count by up to 4% over four-bit (Tables 4.4 and 4.5) and up to 45% over ETX (Table 4.4). The ParentCh metric implies on the topology stability. FLQE-RM improves topology stability by up to 47% over four-bit (Table 4.4) and up to 92% over ETX (Table 4.5).

Table 4.6: Memory footprint of four-bit, ETX, and FLQE-RM.

	<b>four-bit</b>	<b>ETX</b>	<b>FLQE-RM</b>
<b>ROM</b> (in KiloBytes)	22.28	22	27.10
<b>RAM</b> (in KiloBytes)	4.04	4.06	4.47

#### 4.5.3.6 Memory footprint and computation complexity

We measured the memory footprint with respect to four-bit, ETX, and FLQE-RM, in terms of RAM and ROM consumptions. As shown in Table 4.6, a sensor node (precisely, TelosB mote) running FLQE-RM as routing metric consumes a total ROM footprint equal to 27.10 KB and a total RAM footprint equal to 4.47 KB. Compared to four-bit and ETX, FLQE-RM has more memory footprint as depicted in Table 4.6. Nevertheless, today’s sensor platforms provide higher memory than that consumed by FLQE-RM. For example, a TelosB mote has total ROM of 48 KB and a total RAM of 10 KB. Our experimental study with Indriya and MoteLab proves that FLQE-RM metric can be implemented on TelosB and TMote Sky motes.

FLQE-RM relies on F-LQE estimator, which is computationally more complex than four-bit and ETX. Typically, F-LQE computes four link quality metrics (SPRR, ASL, SF, and ALQI) applies these metrics to piecewise linear membership functions, then combines the different membership levels into a particular equation. On the other hand four-bit combines two link quality metrics through a simple weighted sum (the EWMA filter), and ETX uses a single link quality metric.

#### 4.5.3.7 Discussion

Each of FLQE-RM, four-bit, and ETX selects routing paths, which corresponds to the establishment of the routing tree in the context of collection tree routing, based on link quality estimation. Typically, an efficient routing metric (i.) reduces the number of packet transmissions and retransmissions in the network, (ii.) increases its delivery and (iii.) ensures a stable topology. Our experimental study demonstrates that FLQE-RM establishes and maintains the routing tree better than four-bit, and ETX as it generally presents the highest PDR and lowest RTX, Hop count and ParentCh. The effectiveness of FLQE-RM as a routing metric can be interpreted by (i.) the accuracy of link quality estimation as well as (ii.) the efficiency of path cost evaluation:

In the context of CTP routing, all routing decisions are based on link quality estimation. Therefore, the accuracy of link quality estimation significantly impacts the effectiveness of routing metrics: the more accurate the estimate is, the more correct routing decisions are. In the previous chapter, we have shown that F-LQE is more accurate than four-bit and ETX (viewed as LQEs) as it provides a fine grain classification of links, especially intermediate links (these are the most difficult to assess). Thus, our experimental results confirms the accuracy of F-LQE, which is traduced by the correctness of routing decisions.

The effectiveness of a routing metric depends not only on the accuracy of link quality estimation, but also on how to use link estimates to evaluate the path cost. FLQE-RM path cost function allows to select paths constituted with

high quality links (in terms of F-LQE), while avoiding those having some weak links among high quality links. This path cost function also favors the selection of short paths. In fact, the path cost functions of four-bit and ETX metrics also share these features. That is, they take into account the path global quality and implicitly favor the selection of short paths that do not have poor links. Hence, what makes FLQE-RM more effective than four-bit and ETX would be the accuracy of link quality estimation through the use of F-LQE.

Our experimental results also show that four-bit performs better than ETX. Definitely, this result mainly pertains to the accuracy of link quality estimation. Four-bit takes into account more link aspects compared to ETX, as it combines RNP and estETX. estETX is not other than a smoothed ETX using the EWMA filter.

The outperformance of FLQE-RM over four-bit and ETX, which are representative and well-known metrics in the WSN community does not come without a price. As we have shown above, FLQE-RM involves higher memory footprint and computation complexity. In terms of energy consumption, FLQE-RM conserves the nodes energy by reducing the number of transmissions and retransmissions in the network, as shown by our experimental study. A sensor node expends most (almost 2/3) of its energy in data communication [111].

## 4.6 Conclusion

In this chapter, we have presented FLQE-RM, an efficient routing metric based on F-LQE. We have shown through both TOSSIM 2 simulation and large scale real experimentation that FLQE-RM boosts CTP routing performance. Particularly, our experimental results show that FLQE-RM establishes and maintains CTP routing tree better than four-bit, and ETX: It improves the end-to-end-delivery by up to 16%, reduces the number of packet retransmissions by up to 32%, reduces the Hop count by up to 4%, and improves the topology stability by up to 47%. These results indeed demonstrate the applicability and the usefulness of F-LQE for routing protocols — specifically, collection tree routing protocols.

---

## Conclusion

---

### Discussion

Link quality estimation has been attracting a lot of attention in the Wireless Sensor Network (WSN) community as it emerges as a fundamental building block for several protocols and mechanisms, such as MAC, routing, mobility management, and localization. In this context, this dissertation presents several contributions, namely (i.) an overview of link quality estimation in low-power WSNs, (ii.) the design and implementation of RadiaLE: a framework that automates the experimental evaluation, design and optimization of link quality estimators (LQEs), (iii.) a comparative performance study of most well-known LQEs, using both simulation and experimentation, (iv.) the design and evaluation of F-LQE, a new LQE based on Fuzzy Logic that overcomes the limitations of existing LQEs, and (v.) the impact of LQEs, including F-LQE, on the performance of collection tree routing. From this array of contributions, several lessons can be learnt.

**Lesson 1:** It is well known that wireless links are unreliable, in contrast to wired links. However, WSN links are even more unreliable than traditional wireless links, due to the radio transceivers typically used by sensor devices. These radios transmit low-power signals, which makes radiated signals more prone to noise, interference, and multi-path distortion. Consequently, low-power links experience a complex and dynamic behavior, e.g., intensive quality fluctuations, high asymmetric connectivity, large transitional region. Several recent research efforts were devoted to the understanding of low-power links behaviour through (i.) their empirical characterization as well as (ii.) their statistical characterization using estimation theory — the so called Link Quality Estimation.

We have shown in Chapter 1 that some empirical observations from different studies were contradictory. This is due to the discrepancies in experimental conditions between these studies, i.e., they do not have the same environment characteristics, neither the same WSN platform or the same experiment settings. Empirical observations are of paramount importance for the channel modeling in general and link quality estimation in particular. Hence, it is important to

draw them under a large number of experiments while varying experimental conditions in order to avoid misleading observations.

**Lesson 2:** We have drawn the following recommendations for the design of an efficient link quality estimator (LQE):

- An efficient LQE must be reactive to persistent changes in link quality, yet stable by ignoring transient (short-term) variations in link quality. A good balance between reactivity and stability can be obtained through the use of EWMA (Exponentially Weighted Moving Average) filtering [70]. This filter has two parameters that should be carefully tuned: the smoothing factor  $\alpha$  and the estimation window  $w$ .
- Efficient link quality estimation that provides a fine grain classification of links, especially intermediate quality links, should be based on several link quality metrics, each metric capturing a particular link property such as link asymmetry or stability. In fact, a single metric (e.g., RSSI, PRR, RNP, ETX) can only assess a particular link property and thus provides just a partial characterization of the link.
- A common error is to design a unidirectional LQE and use it for the assessment of bidirectional links, assuming that both link directions have the same quality, i.e., the link is symmetric. This misconception (typically found in mesh routing) has a negative impact on the performance of network protocols and can lead to dramatic performance due to the prevalence of asymmetric links in WSNs. This does not mean that all LQEs should be bidirectional and unidirectional LQEs are useless. Specific applications such as data collection based on tree routing only need to assess one link direction (from child to parent). Thus, using a unidirectional LQE for these applications, specifically a sender-side LQE, is a convenient choice [25]. The design of bidirectional LQEs is not a trivial task. A bidirectional LQE should combine feedback from both link directions. The main challenge is that these feedbacks should be obtained at the same time in order to cope with link dynamic. ETX and four-bit are bidirectional LQEs, but they do not meet this challenge.

**Lesson 3:** PRR and RNP are two representative and basic LQEs. They have been extensively used for routing protocols and also for the design of composite LQEs. Hence, it is important to understand their features:

- For good-quality and bad-quality links, i.e., links having high (e.g.,  $> 90\%$ ) and low reception rates (e.g.,  $< 50\%$ ) respectively, PRR follows the same behavior as RNP. However, for intermediate quality links, PRR *overestimates* the link quality because it does not take into account the underlying distribution of packet losses. When the link exhibits short periods during which packets are not received, the PRR can still have high value but the RNP is high so that it indicates the real link state. As a matter of fact, a packet that cannot be delivered may be retransmitted several times before aborting transmission.



- RNP is more reactive than PRR but it can underestimate link quality. In fact, RNP is a sender side LQE, i.e., it is computed based on transmitted packets. Consequently, RNP is able to provide link quality estimates as long as there is traffic generated from the sender. On the other hand, PRR is receiver side, i.e., it is computed based on received packets. Consequently, when the link is of poor quality, packets are not delivered and PRR cannot be computed. However, RNP can underestimate link quality in particular situations, as sometimes packets are retransmitted many times before being successfully received. This situation yields to good PRR but bad RNP. Further, RNP is unstable compared with PRR.

**Lesson 4:** The design of LQEs that provide a holistic view on the link quality is relatively new research problem, thus, several research challenges still remain open. One challenging problem is to select representative link quality metrics for the specification of a holistic link quality estimation. For instance, a big emphasis has been made in the literature about the goodness of hardware metrics namely RSSI, LQI and SNR in quantifying some properties of the link. Another challenging problem is to devise convenient techniques for combining these metrics and producing a single link quality estimate. In Chapter 3, we have addressed these challenges by introducing F-LQE, a Fuzzy Link Quality Estimator. F-LQE combines four link metrics (SPRR, ASNR, ASL, and SF) using Fuzzy Logic, since we believed (and proved) to be an appropriate strategy to fuse different and imprecise metrics.

We have extensively evaluated F-LQE both by simulation and experimentation, demonstrating greater performance over existing and representative LQEs, in terms of reliability and stability. In chapter, 4, we have demonstrated the usefulness and applicability of F-LQE by investigating its impact on the Collection Tree routing Protocol (CTP). We have shown through both simulation and large scale real experimentation that using F-LQE for link quality estimation boosts CTP performance by improving the end-to-end delivery, reducing the number of packet retransmissions, reducing the hop count, and improving the topology stability. Nevertheless F-LQE has some limitations:

First, F-LQE is computationally more complex than traditional LQEs, such as PRR, RNP, four-bit, ETX, and WMEMWA. This is due to the fact that F-LQE computes four link quality metrics (SPRR, ASL, SF, and ASNR/ALQI) applies these metrics to piecewise linear membership functions, then combines the different membership levels into a given equation. On the other hand traditional LQEs either are based on a single link quality metric, or combines less metrics than F-LQE. For example, four-bit combines two link quality metrics through a simple weighted sum (the EWMA filter). F-LQE also consumes more memory footprint, which is a consequence of its computation complexity.

Second, F-LQE is receiver-side LQE as all considered link quality metrics are computed based on received packets. Consequently, when the link is of poor quality, packets are not delivered and F-LQE estimate can not be updated. This limitation has negative impact on mobility management schemas, where responsiveness to link quality dynamic is an major concern. Nevertheless, F-LQE stands for the methodology of combing representative link quality metrics using Fuzzy logic, for a holistic characterization of the link. Hence, another possible version of F-LQE would be the combination of sender-side link quality

metrics such as RNP, in order better cope with link dynamics.

## Future directions

Several network protocols and mechanisms are built upon efficient link quality estimation. A LQE can be efficient on a link basis, but leads to poor performance when integrated in a particular protocol or mechanism. In Chapter 4, we have shown how to use F-LQE to be optimally used for collection tree routing. As future work, it would be also interesting to tune F-LQE to be used by other protocols and mechanisms, namely mobility management and localization. Particularly, several localization systems are based on link RSSI measurement to determine the distance separating the two link ends. However, RSSI is not a good indicator of link quality at least because it only assess one link aspect. Therefore, a possible future direction is to find a mapping function that returns the correct distance given F-LQE estimate.

Link quality can be assessed in different ways, based on reliability, latency, energy etc. This dissertation focuses on the assessment of links based on their reliability. This reliability can be defined in terms of packet reception, or in terms of number of packet retransmissions. It can also be assessed by hardware metrics such as RSSI. Most relevant LQEs that are suitable for WSNs assess links based on their reliability. Nevertheless, as WSN applications have different requirements, it would be conceivable to consider other criteria in link quality assessment other than link reliability, such as latency for real-time constrained applications. Several metrics based on latency and energy have been introduced for mesh and Ad Hoc networks, such as the ETT (Expected Transmission Time) [112]. Hence, the study of these metrics and their adequacy for WSN context would also be an interesting future work.

---

## Bibliography

---

- [1] G. Zhou, T. He, S. Krishnamurthy, and J. A. Stankovic, "Impact of radio irregularity on wireless sensor networks," in *Proc. of the 2<sup>nd</sup> Int. Conf. on Mobile Systems, Applications, and Services (MobiSys '04)*. ACM, 2004, pp. 125–138.
- [2] D. Ganesan, B. Krishnamachari, A. Woo, D. Culler, D. Estrin, and S. Wicker, "Complex behavior at scale: An experimental study of low-power wireless sensor networks," Tech. Rep., 2002.
- [3] N. Baccour, A. Koubâa, M. B. Jamaa, D. do Rosário, H. Youssef, M. Alves, and L. B. Becker, "Radiale: A framework for designing and assessing link quality estimators in wireless sensor networks," *Ad Hoc Networks*, vol. 9, no. 7, pp. 1165 – 1185, 2011.
- [4] K. Srinivasan, P. Dutta, A. Tavakoli, and P. Levis, "An empirical study of low-power wireless," *ACM Trans. Sen. Netw.*, vol. 6, pp. 1–49, 2010.
- [5] (2009) Topology configuration. [Online]. Available: <http://www.tinyos.net/dist-2.0.0/tinyos-2.x/doc/html/tutorial/usc-topologies.html>
- [6] A. Cerpa, J. L. Wong, M. Potkonjak, and D. Estrin, "Temporal properties of low power wireless links: Modeling and implications on multi-hop routing," in *Proc. of the 6<sup>th</sup> Int. Symposium on Mobile ad hoc networking and computing (MobiHoc '05)*. ACM, 2005, pp. 414–425.
- [7] G. Zhou, T. He, S. Krishnamurthy, and J. A. Stankovic, "Models and solutions for radio irregularity in wireless sensor networks," *ACM Trans. Sen. Netw.*, vol. 2, no. 2, pp. 221–262, 2006.
- [8] J. Zhao and R. Govindan, "Understanding packet delivery performance in dense wireless sensor networks," in *Proc. of the 1<sup>st</sup> Int. Conf. on Embedded Networked Sensor Systems (SenSys '03)*. ACM, 2003, pp. 1–13.
- [9] A. Cerpa, J. L. Wong, L. Kuang, M. Potkonjak, and D. Estrin, "Statistical model of lossy links in wireless sensor networks," in *Proc. of the 4<sup>th</sup> Int. Symposium on Information Processing in Sensor Networks (IPSN '05)*. IEEE Press, 2005, pp. 81 – 88.

- [10] P. Jiang, Q. Huang, J. Wang, X. Dai, and R. Lin, "Research on wireless sensor networks routing protocol for wetland water environment monitoring," in *Proc. of the 1<sup>st</sup> Int. Conf. on Innovative Computing, Information and Control (ICICIC '06)*. IEEE Computer Society, 2006, pp. 251–254.
- [11] A. Woo, T. Tong, and D. Culler, "Taming the underlying challenges of reliable multihop routing in sensor networks," in *Proc. of the 1<sup>st</sup> Int. Conf. on Embedded Networked Sensor Systems (SenSys '03)*. ACM, 2003, pp. 14–27.
- [12] O. Gnawali, R. Fonseca, K. Jamieson, D. Moss, and P. Levis, "Collection tree protocol," in *Proc. of the 7<sup>th</sup> ACM Conf. on Embedded Networked Sensor Systems (SenSys '09)*. ACM, 2009, pp. 90–100.
- [13] Y. Li, J. Chen, R. Lin, and Z. Wang, "A reliable routing protocol design for wireless sensor networks," in *Proc. of the IEEE Int. Conf. on Mobile Adhoc and Sensor Systems (MASS '05)*. IEEE Computer Society, 2005, pp. 61–65.
- [14] G. Lim, "Link stability and route lifetime in ad-hoc wireless networks," in *Proc. of the Int. Conf. on Parallel Processing Workshops (ICPPW '02)*. IEEE Computer Society, 2002, p. 116.
- [15] C. Koksal and H. Balakrishnan, "Quality-aware routing in time-varying wireless networks," *IEEE Journal on Selected Areas of Communication Special Issue on Multi-Hop Wireless Mesh Networks*, vol. 24, no. 11, pp. 1984–1994, 2006.
- [16] K. Seada, M. Zuniga, A. Helmy, and B. Krishnamachari, "Energy-efficient forwarding strategies for geographic routing in lossy wireless sensor networks," in *Proc. of the 2<sup>nd</sup> Int. Conf. on Embedded Networked Sensor Systems (SenSys '04)*. ACM, 2004, pp. 108–121.
- [17] A. Cerpa and D. Estrin, "ASCENT: Adaptive Self-Configuring sEnSOr Networks Topologies," *IEEE Transactions on Mobile Computing*, vol. 3, no. 3, pp. 272–285, 2004.
- [18] A. Cerpa, N. Busek, and D. Estrin, "Scale: A tool for simple connectivity assessment in lossy environments," Tech. Rep., 2003.
- [19] D. Son, B. Krishnamachari, and J. Heidemann, "Experimental study of concurrent transmission in wireless sensor networks," in *Proc. of the 4<sup>th</sup> Int. Conf. on Embedded Networked Sensor Systems (SenSys '06)*. ACM, 2006, pp. 237–250.
- [20] L. Tang, K.-C. Wang, Y. Huang, and F. Gu, "Channel characterization and link quality assessment of ieee 802.15.4-compliant radio for factory environments," *IEEE Trans. Industrial Informatics*, vol. 3, no. 2, pp. 99–110, 2007.
- [21] C.-J. M. Liang, N. B. Priyantha, J. Liu, and A. Terzis, "Surviving wi-fi interference in low power zigbee networks," in *Proc. of the 8<sup>th</sup> ACM Conf. on Embedded Networked Sensor Systems (SenSys '10)*. ACM, 2010, pp. 309–322.

- [22] M. Rondinone, J. Ansari, J. Riihijärvi, and P. Mähönen, “Designing a reliable and stable link quality metric for Wireless Sensor Networks,” in *Proc. of the Workshop on Real-world Wireless Sensor Networks (RealWSN '08)*, 2008, pp. 6–10.
- [23] N. Baccour, A. Koubâa, L. Mottola, M. A. Zuniga, H. Youssef, C. A. Boano, and M. Alves, “Radio link quality estimation in wireless sensor networks: a survey,” (*To appear in*) *ACM Transactions on Sensor Networks*, vol. 8, no. 4, 2012.
- [24] (2010) Radiale benchmarking tool. [Online]. Available: <http://www.open-LQE.net>
- [25] N. Baccour, A. Koubaa, M. Ben Jamaa, H. Youssef, M. Zuniga, and M. Alves, “A comparative simulation study of link quality estimators in wireless sensor networks,” in *Proc. of the 17<sup>th</sup> IEEE/ACM Int. Symposium on Modelling, Analysis and Simulation of Computer and Telecommunication Systems (MASCOTS '09)*. IEEE, 2009, pp. 301–310.
- [26] N. Baccour, A. Koubaa, H. Youssef, M. Ben Jamaa, D. do Rosário, , M. Alves, and L. B.Becker, “F-LQE: A Fuzzy Link Quality Estimator for Wireless Sensor Networks,” in *Proc. od the 7<sup>th</sup> European Conf. on Wireless Sensor Networks (EWSN 2010)*. Springer, 2010, pp. 240–255.
- [27] N. Baccour, A. Koubâa, W. Mefteh, M. B. Jamâa, H. Youssef, and M. Alves, “Boosting collection-tree routing protocols through enhanced link quality estimation,” Tech. Rep., 2011.
- [28] N. Reijers, G. Halkes, and K. Langendoen, “Link layer measurements in sensor networks,” in *Proc. of the 1<sup>st</sup> IEEE Intl Conf. on Mobile Ad-hoc and Sensor Systems (MASS '04)*. IEEE Computer Society, 2004, pp. 24–27.
- [29] M. Zuniga and B. Krishnamachari, “Analyzing the transitional region in low power wireless links,” in *Proc. of the 1<sup>st</sup> Int. Conf. on Sensor and Ad hoc Communications and Networks (SECON '04)*. IEEE Communications Society, 2004, pp. 517–526.
- [30] BTNode,  
[www.btnode.ethz.ch](http://www.btnode.ethz.ch).
- [31] M. Dyer, J. Beutel, L. Thiele, T. Kalt, P. Oehen, K. Martin, and P. Blum, “Deployment support network - A toolkit for the development of WSNs,” in *Proc. of the 4<sup>th</sup> European Conference on Wireless Sensor Networks (EWSN '07)*. Springer, 2007, pp. 195–211.
- [32] J. Polastre, R. Szewczyk, and D. Culler, “Telos: Enabling ultra-low power wireless research,” in *Proc. of the 4<sup>th</sup> Int. Symposium on Information Processing in Sensor Networks (IPSN '05)*. IEEE Press, 2005, pp. 364 – 369.
- [33] B. Raman and K. Chebrolu, “Censor networks: a critique of ”sensor networks” from a systems perspective,” *SIGCOMM Comput. Commun. Rev.*, vol. 38, pp. 75–78, 2008.

- [34] G. Werner-Allen, K. Lorincz, J. Johnson, J. Lees, and M. Welsh, "Fidelity and yield in a volcano monitoring sensor network," in *Proc. of the 7<sup>th</sup> Symposium on Operating Systems Design and Implementation (OSDI '06)*. USENIX Association, 2006, pp. 381–396.
- [35] B. Raman, K. Chebrolu, N. Madabhushi, D. Y. Gokhale, P. K. Valiveti, and D. Jain, "Implications of link range and (in)stability on sensor network architecture," in *Proc. of the 1<sup>st</sup> Int. Workshop on Wireless Network Testbeds, Experimental Evaluation & Characterization (WiNTECH '06)*. ACM, 2006, pp. 65–72.
- [36] K. Bannister, G. Giorgetti, and S. K. Gupta, "Wireless Sensor Networking for Hot Applications: Effects of Temperature on Signal Strength, Data Collection and Localization," in *Proceedings of the 5th Workshop on Embedded Networked Sensors (HotEmNets)*, Charlottesville, Virginia, USA, Jun. 2008.
- [37] C. A. Boano, J. Brown, N. Tsiftes, U. Roedig, and T. Voigt, "The Impact of Temperature on Outdoor Industrial Sensor Network Applications," *IEEE Transactions on Industrial Informatics*, vol. 6, no. 3, pp. 451–459, Aug. 2010.
- [38] J. Thelen, D. Goense, and K. Langendoen, "Radio-wave propagation in potato fields," in *Proc. of 1<sup>st</sup> Wkshp. on Wireless Network Measurements*, 2005.
- [39] D. Lymberopoulos, Q. Lindsey, and A. Savvides, "A.: An empirical characterization of radio signal strength variability in 3-d ieee 802.15.4 networks using monopole antennas," in *Proc. of the 7<sup>th</sup> European Conf. on Wireless Sensor Networks (EWSN' 10)*. Springer, 2006, pp. 326–341.
- [40] M. Zuniga and B. Krishnamachari, "An analysis of unreliability and asymmetry in low-power wireless links," *ACM Trans. Sen. Netw.*, vol. 3, no. 2, pp. 63–81, 2007.
- [41] IEEE 802.15.4 Standard, <http://standards.ieee.org/getieee802/download/802.15.4-2003.pdf>, 2003.
- [42] (2009) Chipcon cc2420: Data sheet. [Online]. Available: <http://enaweb.eng.yale.edu/drupal/system/files/CC2420\unhbox\voidb@x\vbox{\hrulewidth0.4em}Data\unhbox\voidb@x\vbox{\hrulewidth0.4em}Sheet\unhbox\voidb@x\vbox{\hrulewidth0.4em}1\unhbox\voidb@x\vbox{\hrulewidth0.4em}4.pdf>
- [43] D. Kotz, C. Newport, and C. Elliott, "The mistaken axioms of wireless-network research," Dartmouth College, Tech. Rep., July 2003.
- [44] L. Mottola, G. P. Picco, M. Ceriotti, c. Gună, and A. L. Murphy, "Not all wireless sensor networks are created equal: A comparative study on tunnels," *ACM Trans. Sen. Netw.*, vol. 7, pp. 15:1–15:33, September 2010.
- [45] G. Zhou, T. He, J. A. Stankovic, and T. Abdelzaher, "Rid: Radio interference detection in wireless sensor networks," in *Proc. of the 24<sup>th</sup> Annual Joint Conf. of the IEEE Computer and Communications Societies (INFOCOM '05)*. IEEE, 2005, pp. 891 – 901.

- [46] K. Srinivasan, M. Jain, J. I. Choi, T. Azim, E. S. Kim, P. Levis, and B. Krishnamachari, "The  $\beta$  factor: inferring protocol performance using inter-link reception correlation," in *Proc. of the 16<sup>th</sup> Annual Int. Conf. on Mobile Computing and Networking (MobiCom '10)*. ACM, 2010, pp. 317–328.
- [47] T. S. Rappaport, *Wireless Communications: Principles and Practice*. Prentice Hall, 2001.
- [48] A. Goldsmith, *Wireless Communications*. Cambridge University Press, 2005.
- [49] H. Liu, J. Li, Z. Xie, S. Lin, K. Whitehouse, J. A. Stankovic, and D. Siu, "Automatic and robust breadcrumb system deployment for indoor fire-fighter applications," in *Proc. of the 8<sup>th</sup> Int. Conf. on Mobile Systems, Applications, and Services (MobiSys '10)*. ACM, 2010, pp. 21–34.
- [50] S. Munir, S. Lin, E. Hoque, S. M. S. Nirjon, J. A. Stankovic, and K. Whitehouse, "Locationing burstiness for reliable communication and latency bound generation in wireless sensor networks," in *Proc. of the 9<sup>th</sup> ACM/IEEE Int. Conf. on Information Processing in Sensor Networks (IPSN '10)*. ACM, 2010, pp. 303–314.
- [51] J. Brown, B. McCarthy, U. Roedig, T. Voigt, and C. J. Sreenan, "Burst-probe: debugging time-critical data delivery in wireless sensor networks," in *Proc. of the 8<sup>th</sup> European Conf. on Wireless sensor networks (EWSN '11)*. Springer-Verlag, 2011, pp. 195–210.
- [52] K. Srinivasan, M. A. Kazandjieva, S. Agarwal, and P. Levis, "The  $\beta$ -factor: measuring wireless link burstiness," in *Proc. of the 6<sup>th</sup> Int. Conf. on Embedded Network Sensor Systems (SenSys '08)*. ACM, 2008, pp. 29–42.
- [53] S. Lin, J. Zhang, G. Zhou, L. Gu, J. A. Stankovic, and T. He, "Atpc: adaptive transmission power control for wireless sensor networks," in *Proc. of the 4<sup>th</sup> Int. Conf. on Embedded Networked Sensor Systems (SenSys '06)*. ACM, 2006, pp. 223–236.
- [54] S. Lin, G. Zhou, K. Whitehouse, Y. Wu, J. A. Stankovic, and T. He, "Towards stable network performance in wireless sensor networks (rtss '09)," in *Proc. of the 30<sup>th</sup> IEEE Real-Time Systems Symposium*. IEEE Computer Society, 2009, pp. 227–237.
- [55] D. Lal, A. Manjeshwar, and F. Herrmann, "Measurement and characterization of link quality metrics in energy constrained wireless sensor networks," in *Proc. of the IEEE Global Telecommunications Conference (Globecom '03)*. IEEE Communications Society, 2003, pp. 446–452.
- [56] H. Lee, A. Cerpa, and P. Levis, "Improving wireless simulation through noise modeling," in *Proc. of the 6<sup>th</sup> Int. Conf. on Information Processing in Sensor Networks (IPSN '07)*. ACM, 2007, pp. 21–30.

- [57] A. Sikora and V. F. Groza, "Coexistence of IEEE 802.15.4 with other systems in the 2.4 GHz-ISM-Band," in *Proc. of the IEEE Conf. on Instrumentation and Measurement Technology*, 2005, pp. 1786–1791.
- [58] M. Petrova, L. Wu, P. Mahonen, and J. Riihijarvi, "Interference measurements on performance degradation between colocated ieee 802.11g/n and ieee 802.15.4 networks," in *Proc. of the 6<sup>th</sup> Int. Conf. on Networking*. IEEE Computer Society, 2007, pp. 93–.
- [59] D. Yang, Y. Xu, and M. Gidlund, "Coexistence of IEEE802.15.4 Based Networks A Survey," in *Proc. of the 36<sup>th</sup> Annual Conf. on IEEE Industrial Electronics Society (IECON '10)*. IEEE, 2010, pp. 2107–2113.
- [60] C. A. Boano, T. Voigt, C. Noda, K. Römer, and M. A. Zúñiga, "JamLab: Augmenting Sensornet Testbeds with Realistic and Controlled Interference Generation," in *Proc. of the 10<sup>th</sup> Int. Conf. on Information Processing in Sensor Networks (IPSN '11)*. ACM Press, 2011, pp. 175–186.
- [61] G. Zhou, J. A. Stankovic, and S. H. Son, "Crowded Spectrum in Wireless Sensor Networks," in *Proc. of the 3<sup>rd</sup> Workshop on Embedded Networked Sensors (EmNets '06)*, 2006.
- [62] O. D. Incel, S. Dulman, P. Jansen, and S. Mullender, "Multi-Channel Interference Measurements for Wireless Sensor Networks," in *Proc. of the 31<sup>th</sup> Int. Conf. on Communications*. IEEE Communications Society, 2006, pp. 694–701.
- [63] E. Toscano and L. L. Bello, "Cross-channel interference in IEEE 802.15.4 networks," in *Proc. of the 7<sup>th</sup> Int Workshop on Factory Communication Systems (WFCS '08)*, 2008, pp. 139–148.
- [64] Y. Wu, J. A. Stankovic, T. He, and S. Lin, "Realistic and Efficient Multi-Channel Communications in Wireless Sensor Networks," in *Proc. of the 27<sup>th</sup> Conference on Computer Communications (INFOCOM '08)*. IEEE, 2008, pp. 1193–1201.
- [65] G. Xing, M. Sha, J. Huang, G. Zhou, X. Wang, and S. Liu, "Multi-Channel Interference Measurement and Modeling in Low-Power Wireless Networks," in *Proc. of the 30<sup>th</sup> IEEE Real-Time Systems Symposium (RTSS '09)*. IEEE Computer Society, 2009, pp. 248–257.
- [66] M. H. Alizai, O. Landsiedel, J. A. B. Link, S. Götz, and K. Wehrle, "Bursty traffic over bursty links," in *Proc. of the 7<sup>th</sup> ACM Conference on Embedded Networked Sensor Systems (SenSys '09)*. ACM, 2009, pp. 71–84.
- [67] D. S. J. D. Couto, D. Aguayo, J. Bicket, and R. Morris, "A high-throughput path metric for multi-hop wireless routing," in *Proc. of the 9<sup>th</sup> Annual Int. Conf. on Mobile Computing and Networking (MobiCom '03)*. ACM, 2003, pp. 134–146.
- [68] K.-H. Kim and K. G. Shin, "On accurate measurement of link quality in multi-hop wireless mesh networks," in *Proc. of the 12<sup>th</sup> Annual Int. Conf. on Mobile Computing and Networking (MobiCom '06)*. ACM, 2006, pp. 38–49.



- [69] H. Zhang, L. Sang, and A. Arora, "Comparison of data-driven link estimation methods in low-power wireless networks," *IEEE Transactions on Mobile Computing*, vol. 9, pp. 1634–1648, 2010.
- [70] A. Woo and D. Culler, "Evaluation of efficient link reliability estimators for low-power wireless networks," EECS Department, University of California, Berkeley, Tech. Rep. UCB/CSD-03-1270, 2003. [Online]. Available: <http://www.eecs.berkeley.edu/Pubs/TechRpts/2003/6239.html>
- [71] Y. Xu and W.-C. Lee, "Exploring spatial correlation for link quality estimation in wireless sensor networks," in *Proc. of the 4<sup>th</sup> Annual IEEE Int. Conf. on Pervasive Computing and Communication (PERCOM '06)*. IEEE Computer Society, 2006, pp. 200–211.
- [72] M. Yunqian, "Improving wireless link delivery ratio classification with packet snr," in *Proc. of the Int. Conf. on Electro Information Technology*. IEEE, 2005, pp. 6–12.
- [73] Y. Wang, M. Martonosi, and L.-S. Peh, "Predicting link quality using supervised learning in wireless sensor networks," *ACM SIGMOBILE Mobile Computing and Communications Review*, vol. 11, no. 3, pp. 71–83, 2007.
- [74] D. Puccinelli and M. Haenggi, "Reliable data delivery in large-scale low-power sensor networks," *ACM Trans. Sen. Netw.*, vol. 6, no. 4, pp. 1–41, 2010.
- [75] H. Zhang, L. Sang, and A. Arora, "Unravelling the subtleties of link estimation and routing in wireless sensor networks," Tech. Rep., 2008.
- [76] R. Fonseca, O. Gnawali, K. Jamieson, and P. Levis, "Four bit wireless link estimation," in *Proc. of the 6<sup>th</sup> Int. Workshop on Hot Topics in Networks (HotNets VI)*. ACM SIGCOMM, 2007.
- [77] M. Kim and B. Noble, "Mobile network estimation," in *Proc. of the 7<sup>th</sup> Annual Int. Conf. on Mobile Computing and Networking (MobiCom '01)*. ACM, 2001, pp. 298–309.
- [78] M. Senel, K. Chintalapudi, D. Lal, A. Keshavarzian, and E. J. Coyle, "A Kalman Filter Based Link Quality Estimation Scheme for Wireless Sensor Networks," in *Proc. of the IEEE Global Telecommunications Conference (GLOBECOM '07)*. IEEE, 2007, pp. 875–880.
- [79] D. Puccinelli and M. Haenggi, "DUCHY: Double Cost Field Hybrid Link Estimation for Low-Power Wireless Sensor Networks," in *Proc. of the 5<sup>th</sup> Fifth Workshop on Embedded Networked Sensors (Hot EmNets'08)*. ACM, 2008.
- [80] K. Srinivasan, P. Dutta, A. Tavakoli, and P. Levis, "Understanding the causes of packet delivery success and failure in dense wireless sensor networks," in *Proc. of the 4<sup>th</sup> Int. Conf. on Embedded Networked Sensor Systems (SenSys '06)*. ACM, 2006, pp. 419–420.

- [81] K. Srinivasan and P. Levis, "Rssi is under appreciated," in *Proc. of the 3<sup>rd</sup> In. Workshop on Embedded Networked Sensors (EmNets'06)*, 2006.
- [82] C. A. Boano, T. Voigt, A. Dunkels, F. Osterlind, N. Tsiftes, L. Mottola, and P. Suarez, "Poster abstract: Exploiting the LQI variance for rapid channel quality assessment," in *Proc. of the Int. Conf. on Information Processing in Sensor Networks (IPSN '09)*. IEEE Computer Society, 2009, pp. 369–370.
- [83] D. Aguayo, J. Bicket, S. Biswas, G. Judd, and R. Morris, "Link-level measurements from an 802.11b mesh network," *SIGCOMM Comput. Commun. Rev.*, vol. 34, no. 4, pp. 121–132, 2004.
- [84] C. Gomez, A. Boix, and J. Paradells, "Impact of LQI-based routing metrics on the performance of a one-to-one routing protocol for IEEE 802.15.4 multihop networks," *EURASIP J. Wirel. Commun. Netw.*, vol. 2010, pp. 6:1–6:20, February 2010.
- [85] C. A. Boano, M. Zuniga, T. Voigt, A. Willig, and K. Römer, "The Triangle Metric: Fast Link Quality Estimation for Mobile Wireless Sensor Networks," in *Proc. of the 19<sup>th</sup> Int. Conf. on Computer Communications and Networks (ICCCN '10)*. IEEE Communications Society, 2010, pp. 1 – 7.
- [86] G. Fairhurst and L. Wood, "Rfc 3366 : Advice to link designers on link automatic repeat request (arq)," Tech. Rep., 2002.
- [87] TinyOS MultiHopLQI routing algorithm, <http://www.tinyos.net/tinyos-1.x/tos/lib/MultiHopLQI/>, 2004.
- [88] K. Srinivasan, M. A. Kazandjieva, M. Jain, E. Kim, and P. Levis, "Demo abstract: Swat: enabling wireless network measurements," in *Proc. of the 6<sup>th</sup> ACM Conf. on Embedded Network Sensor Systems (SenSys '08)*. ACM, 2008, pp. 395–396.
- [89] P. Levis, N. Lee, M. Welsh, and D. Culler, "Tossim: Accurate and scalable simulation of entire tinyos applications," in *Proc. of the 1<sup>st</sup> In. Conf. on Embedded networked sensor systems (SenSys '03)*. ACM, 2003, pp. 126–137.
- [90] Tinyos. [Online]. Available: [www.tinyos.net/](http://www.tinyos.net/)
- [91] D. Gay, P. Levis, R. von Behren, M. Welsh, E. Brewer, and D. Culler, "The nesc language: A holistic approach to networked embedded systems," in *Proc. of the ACM SIGPLAN conf. on Programming Language Design and Implementation (PLDI '03)*. ACM, 2003, pp. 1–11.
- [92] G. Werner-Allen, P. Swieskowski, and M. Welsh, "Motelab: a wireless sensor network testbed," in *Proc. of the Int. Symposium on Information Processing in Sensor Networks (IPSN '05)*. IEEE Press, 2005, pp. 483–488.

- [93] B. N. Chun, P. Buonadonna, A. AuYoung, C. Ng, D. C. Parkes, J. Shneidman, A. C. Snoeren, and A. Vahdat, "Mirage: a microeconomic resource allocation system for sensornet testbeds," in *IEEE workshop on Embedded Networked Sensors*. IEEE Computer Society, 2005, pp. 19–28.
- [94] V. Handziski, A. Köpke, A. Willig, and A. Wolisz, "Twist: a scalable and reconfigurable testbed for wireless indoor experiments with sensor networks," in *Proc. of the 2<sup>nd</sup> Int. Workshop on Multi-hop Ad hoc Networks: From Theory to Reality (REALMAN '06)*. ACM, 2006, pp. 63–70.
- [95] A. Arora, E. Ertin, R. Ramnath, M. Nesterenko, and W. Leal, "Kansei: a high-fidelity sensing testbed," *Internet Computing, IEEE*, vol. 10, no. 2, pp. 35–47, March-April 2006.
- [96] D. Johnson, D. Flickinger, T. Stack, R. Ricci, L. Stoller, R. Fish, K. Webb, M. Minor, and J. Lepreau, "Emulab's wireless sensor net testbed: true mobility, location precision, and remote access," in *Proc. of the 3<sup>rd</sup> Int. Conf. on Embedded networked sensor systems (SenSys '05)*. ACM, 2005, pp. 306–306.
- [97] (2009) Tinyos 2. [Online]. Available: <http://www.tinyos.net/tinyos-2.x/tos/>
- [98] L. A. Zadeh, "The concept of a linguistic variable and its application to approximate reasoning," *Information Sciences*, vol. 8, p. 199249, 1975.
- [99] —, "Fuzzy sets," *Information and Control*, vol. 8, p. 338353, 1965.
- [100] R. R. Yager, "On ordered weighted averaging aggregation operators in multicriteria decisionmaking," *IEEE Trans. Syst. Man Cybern.*, vol. 18, no. 1, pp. 183–190, 1988.
- [101] H. Youssef, S. M. Sait, and S. A. Khan, "Fuzzy evolutionary hybrid metaheuristic for network topology design," in *Proc. of the First Int. Conf. on Evolutionary Multi-Criterion Optimization (EMO '01)*. Springer-Verlag, 2001, pp. 400–415.
- [102] A. K. Dwivedi and O. P. Vyas, "A survey on routing protocols for wireless sensor networks," *Ad Hoc Networks*, vol. 3, pp. 325–349, 2005.
- [103] K. Akkaya and M. Younis, "Network layer protocols for wireless sensor networks: Existing classifications and design challenges," *International Journal of Computer Applications*, vol. 8, pp. 30–34, 2010.
- [104] S. Moeller, A. Sridharan, B. Krishnamachari, and O. Gnawali, "Routing without routes: the backpressure collection protocol," in *Proc. of the 9<sup>th</sup> ACM/IEEE Int. Conf. on Information Processing in Sensor Networks (IPSN '10)*, ser. IPSN '10. ACM, 2010, pp. 279–290.
- [105] B.-r. Chen, K.-K. Muniswamy-Reddy, and M. Welsh, "Ad-hoc multicast routing on resource-limited sensor nodes," in *Proc. of the 2<sup>nd</sup> Int. Workshop on Multi-hop ad hoc networks: from theory to reality*, ser. REALMAN '06. New York, NY, USA: ACM, 2006, pp. 87–94.

- 
- [106] Ctp:collection tree protocol. [Online]. Available: <http://www.tinyos.net/tinyos-2.x/doc/html/tep123.html>
- [107] LEEP protocol, <http://www.tinyos.net/tinyos-2.x/doc/html/tep124.html>, 2007.
- [108] J. Polastre, J. Hill, and D. Culler, “Versatile low power media access for wireless sensor networks,” in *Proc. of the 2<sup>nd</sup> Int. Conf. on Embedded networked sensor systems*, ser. SenSys ’04. ACM, 2004, pp. 95–107.
- [109] M. Doddavenkatappa, M. Choon Chan, , and A. A.L, “Indriya: A low-cost, 3d wireless sensor network testbed,” in *Proc. of the 8<sup>th</sup> Int. ICST Conf. on Testbeds and Research Infrastructures for the Development of Networks and Communities*, 2011.
- [110] D. Puccinelli, O. Gnawali, S. Yoon, S. Santini, U. Colesanti, S. Giordano, and L. Guibas, “The impact of network topology on collection performance,” in *Proc. of the 8<sup>th</sup> European conference on Wireless sensor networks*, ser. EWSN’11. Springer-Verlag, 2011, pp. 17–32.
- [111] I. F. Akyildiz, W. Su, Y. Sankarasubramaniam, and E. Cayirci, “Wireless sensor networks: a survey,” *Computer Networks*, vol. 38, pp. 393–422, 2002.
- [112] R. Draves, J. Padhye, and B. Zill, “Routing in multi-radio, multi-hop wireless mesh networks,” in *Proc. of the 10<sup>th</sup> Annual Int. Conf. on Mobile Computing and Networking (MobiCom ’04)*, ser. MobiCom ’04. ACM, 2004, pp. 114–128.



---

---

## **Link Quality Estimation in Wireless Sensor Networks: Analysis, Design, and Experimentation**

---

---

**Nouha Baccour Sellami**

---

---

**Résumé :** Cette thèse adresse la conception, l'évaluation et l'expérimentation de nouvelles méthodologies pour une estimation plus fiable de la qualité des liens dans les réseaux de capteurs sans fil (RCSFs). Parmi les contributions de cette thèse est la conception d'un nouvel estimateur de qualité de liens, appelé *F-LQE*, basé sur la logique floue et qui fournit une caractérisation globale des liens dans les RCSFs. Une analyse de performances extensive, basée sur des simulations et des expérimentations réelles, montre que *F-LQE* est plus fiable que les estimateurs existants.

**Abstract:** This thesis addresses the design, evaluation and experimentation of new methodologies for more reliable link quality estimation in Wireless Sensor Networks (WSNs). Among the contributions of this thesis is the design of *F-LQE*, a new Link Quality Estimator based on Fuzzy Logic that provides a holistic characterization of low-power links. An extensive performance analysis based on both simulation and real experimentation shows that *F-LQE* outperforms existing estimators.

**Mots clés:** Estimation de la qualité des liens, liens dans les réseaux de capteurs, Expérimentation, Testbed, Mesures, Performance, Routage.

**Key-words:** Link quality estimation, Low-power links, Experimentation, Testbed, Measurements, Performance, Routing.